2014

Evaluate the fracture and fatigue resistances of hot mix asphalt containing high percentage reclaimed asphalt pavement (RAP) materials at low and intermediate temperatures

Sheng Tang
Iowa State University

Evaluate the fracture and fatigue resistances of hot mix asphalt containing high percentage reclaimed asphalt pavement (RAP) materials at low and intermediate temperatures

by

Sheng Tang

A dissertation submitted to the graduate faculty

in partial fulfillment of the requirement for the degree of

DOCTOR OF PHILOSOPHY

Major: Civil Engineering (Civil Engineering Materials)

Program of Study Committee:
R. Christopher Williams, Major Professor
Kejin Wang
Charles Jahren
W. Robert Stephenson
Sigurdur Olafsson

Iowa State University

Ames, Iowa

2014

TABLE OF CONTENTS

LIST OF FIGURES

LIST OF TABLES

ACKNOWLEDGMENTS

First, I would like to thank all my family members who have supported me throughout this journey in United States, especially my parents and wife. Their encouragement and unconditional love kept me going during hard times.

I would like to thank my major professor, Dr. Chris Williams, for all his help and support throughout my studies at Iowa State. I owe my deepest gratitude to him for placing me in the PhD program, providing guidance, and also constantly looking out for my interests and career development. This would not been possible without his generosity and kindness.

I would like to extend my great thanks to Drs. Robert Stephenson, Sigurdur Olafsson, Kejin Wang, and Charles Jahren for serving on my graduate committee and providing one-on-one help with my education. Their knowledge of statistics, data mining, operation research, concrete materials, and heavy construction I learned during classes will definitely benefit me in the future for many years.

I would also like to thank Dr. Wei Hong for providing insightful guidance on this thesis. Many thanks are also given to the Iowa Department of Transportation and the University of Iowa for their technical support.

Last, but not least, I would like to thank my dear friends and colleagues. Your companionship made living in Ames at Iowa State a memorable experience.

ABSTRACT

When applying recycled asphalt technology in a flexible pavement project, most of the concerns are related to low-temperature fracture and fatigue cracking, since the stiffness of hot mix asphalt (HMA) mixtures could dramatically increase through adding a high percentage of reclaimed asphalt pavement (RAP) materials. Therefore, the purpose of this research was to evaluate fracture and fatigue resistance of asphalt mixtures in relationship to various proportions of reclaimed asphalt pavement materials, and two RAP addition methods (Traditional and Fractionated Methods) at different temperatures (-10, -20, and -30°C for fracture resistance assessment, and 20°C for examination to fatigue resistance). Fracture and fatigue experiments, separately, utilized two types of RAP from different resources. Asphalt mixture samples for both facture and fatigue tests were prepared with RAP using the as is gradation (Traditional) and splitting of the RAP into coarse and fine fractions (Fractionated) methods with three RAP binder content replacement percentages (30, 40, and 50%).

Based on the findings and experimental observations on the fracture energy test results, which underestimate fracture resistance at certain testing temperatures, this research was extended to critically investigate the suitability for the semi-circular bend (SCB) test protocol to evaluate the fracture resistance of asphalt mixtures. By applying fracture mechanistic theories, some test procedures were modified to ensure measurement is the toughness, which better represents fracture resistance of the material. Fracture toughness tests performed on asphalt mixtures containing 30, 40, and 50% RAP reveal their fracture resistance changes with varying temperatures. None of the asphalt mixtures evaluated in this research preserves its own advantage for the entire temperature range from -30 to -10°C. The toughness of traditionally

batched mixtures is generally larger than the fractionated prepared mixtures. However, a statistically significant difference is not detected.

Moreover, asphalt mixture beam fatigue and binder fatigue tests (time-sweep test) were performed as well. The RAP materials evaluated in beam fatigue and binder fatigue tests were different from the RAP materials utilized in the fracture experiments. Beam fatigue samples also underwent free-thaw cycling treatments for evaluation. Rather than based solely on S-N_f curves to illustrate the fatigue performance, the beam fatigue test data were analyzed through a dissipated energy approach. Basically, the 40% RAP materials were weaker than those with 30 and 50% RAP. Furthermore, traditional RAP mixes exhibit better fatigue resistance than the fractionated mixes. From the morphology aspects, the binder's phase separation and physical hardening effects could explain the faster fatigue degradation of the 40% RAP binder and beam mixture subjected to the repeated loading.

CHAPTER 1. GENERAL INTRODUCTION

Background

Reclaimed asphalt material technology has been applied in the United States for more than 30 years, and there is a tendency for many owner agencies to utilize more reclaimed asphalt materials (RAP) by increasing the RAP percentage. This increasing RAP utilization is and will continue to be driven by historically high asphalt binder prices, high quality aggregates existing in pavement rehabilitation projects, and increasing awareness of environmental stewardship and sustainability issues.

From the application perspective, one of the challenges of the mix design process for using a high percentage of RAP in the United States is to meet the volumetric mix design criteria. Often volumetric criteria, such as voids in the mineral aggregate (VMA) and film thickness, are intended to ensure sufficient asphalt binder coating of the aggregate structure and sound performances. However, a large amount of fine materials introduced into an asphalt mix via RAP often makes volumetric criteria, including film thickness requirements, difficult to achieve (State agency specification, e.g. Iowa Department of Transportation Specifications). To address this issue, two RAP addition methods (Traditional and Fractionated) were designed. The only difference between these two mix procedures is the fractionated method removes a portion of fine RAP materials passing the No. 30 sieve (0.6mm), so the RAP materials remaining on and above the No. 30 sieve could be used to add to the HMA mixtures. This sieve size could be adjusted depending on the design purpose and the RAP gradation. By removing more fine RAP materials, the Fractional RAP addition method was proposed to address the film thickness design criteria. Determining the distribution of fine aggregates in RAP stockpiles, asphalt

mixture design and volumetric properties variation with changing RAP content were accomplished as the first stage of this research work at the University of Iowa. The resulting analysis showed this fractionated addition method had positive, but limited effects on increasing film thickness of asphalt mixtures (Shannon, 2012).

From the serviceability perspective, when applying recycled asphalt technology in a flexible pavement project, most of the concerns for applying RAP are related to low-temperature fracture and fatigue cracking, considering the stiffness of the asphalt mixture can dramatically increase through introducing RAP (McDaniel et al., 2000). Evaluating the outcome of adding RAP in three different percentages (30, 40, and 50%), based on the mechanical properties of the mixture, and examining the aged material (RAP binder) blended binder properties were completed as the second stage at Iowa State University. In this research, two types of RAP materials from different resource were utilized for fracture tests and fatigue tests, separately.

Objective and Scope of Research

The original objective of this study was to investigate the feasibility of using reclaimed asphalt materials up to more than 25% of the total weight of the mix. The evaluated asphalt mixture was targeted to contain the amount of RAP to provide 30, 40, and 50% RAP binder replacement. Rather than rely on volumetric properties alone, evaluations were based upon the performances of low-temperature fracture and fatigue cracking resistance of asphalt mixture, and binder properties.

Two tasks were accomplished for this research work. The first task was to design and assemble a rotary evaporator system to extract the aged binder from RAP without extensive aging. Thus, extracted binder can be obtained for sequence tests to evaluate physical properties. Second, the specimen jig (supporting frame) of the semi-circular bend (SCB) test was designed and fabricated, as well as the SCB testing software was programed following the proposed American Association of State Highway and Transportation Officials (AASHTO) test protocol. Thus, fracture experiments can be applied to estimate the fracture resistance of asphalt mixtures.

Both convenient fracture energy, G_f, and the toughness, K_C, test were utilized to quantify the influence by adding RAP in varying percentages and the effects introduced by applying different RAP addition methods on asphalt materials' fracture resistance. Variations of experimental measurements with different specimen geometries were discussed. After identifying the limitations of the original SCB (G_f and K_C) test application, a new test procedure and two data analysis methods were proposed.

Additionally, the asphalt mixture beam fatigue and binder fatigue tests (binder fatigue test) were performed. Normally, examining the traditional S-N_f fatigue curve is used to illustrate mix fatigue testing results. In this project, the beam fatigue test data were analyzed through a dissipated energy approach. Compared with normal performance grading evaluations for asphalt binder, a time-sweep test providing a better indicator of expected fatigue performance of mixes rather than the loss modulus G" was implemented.

Organization of Dissertation

This dissertation is organized as follows:

Chapter 2 is a review of the current state of the practice for SCB testing, which demonstrates the application's limitations. In Chapter 3, a development of the modified semi-circular bending test and data analysis methods, based on the fracture mechanics approach is presented. Chapter 4 outlines the application of the modified semi-circular bending test to asphalt mixtures containing high percentage RAP materials and

Chapter 5 is an evaluation of fatigue resistance of asphalt mixtures and binders containing RAP materials.

Chapter 6 presents conclusions for this study, limitations and suggestions for SCB and fatigue test specifications, and recommendations for further research.

References

Iowa DOT Standard Specifications, 2012. Section 2303. *Hot Mix Asphalt Mixtures.*

Shannon, C.P., 2012. Fractionation of recycled asphalt pavement materials: improvement of volumetric mix design criteria for High-RAP content surface mixtures. *Master's thesis,* University of Iowa.

McDaniel, S.R., Soleymani, H., Anderson, R.Mj., Turner, P., and Peterson, R., Oct. 2000. Recommended use of reclaimed asphalt pavement in the superpave mix design method. *National Cooperative Highway Research Program, Washington,* D.C.

CHAPTER 2. RECONSIDERATION OF THE SEMI CIRCULAR BENDING (SCB) FRACTURE ENERGY TEST FOR EVALUATING ASPHALT MIXTURES

A paper to be submitted to ASCE Journal of Materials in Civil Engineering as a Technical Note

Sheng Tang and R. Christopher Williams

Abstract

Researchers have prevalently used the semi-circular bending (SCB) fracture energy test to evaluate fracture resistance for asphalt pavement materials at low temperatures. A number of papers have been published, based on this testing method and subsequent analysis of measurements, including fracture energy, stiffness, peak load, and stress intensity factor (Mull et al. 2002, Wu et al. 2005, Shu et al. 2008, Li and Marasteanu 2010). However, under certain temperature and specimen geometry conditions, these measured parameters can be inappropriately employed, and lead to incorrect conclusions. The correct application of the current fracture energy test is very much limited by SCB sample sizes and testing temperatures. New and applicable SCB test procedures providing toughness measurements with a wider application range should be developed. More rigorous fracture mechanics-based approaches are necessary, and should be adopted to better analyze the SCB test data.

In reference to fracture mechanic theories and existing American Society for Testing and Materials (ASTM) fracture toughness test procedures, the peak load is insufficient to assess fracture resistance of asphalt mixtures, because of its extensive variability and miscorrelation with fracture toughness. The experimentally measured K value is not appropriate to evaluate

fracture resistance for tests at sufficiently high temperatures. Moreover, the simple measurement of the fracture energy is also inaccurate to evaluate asphalt mixtures at temperatures when the material deforms more in an elastic–plastic manner. After identifying the limitations of the current SCB fracture energy test, an applicable fracture toughness test should be developed with a wider application range. This SCB toughness test suitable for asphalt mixtures may be adopted, based upon Begley and Landes' paper (1972) and ASTM E1820.

Introduction

In the asphalt research field, the "SCB test" is a general term to broadly define a series of three-point bending tests using semi-circular geometry based specimens with a single notch on one edge. A simplified SCB loading setup with a specimen is shown in Figure 1.

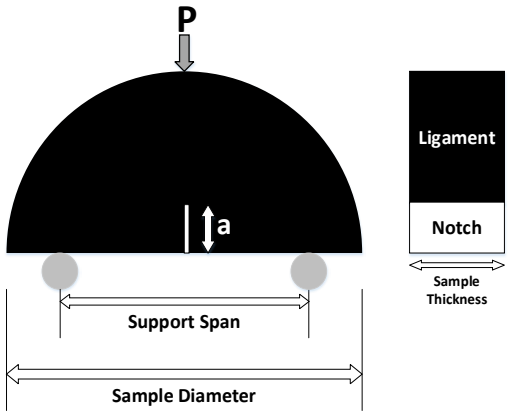

Figure 1. Simplified SCB loading setup with a specimen

Different labs and institutions use varying test procedures, devices, loading methods and sample sizes. Generally, four parameters obtained from different SCB tests are commonly utilized by asphalt researchers to evaluate fracture resistance—fracture energy (G_f), peak load, stress intensity factor (K) and J-integral. Based upon fracture mechanics theories, all current

SCB test procedures implemented in asphalt research field can be classified into two catalogs: (1) the SCB fracture energy, G_f, test and (2) the SCB fracture toughness test. (The reason for the conventional calculated fracture energy, G_f, to be independently listed from toughness and its correct interpretation will be explained after a review on the basics of fracture mechanics.) Moreover, because of the complexity of asphalt materials involving temperature-sensitive rheological properties, the binder's viscoelastic property, and the mixture's composite material property, the fracture toughness parameters should be carefully selected to analyze asphalt mixture fracture mechanical properties as well.

This paper first reviews the elements of fracture mechanics and then discusses the differences between the SCB fracture energy with SCB fracture toughness test. Finally, analysis of different fracture resistance parameters (conveniently estimated fracture energy G_f, peak load, stress intensity factor K, and J-integral toughness) is achieved to investigate their effectiveness and suitability for applications to evaluate asphalt mixtures at low temperatures.

Elements of Fracture Mechanics

Fracture mechanics is a field which, in part, focuses on the study of crack initiation and propagation in different materials. It provides a series of tests and analysis methods to capture the physical parameters describing materials' resistance to fracture (e.g. fracture toughness), which can be further used in the engineering design and material selection.

Generally, three critical experimental measurements—(1) stress intensity factor K_C, (2) energy release rate G_C or J-integral (J_C), and (3) Crack-Tip Opening Displacement (CTOD (δ_C))—can be commonly used to assess fracture toughness (ASTM 1823), based on three

different perspectives. K_C is based on stress intensity, G_C and J_C are established from the energy release and consumption concepts, respectively, and the CTOD (δ_C) is grounded in the correlation between fracture resistances with crack tip geometry.

Correctly selecting the appropriate fracture toughness parameter is the key to properly analyze and evaluate the fracture resistance of the interested materials. This selection should depend upon material's mechanical behavior (linear elastic or elastic-plastic) and the size of the fracture process zone (small or large). The differences and applications of fracture toughness are described in the following sections.

Griffith Theory and Surface Energy

The origin of fracture mechanics dates back to early 1920s, when Griffith correlated between the strength of glass and the size of a pre-existing crack through an energy approach (Griffith 1921). The surface energy is the energy needed to create a unit area of a new element. More specifically, it is the energy that purely separates two atomic layers without moving and rearranging those adjacent atoms. For a large plate containing a center crack with length $2a$, the strength σ_c is related to the surface energy γ and Young's modulus E as

$$\sigma_c\sqrt{a} = \sqrt{\frac{2\gamma E}{\pi}} \ . \qquad \text{(equation 1)}$$

The letter γ represents the surface energy and E denotes Young's modulus of the material. This equation shows strength depends upon crack size. Because different samples have varying crack sizes, the fracture strength is not a material property. The measured strength can have notable scatter in the experimental data. If the strength-based design philosophy is applied, the defect size in the material must be addressed carefully.

The practice of modeling fracture cracking with surface energy is theoretically correct, based on Griffith's theory, if very brittle materials, such as glass, are tested. On the other hand, surface energy has its application limitations for ductile materials, since the energy needed to break the atomic bonds is only a very small portion of the total energy to create cracking, such as an asphalt mixture's fracture at intermediate temperatures. Later, Irwin and Rice (Irwin 1956, Rice 1968) developed two other fracture parameters, still utilizing the energy concept "energy release rate G" and "J-integral," respectively.

In the asphalt materials research field, the surface energy concept is rarely utilized to model the abrupt failure of asphalt pavement (fast fracture) at low temperatures. However, the surface energy concept has been widely used in micromechanical models to predict *fatigue* cracking and healing behaviors of asphalt mixtures (Little et al., 1997, 1999, Cheng et al., 2002, Kim 2009). The surface energy covering many common asphalt binders, such as AAD and AAM, and several types of aggregates have been experimentally evaluated. From a microscopic point of view, the atoms on a sample's surface are at a higher energy level than the atoms in the center of an element, in which case the entire element could be held and clamped together as one piece and, thus retained from collapsing. From this point of view, surface energy is intuitively correlated with a material's healing ability against fatigue cracking.

Energy Release Rate

In the 1940s, researches following Griffith's theory agreed with the experimental observations of brittle materials. However, researches disagreed with the observations based upon ductile materials. Both fracture and surface energy tests utilizing steel were performed.

The fracture test showed $\pi \frac{{\sigma_c}^2}{E} a$ was nearly 100kJ/m^2. Surface energy was only about 1 kJ/m^2. Based upon Griffith's theory, they should equal following equation,

$$\pi \frac{{\sigma_c}^2}{E} a = 2\gamma \ . \qquad \text{(equation 2)}$$

The left side $\pi \frac{{\sigma_c}^2}{E} a$, is much more than two times the surface energy for steel, which means the input energy from loading is more than the surface energy required to create a new surface by cracking. This additional energy must be consumed somewhere else, considering energy conservation theory. Later, Irwin (1948) and Orowan (1948) independently developed a similar equation,

$$\pi \frac{{\sigma_c}^2}{E} a = \Gamma \ , \qquad \text{(equation 3)}$$

to define fracture toughness (Γ), and created a new loading parameter, G, termed energy release rate. This was the first time "fracture toughness" was utilized. The energy release rate is also referred to as "crack-extension force" and notation uses the same letter. Energy release rate is the elastic energy reduction per unit area, associated with crack extensions,

$$G = \frac{\partial U}{\partial A} \ , \qquad \text{(equation 4)}$$

where ∂U is the change in elastic energy and ∂A is the cracking area.

The critical G value (G_C) obtained prior to fracture instability is fracture toughness, Γ. The relationship between G and Γ is analogous to the relationship between stress and strength. However, the critical G value (G_C) is interchangeably used with fracture toughness, Γ, in many textbooks and other documents. Additionally, if *fracture energy* is defined as the energy

consumption required to create a unit surface area of a crack, it quantitatively equals to the average number of critical energy release rates obtained between certain crack extension.

As shown in Figure 2(a) from Griffith's picture of fracture, *fracture energy* equals the energy needed for atomic bond breaking (surface energy) used for brittle materials like glass. Figure 1(b) shows Irwin and Orowan's representation of fracture (Irwin, 1948; Orowan, 1948). *Fracture energy* is the surface energy plus the plastic deformation work and

$$\Gamma = 2\gamma + W_p \ . \qquad \text{(equation 5)}$$

In this way, the energy concept built for fracture mechanics is extended and can be applied to ductile materials under the small scale yielding condition. Furthermore, a J-integral proposed by Rice in 1968 extended the energy concept further to ductile materials under the large scale yielding condition (Rice 1968).

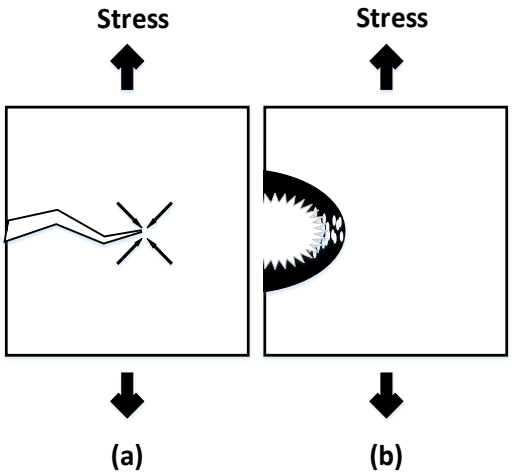

Figure 2. Provoked areas for (a) brittle and (b) ductile materials

Besides utilizing the energy concept (surface energy, energy release rate or J-integral) to interpret fracture mechanics, two other parameters are broadly utilized as well. One

parameter is the stress intensity factor (K), and the other one is crack tip opening displacement (CTOD).

Stress Intensity Factor (K)

A loading parameter, stress intensity factor (K), is employed to calculate local stress and describes the stress field around a crack tip. The critical (maximum) value for the stress intensity factor determines the fracture toughness, K_C. The relationship between the loading parameter (K) and the material property (K_C) is similar to the relationship between stress and strength. Roman numeral subscripts indicate the mode of fracture illustrated in Figure 3 (Anderson 1991).

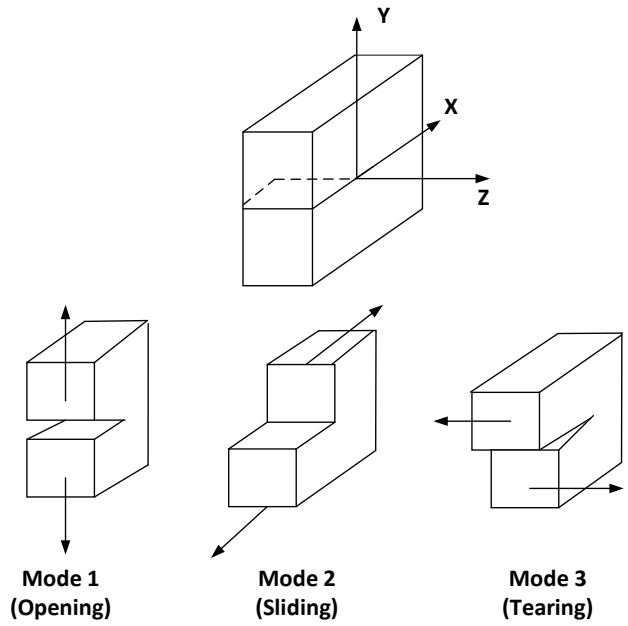

Figure 3. Fracture loading mode (Anderson 1991)

Mode I opening fracture is the condition in which the crack plane is normal to the direction of the largest tensile loading. This is the most commonly encountered mode. Modes II and III are defined as sliding and tearing, respectively. Thus, K_I represents the stress

intensity factor dominating around the crack tip for the material under the open loading condition, and it can be expressed as

$$K_I = \sigma\beta\sqrt{\pi a}\ , \qquad \text{(equation 6)}$$

where K_I is the calculated parameter, depending upon the applied remote stress (σ), crack length (a), and specimen component geometry factor (β). The remote stress is the global stress applied on the outside boundary of the subject. It is different from the local stress used to describe the stress conditions around the crack tip. When the fracture phenomenon occurs, the local stress around the crack tip field can be much larger than the remote stress applied on the subject. This can explain why some objects with small and sharp cracks are broken under the load (remote) much smaller than the material's yield strength. β is a dimensionless factor and corresponds with the shape of the testing specimen and crack length, a.

Figure 4 illustrates an infinite wide elastic plate containing a crack of length $2a$ (Anderson 1991). The plate is subjected to a tensile remote stress far from the crack opening. The local stress for any point (r, ɵ) near the crack tip can be provided by the following equations (Irwin 1957),

$$\sigma_x = \frac{K}{\sqrt{2\pi r}} cos\frac{\theta}{2}\left(1 - sin\frac{\theta}{2} sin\frac{3\theta}{2}\right), \qquad \text{(equation 7)}$$

$$\sigma_y = \frac{K}{\sqrt{2\pi r}} cos\frac{\theta}{2}\left(1 + sin\frac{\theta}{2} sin\frac{3\theta}{2}\right), \text{and} \qquad \text{(equation 8)}$$

$$\sigma_{xy} = \frac{K}{\sqrt{2\pi r}} sin\frac{\theta}{2}\left(cos\frac{\theta}{2} cos\frac{3\theta}{2}\right). \qquad \text{(equation 9)}$$

r is the distance between the point and the crack tip, and the value of the K factor can be calculated from equation $K_I = \sigma\beta\sqrt{\pi a}$. The three local stress equations above demonstrate

how the materials near the crack tip respond to remote stress, σ. If the stress intensity factor (K) becomes larger, the stress near the crack tip will dramatically increase as well. The factor K depends upon the size of the crack, the sharpness of the crack, and remote loading. The stress intensity factor quantifies the amplification effects of global stress. This amplification makes the local stress near the crack tip beyond the yielding strength of the material and then leads the crack to initiate and propagate.

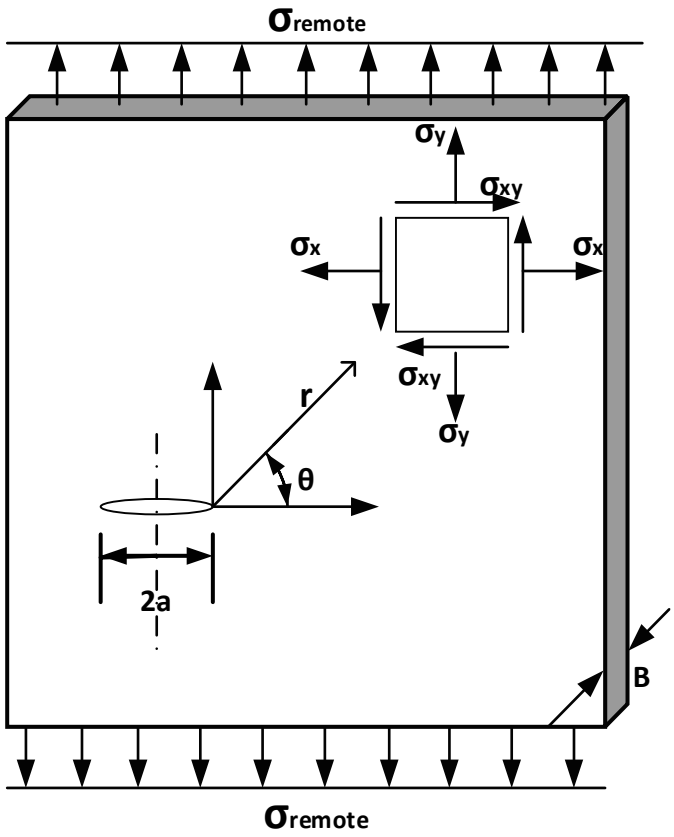

Figure 4. Infinite elastic plate with a central crack (Anderson 1991)

Fracture toughness, K_C, is determined by a test method taking values at the onset of fracture instability. Therefore, the material property, K_C, is a point value. The notch tip sharpness and the homogeneity of the material play a significant role to affect the test results.

Thus, sample pretreatments and special data selection methods are required. ASTM E399, E561, and E1820 describe the standard testing methods for obtaining the stable K_{IC} and K–R curve for materials under a small scale yielding condition.

Small Scale Yielding

Linear elastic fracture mechanics (LEFM) applies the theory of linear elasticity to model the phenomenon of fracture propagation, if the material mainly demonstrates linear elasticity. Only when the small-scale yielding condition is satisfied can the problem be solved by applying LEFM. The small-scale yielding condition is satisfied when the size of the fracture process zone (FPZ) is much smaller than the external boundary zone (Figure 5). The external boundary zone includes all the geometries of the test specimen as well as the preexisting crack size. Under the small-scale yielding condition, most of the specimen deforms elastically. When the FPZ is much smaller than the size of the other geometries under small-scale yielding, which provides sufficient space for cracking extension, the fracture resistance can attain a steady state determinately. Generally, the scale difference should be at least one order of magnitude to ensure the small scale condition.

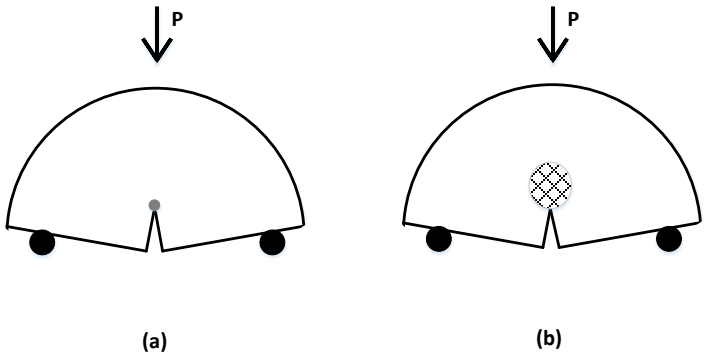

Figure 5. Process zone size for (a) small and (b) large scale yielding SCB samples

To assess the process zone size, two criteria were established, based on the material deformation behavior. For brittle glass and ceramic materials, the fracture process mostly involves only the atom bond breaking. Therefore, the fracture process zone encloses the bond-breaking atoms. The FPZ is usually a nanometer scale. For ductile materials, the fracture process not only breaks the atom level bonds, but also includes the rearrangement of the adjacent atoms around the crack tip. This rearrangement facilitates a certain amount of materials around the cracking surface to undergo plastic deformation. Under this situation, the fracture process zone should enclose the plastic zone around the tip. The FPZ ranges from the millimeter to centimeter scale. When the FPZ reaches the centimeter level scale, to satisfy the small scale yielding condition, the specimen must be meters in size. Thus, it can be very expensive to attain experimentally.

Most tests that meet the small scale yielding condition often use K_C to define fracture toughness. Surface energy and critical energy release rate (Gc) can be selected as well. However, beyond the LEFM, when the small scale yielding condition cannot be satisfied, the elastic-plastic fracture parameters should be used—J-integral and CTOD.

Fracture Parameter in Terms of J-integral

The J-integral is a mathematical expression. It is a line or surface integral that encloses the cracking front from one crack surface to the other, used to characterize the local stress-strain field around the crack front (ASTM E1820). The basic relationship is

$$J = \int_{\Gamma} w d_y - T \frac{\partial U}{\partial x} d_s \ . \qquad \text{(equation 10)}$$

Γ is the curve that surrounds the crack-tip, T is the traction vector, U is the displacement vector, ds is a length increment along the curve Γ, w is the strain energy density, x direction is as same as the crack line, and the y direction is taken normal to the crack line (Anderson 1991). The J-integral concept proposed by Rice in 1968 provides a mathematical equation to calculate the potential energy difference between two identically loaded bodies with neighboring crack sizes (Rice 1968). Based on this equation, the energy balance concept for fracture mechanics can be extended from linear elastic behavior to elastic-plastic behavior. From a practical engineering perspective, J-integral represents, similarly to G (elastic energy release rate), an elastic-plastic energy release rate. This is related to the area under the load displacement curve divided by the advanced cracking length for specimen with unit thickness, (Begley and Landes 1972). J-integral as the energy changing rate is given by

$$J = -\frac{1}{B}\left(\frac{\partial U}{\partial a}\right)_{\Delta} = -\left(\frac{\partial U}{\partial A}\right)_{\Delta}, \qquad \text{(equation 11)}$$

where U is the strain energy, B is the specimen thickness, and a is the length of cracking extension. Thus, A represents the cracking area. Note, "U" is different from U when introducing the energy release rate, even though both are in the same format. U in the elastic energy release rate refers to the elastic energy and is 100% recoverable. U in the J-integral has a broader definition and is the strain energy, regardless whether the energy comes from plastic or elastic deformations. The Δ suffix means the derivative is taken at a certain load-line displacement.

The critical J_C value can be determined experimentally from load displacement tests. Begley and Landes (1972) first described an experimental method to evaluate J_C toughness for

type I fracture by using multiple specimens with varying crack lengths. ASTM standards E813, E1152, E1737, and E1820 provide testing procedures for obtaining J_{IC} and the J R-curve.

Fracture Parameter in Terms of δ (CTOD)

CTOD (δ) is a crack tip opening displacement due to elastic and plastic deformation at various defined locations near the original crack tip (Figure 6 (a)). Those various defined locations are shown in Figure 6 (b) (Anderson 1991).

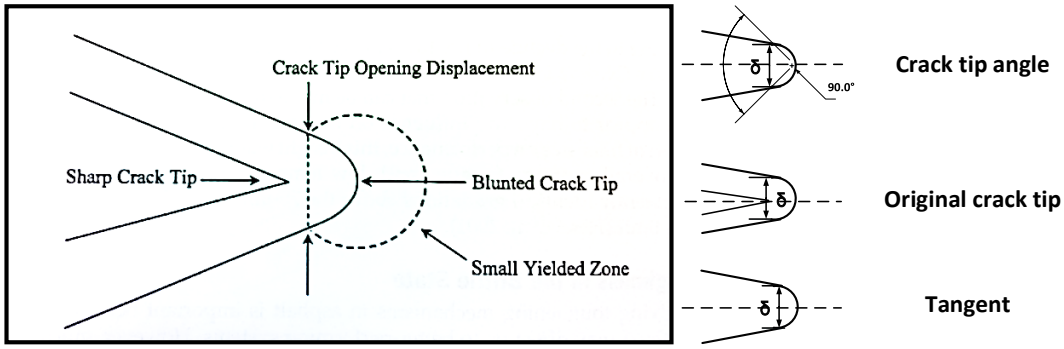

Figure 6. CTOD (δ) the crack displacement near the crack tip region (Anderson 1991)

Wells (1961) did early research on CTOD applications in structural steel, where small scale yielding was difficult to achieve, simply because the experiments under small scale yielding required sample sizes in meters scale level for steel. It is easy to determine steel in meters long, but difficult in meters wide. Thus, it is inadequate to apply LEFM theories. Then Wells defined a new parameter, "the crack opening displacement (δ) of a blunted crack", and proposed this crack-tip characteristic could be used to quantify a material's toughness (Wells 1961). ASTM E1290 and E1820 describe the testing procedures and data analysis methods.

Generally, the measured CTOD (δ) is positively proportional to the material's fracture toughness. Therefore a larger blunting of the crack tip, a larger plastic yielding zone, and a bigger δ value will be observed. On the contrary, the sharper the crack tip, the smaller plastic yielding zone and results in a smaller δ value. This model explains the significant importance of the crack tip shape. Thus, it should be understood why the ASTM testing standards require a fatigue pre-cracking treatment procedure *before* measuring a material's toughness.

Fracture Toughness in Terms of K_C,G_C,J_C, and δ_C

Within fracture mechanics, the criteria for fracture instability are when the loading parameters K, G, J-integral, or CTOD reach beyond their critical values—fracture toughness. When it reaches the critical condition, the original length of the crack becomes unfavorable and starts advancing. Fracture toughness is the material's property and can be expressed in terms of K_C, G_C, J_C, and δ_C. Usually, Γ is often used to represent G_C. Most materials under small scale yielding often use K_C to define fracture toughness.

Under linear elastic fracture mechanics, all fracture toughness parameters are interrelated (Begley and Landes 1972). Under plane-strain conditions with type I mode loading, the relationship can be shown as

$$G_C = J_C = \frac{1-v^2}{E} K_C^2 = \delta_C \sigma_Y \,, \qquad \text{(equation 12)}$$

where v is Poisson's ratio.

Beyond the LEFM, when the small scale yielding condition cannot be met, the validation for applying fracture parameters is summarized in Table 1. Elastic-plastic fracture mechanics (EPFM) is developed to solve the problem with large scale yielding. Without estimating the

plastic zone size and checking the small yielding condition, any conclusions for fracture resistance comparisons generated, based upon K or G, are inappropriate.

Depending on the material's properties of the testing sample, toughness parameters, and testing procedures, even the data analysis methods should be appropriately selected to obtain the appropriate fracture toughness. For low-strength and high-toughness materials like soft and ductile asphalt mixtures subjected to an intermediate temperature environment, toughness should be characterized by parameter J-integral or CTOD (Zhu and Joyce 2012). It is inappropriate to utilize K or G to describe an asphalt mixture's behavior at relative high temperatures. On other hand, all toughness parameters can be applied to assess an asphalt mixture's performance when specimens are tested at very low temperatures, such as -25°C or below the glass transition temperature of the asphalt binder utilized in the mixture.

Table 1. Summary of application range for theories and fracture parameters

Theories and Measurements		Surface energy	Stress Intensity Factor	Elastice Energy Release Rate	J Integral	Open Displacement
Fracture Mechics	Deformation scale	Griffith Theory	K	G	J	CTOD
LEFM	Brittle					
	Small scale					
EPFM	Large scale					

Fracture Mechanics Applied to Asphalt Mixtures

The Current SCB Fracture Energy Test and Its Fracture Parameters

Although the SCB fracture energy test has not been accepted in the ASTM standard, its protocol can be found on InTrans website under AMPP. One important feature for this fracture energy test is all specimens only require preparation with one notch size. This one notch size

feature beneficially makes the test convenient, but also limits its application to ductile materials, such as asphalt mixtures at certain temperature ranges. In contrast, the regular fracture toughness test (Not ASTM) for ductile materials requires multiple samples with varying notch sizes (Begley and Landes 1972). As shown by the following results and discussion, the regular fracture toughness test should be applied to better evaluate the fracture resistances of asphalt mixtures.

The obtained load displacement data from SCB fracture energy test is utilized to estimate fracture energy. A conventional formula is commonly applied by researchers in civil engineering field (Li and Marasteanu 2004, 2010),

$$G_f = \frac{W_f}{A_{lig}}\ , \qquad \text{(equation 13)}$$

where

$G_f = fracture\ energy\ (J/m^2)$,

$W_f = work\ of\ fracture\ (J)$;

$W_f = \int P du$,

$P = applied\ load\ (N)$,

$u = average\ load\ line\ displacement\ (m)$,

$A_{lig} = ligament\ area\ (m^2)$;

$A_{lig} = (r - a) \times t$,

$r = specimen\ radius\ (m)$,

$a = notch\ length\ (m)$, and

$t = speciment\ thickness\ (m)$.

The calculated fracture energy with this conventional formula can at best serve as an order-of-magnitude estimator, as the result is specimen dependent and is actually not the

fracture energy of the material. In fracture mechanics, fracture energy is defined as the energy consumption required to create a unit surface area of a crack. In the SCB test at sufficient low temperatures, the work done by the load P is mainly stored as elastic strain energy prior to fracture (neglecting the viscous dissipation of the material). Upon fracture, the energy is dissipated through propagating the crack and irreversibly deforming the material, and partly converted to kinetic energy. The crack propagation in asphalt mixtures is usually unstable at the testing temperatures below -20°C, thus the kinetic energy may not be neglected. In the SCB test at sufficient high temperatures, the work done by the load P is partly converted to thermal energy dissipated through viscous dissipation. Thus, the thermal energy may not be neglected.

As reviewed in previous sections, the facture mechanics defining fracture energy equals the average value of critical energy release rates between certain crack extensions,

$$G_f = \overline{G_C} \quad \text{and} \quad G_c = -\frac{\partial U}{B\partial a}\Big|_{P_{max}} . \qquad \text{(equation 14)}$$

A comparison between these two equations suggests only when the critical energy release rate, G_C, is independent of crack length, a, the conventional formula, $\frac{W_f}{A_{lig}}$, may provide a good (sample geometry independent) estimation (neglecting the other energy dissipations).

Additionally, one fracture toughness parameter, K_{IC} (the maximum value of K_I), based on the equation shown below is commonly calculated as a secondary parameter when conducting fracture energy tests, since the peak load is recorded. The estimated fracture toughness at the onset of crack extension is calculated by directly substituting the peak loading

P_{max}. The approximate stress intensity factor is given by (Lim et al. 1993; Li and Marasteanu. 2004),

$$K_I = \frac{P}{2rt}\sqrt{\pi a}\left\{4.782 + 1.219\left(\frac{a}{r}\right) + 0.063\, exp\left[7.045\left(\frac{a}{r}\right)\right]\right\} \quad \text{(equation 15)}$$

,

where

$P = \ applied\ load\ (N)$,

$r = specimen\ radius\ (m)$,

$t = specimen\ thickness(m)$, and

$a = notch\ length\ (m)$.

Reconsideration of SCB Fracture Energy Test Practice

The Limitations of G_f Fracture Energy

Before presenting the limitations for applying the SCB fracture energy protocol with a conventional estimation, exanimating a gradual process of a crack development can addressed first. Then, the disadvantage of applying the conventional fracture energy test procedure and calculation method becomes evident.

Consider a general fracture process in different states as illustrated in Figure 7 with a preexisting crack, a_0. The complete crack propagation process could be divided into three segments—A, B, and C. Frame 1 includes two fracture states from crack initiation to the beginning of crack steady extension. When applying a small load, a small region of the material around the crack tip starts to yield, which creates the fracture processing zone (FPZ), while the crack is still arrested at original length a_0. With an increasing loading, the plastic zone grows.

When the loading parameter (K, G, J-integral or δ) finally becomes excessive of the material's fracture toughness (K_C, G_C (Γ), J_C, or δ_C), the crack initiates and starts to advance. After the crack extends an additional crack bridging distance (Lss), it approaches a steady cracking state and continues to develop, where frame 2 starts. The average energy used to create a crack extension in the "A" section, representing the crack initiation state to the onset of steady crack extension, is less than or equal to the "B" section for a steady-state cracking. At the time in the "B" section, the crack has the largest FPZ and the FPZ moves farther right with the crack's extension. Along with crack advancing, the adjacent materials of crack tip subject to plastic deformations. However, when the crack advances to the extremely right side (free boundary), unfortunately there is no material that can be affected, as shown by the dash line in frame 3 in Figure 7. Thus, the energy consumption per additional cracking length in section "C" is less than the "B" or "A" section. The object addressed here is for a crack at different states, the energy cost per unit crack distance is different for the material with the large scale yielding deformation. Moreover, not only the energy consumption rate is dependent on crack advancing distances, but also is affected by the sample geometry constraint when the crack approaches the specimen's boundary (Hu and Wittmann 2000, Hu 2002, Duan et al. 2003, Hu and Duan 2010, Yang et al. 2011). Yang et al. (2011) tested concrete materials and illustrated a measured local fracture energy (g_f) changing along the ligament of a specimen as shown in Figure 8. The g_f defined by Yang actually is the strain energy released rate. Figure 8 shows the fracture energy is dependent on crack distance and affected by the sample boundary. Under this situation, the conventional calculation for G_f is *not* a good estimator for fracture toughness.

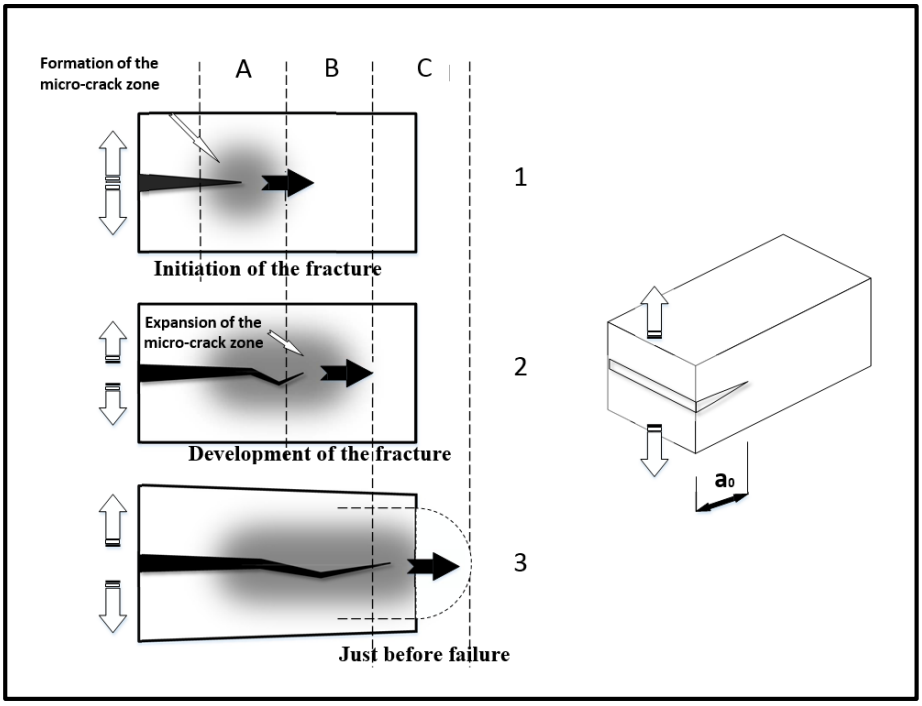

Figure 7. General cracking process

The SCB fracture energy test protocol uses the conventional average method to estimate the critical energy release rate (point value) ,$\frac{\partial U}{B\partial a}$, in section B by utilizing the total energy and dividing by the product of the entire crack advancing distance from A through C (Figure 7) with sample thickness. The G_f value provided by fracture energy test is the average number of energy consumptions per additional cracking length at sections A, B, and C. If the specimen is sufficiently large to provide a relatively "long" section B or the FPZ is extremely small (small scale yielding, linear elastic deformations, brittle material), the G_f, calculated by $\frac{W_f}{A_{lig}}$, can be very close to the value $\frac{\partial U}{B\partial a}$ in section B (if neglect the other energy dissipations). For this condition, the conveniently calculated fracture energy can be used to estimate fracture toughness for stable cracking and the G_f value is almost independent upon notch sizes.

However, when the overall sample size is small with a deep notch or the FPZ is relatively large (large scale yielding, nonlinear plastic deformation, ductile material), then sections A and C dominate the fracture process. The conventional calculation of G_f could underestimate fracture toughness dramatically, since the value of $\frac{\partial U}{B\partial a}$ at section A and C is smaller than the values at B. For this reason, the size effect of the SCB fracture energy test varies with notch depth and the height of the specimen. Thus, G_f is defined as fracture energy rather than fracture toughness. By testing the same materials under identical testing environments, larger notch size results in smaller G_f values.

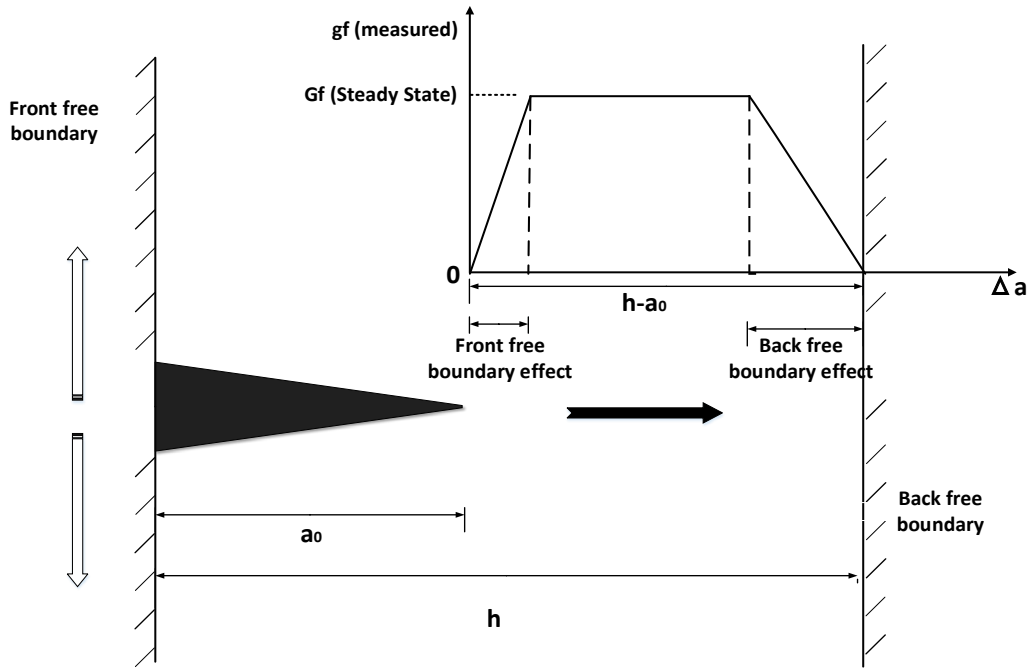

Figure 8. Fracture energy changing along the ligament of a specimen (Yang et al. 2011)

Notch size effects on SCB fracture energy test has been observed by other researchers (Li and Marasteanu 2010) with test results summarized in Table 2. Based upon test results (Li and Marasteanu 2010) illustrated in Figure 9, it is clear all conveniently calculated fracture

energy G_f values converge at -30°C, when the asphalt mixtures are brittle and the small scale yielding conditions are met. All estimated fracture energy G_f values obtained from samples with varying notch sizes agree well with each other. However, with increasing test temperatures, the asphalt mixture becomes more ductile and can sustain large-scale yielding. Then, the test results begin to diversify dramatically for samples with different notch sizes. A larger notch size sample results in smaller G_f values (Table 2). Thus, it is no longer suitable to evaluate fracture toughness for asphalt mixtures at temperatures above approximately -24°C. The conveniently calculated fracture energy depends upon the specimen geometry and size experimentally, and the relatively high temperature test is of limited benefit.

Table 2. Results for samples with varying notch sizes (Li and Marasteanu, 2010)

Test Temp	-6 °C	-18 °C	-30 °C	-6 °C	-18 °C	-30 °C
Notch Length (mm)	Fracture Energy (J/m^2)			Peak Loading (kN)		
5	1488	660	308	2.15	2.72	2.81
15	822	425	303	1.38	2.65	2.96
30	537	471	254	0.64	1.56	1.48

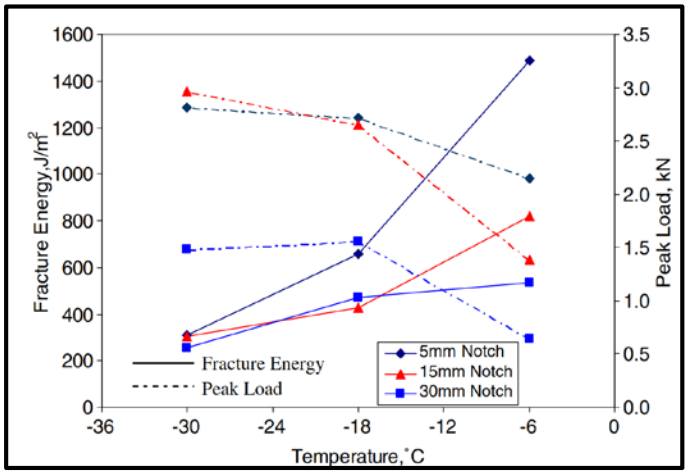

Figure 9. Fracture energy for samples with varying notch sizes (Li and Marasteanu, 2010)

Moreover, the testing data obtained at -6 and -30°C from Li and Marasteanu (2010) (Table 2) can be replotted as shown in Figure 10. The total work is represented on the y-axis, which is the product of estimated fracture energy (G_f) with crack advancing distance and sample thickness. The x-axis is the crack advancing distance obtained by using a 75mm sample radius minus the notch length. Obviously, the total energy consumption for the fracture has a nonlinear relationship with crack propagation at -6°C in Figure 10 (a), but a linear relationship at -30°C in Figure 10 (b). The conventional calculation of the fracture energy, G_f, is actually the slope of the blue lines divided by sample thickness, which connects the black point with the original point. However, based on the concept of toughness is a function describing the total strain energy changing per crack advancing distance and divided by sample thickness ($\frac{\partial U}{B\partial a}$), material toughness actually is the slope of points on the best fit line(as shown in green in Figure 10) divided by sample thickness. Comparing plots (a) and (b) in Figure 10, it shows why conveniently calculated G_f does a fair estimation of toughness for testing at very low temperatures where material is very brittle, but underestimates fracture toughness when the material is ductile and the small scale yielding condition is not satisfied. By further calculating testing data from Li, toughness values can be obtained and Figure 11 illustrates and compares the values of conventional calculated G_f and the estimated J-integral toughness.

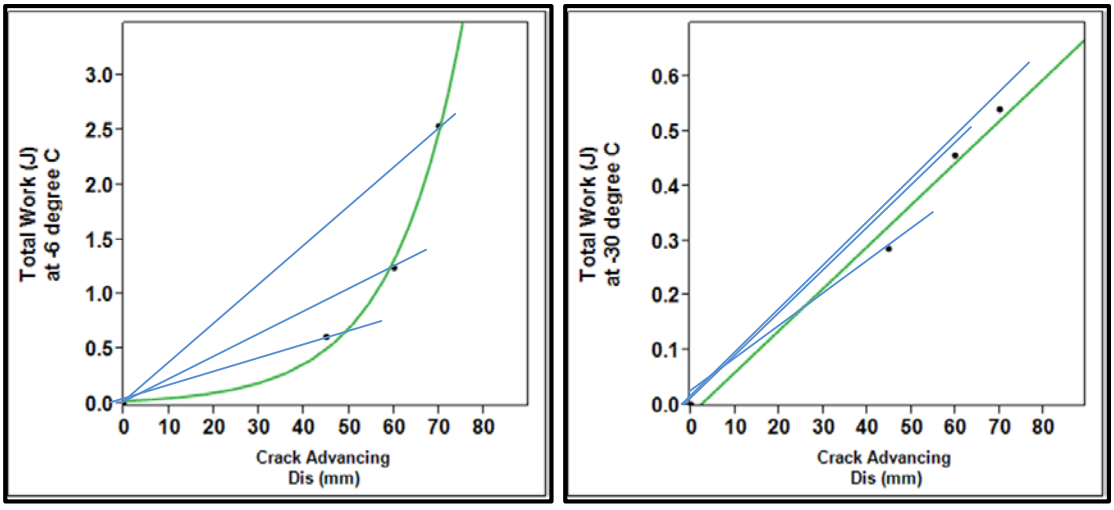

(a) **(b)**

Figure 10. Total energy per unit thickness vs. Crack advancing distance at (a) -6°C and (b) -30°C

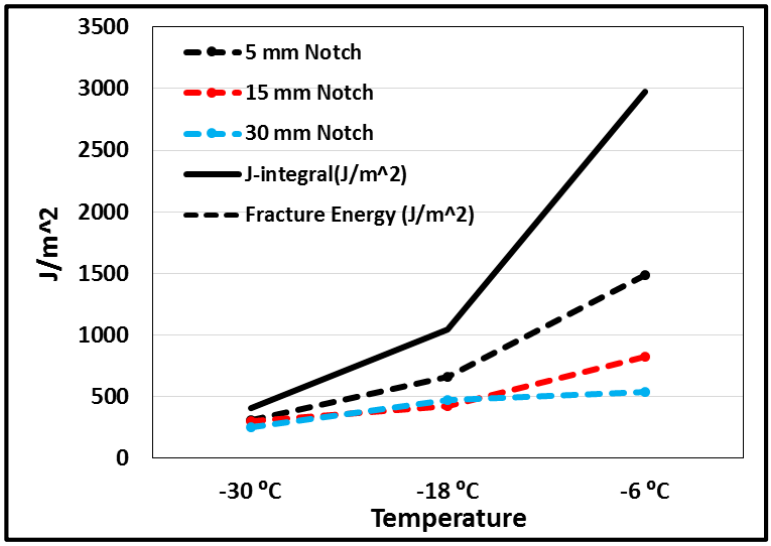

Figure 11. Estimated fracture energy and toughness

This observation can be found in subsequent research as well. Experimental data obtained from testing an asphalt mixture are shown in Figure 12. The conventional fracture energy test application limitation can be verified by testing samples with different notch sizes. A linear relationship demonstrates the small scale yielding condition is satisfied and the conveniently calculated fracture energy G_f may be safe for toughness assessment.

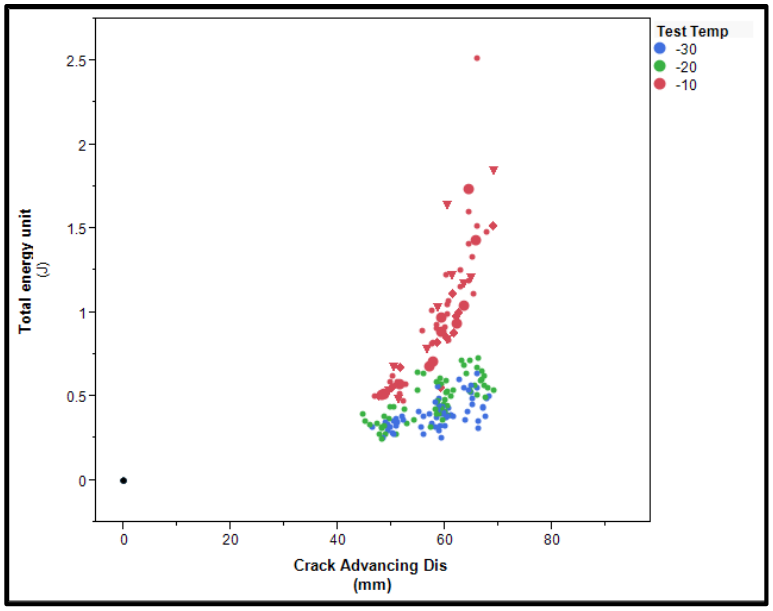

Figure 12. Total energy for 25mm thickness sample vs. Crack advancing distance

The Limitation of Peak Load and K_{IC} Obtained from SCB Fracture Energy Test

As long as the experiments are conducted at sufficiently low temperature to ensure the asphalt mixture behavior is brittle, the experimentally measured K value should be appropriate to estimate toughness, K_{IC}, theoretically. In a simple case when the material could be modeled as linear elastic, the stress intensity factor is approximately given by (Lim et al. 1993; Li and Marasteanu. 2004),

$$K_I = \frac{P}{2rt}\sqrt{\pi a}\left\{4.782 + 1.219\left(\frac{a}{r}\right) + 0.063\, exp\left[7.045\left(\frac{a}{r}\right)\right]\right\}, \qquad \text{(equation 16)}$$

for a crack much smaller than the specimen, $\frac{a}{r} \ll 1$.

However, when testing temperature increases to certain level, the suitability for applying the measured K values should be verified. Based upon Li and Marasteannu's test data from Table 2, the values of the measured stress intensity factor K are calculated. Figure 13 illustrates

conflictions between conveniently estimated fracture energy G_f with the measured K value. Although the conveniently calculated, G_f, values already underestimate fracture resistance at temperatures above -30°C (Figure 11), the measured stress intensity factor K values even demonstrate higher biases with increased temperatures. Li and Marasteannu (2006) recommended calculating the stress intensity factor, only when the fracture process zone is small (Li and Marasteannu 2006).

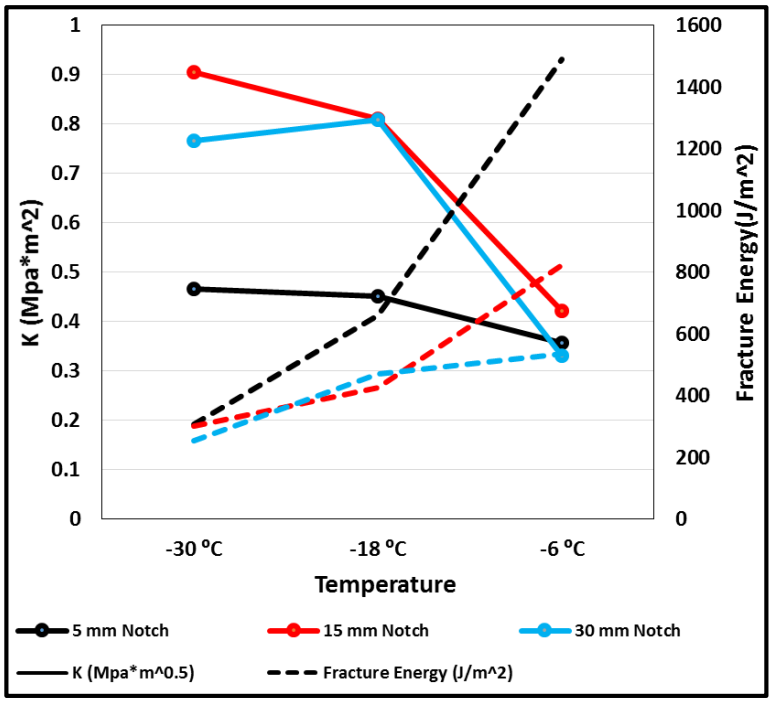

Figure 13. Measured K values and estimated fracture energy G_f

Additionally, since the experimentally determined K is a "point" measurement and highly associated with the crack tip property (sharpness and material), the concern for applying this K measurement to rank asphalt mixtures is also due to the possibility of extensive variability of P_{max} value. The changing trends of peak loads and K values at varying temperatures are illustrated by Figure 14. Correlations between peak loads and K values can be observed.

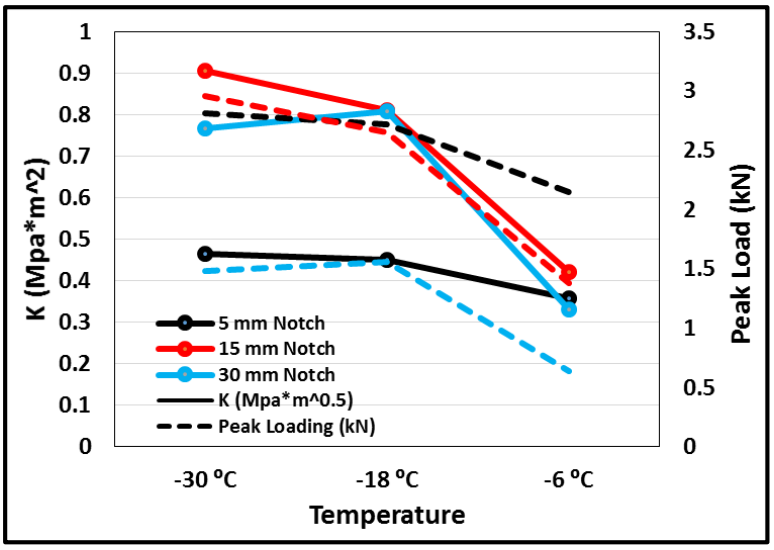

Figure 14. Measured K values and peak load

Testing results with large variances are difficult to detect the statistical differences when several materials are compared. As shown in Figure 15, results used to estimate K_{IC} will be different, if the peak loading P_{max} is directly used in the calculation. Clearly, the notch tip terminating in a rock provides a different P_{max} value when it is in the asphalt binder. This notch tip uncertainty and the geometry (sharpness) variations can result in unstable K measurements, which makes statistical comparisons difficult.

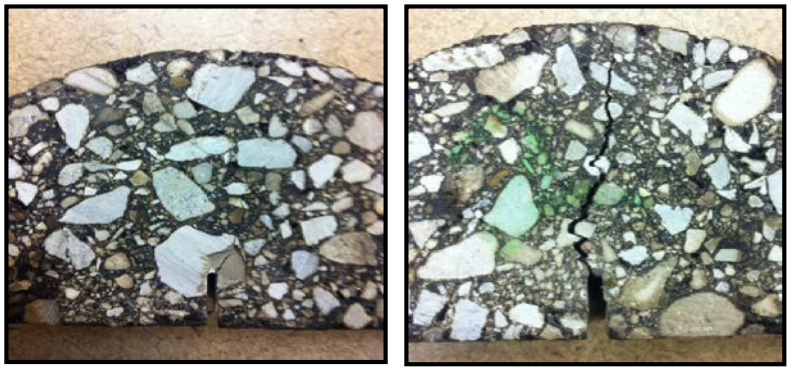

Figure 15. Preexisting crack tip in a large aggregate and paste post SCB testing

First, to obtain precise and conservative toughness measurements, all ASTM standard K_{IC} measurements strictly define the acceptable notch envelopes (Figure 16). Second, to ensure samples with equivalent notch tip sharpness, there is a fatigue pre-cracking treatment to prepare metallic specimens. After cutting notch, the test samples are subjected to the same loading at low magnitude, and then the equal sharpness of the notch tip can be obtained. Third, even after fracture testing, ASTM toughness test specifications recommend a 5% secant line method (Figure 17) and other selection criteria to determine a qualified peak load, $P_{Q,}$ to be used in K_{IC} calculation. These variance reducing methods can provide more precise output calculations when pop-in cracking occurs.

Since asphalt mixtures can be highly variable composite materials, none of these three methods are able to efficiently and fundamentally reduce the test variances in part due to the aggregate to specimen size ratio. Even under small scale yielding condition, when the K_{IC} values from different mixtures can be estimated by K measurements, the statistically significant differences may not be detected, unless the mixtures are dramatically different.

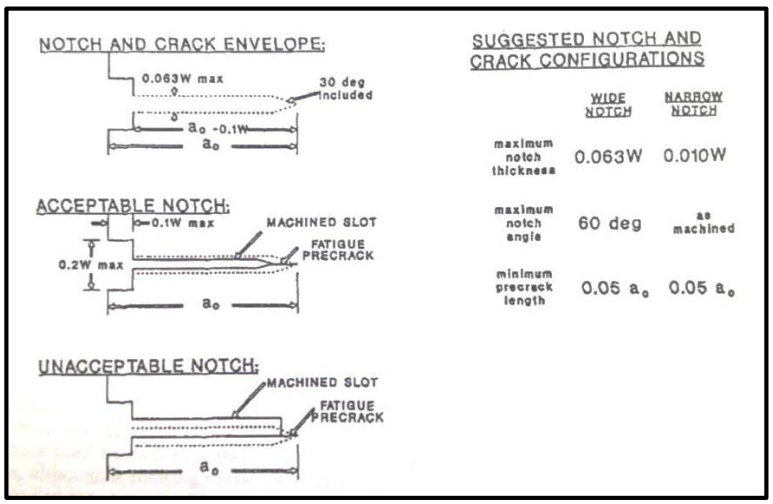

Figure 16. Envelopes of crack notch (ASTM E1820)

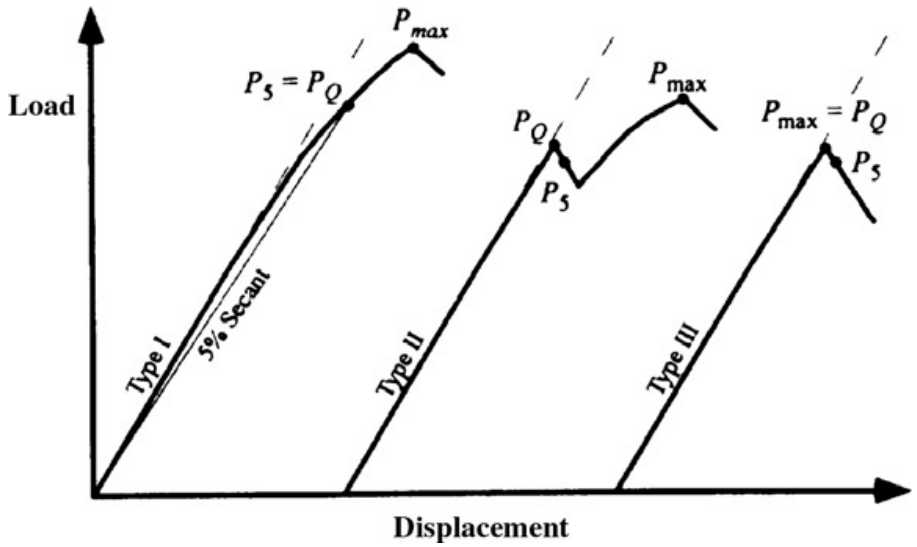

Figure 17. The 5% secant line method and other criteria to determine the qualified peak load P_Q for three types of load displacement curves (ASTM E1820)

Conclusions and Recommendations

The peak load for SCB testing is not recommended as an indicator to rank asphalt mixtures' cracking resistance performance at all temperatures. The variations accounted from the specimen geometry, notch tip sharpness, and miscorrelations with fracture toughness eliminate its application to evaluate fracture resistance of asphalt materials appropriately.

When asphalt materials can be modeled as linear elastic objects with small-scale yielding, the experimentally measured K value should be appropriate to estimate toughness, K_{IC}, theoretically. However, because fatigue pre-cracking treatment is skipped in SCB testing of asphalt mixtures, the preexisting crack tip sharpness and tip location (stone or binder) may result in certain variations to K measurements. The estimated K_{IC} toughness may not be very efficiently used to rank asphalt mixtures (lack of precisions), when the experiment plan consists of a small number of replicate samples and the differences for the compared mixtures

are insignificant. On the other hand, when the small-scale yielding condition is not met, the estimated K_{IC} toughness is a lack of both precisions and accuracies. With a large-scale yielding (testing at high temperatures), K measurements are not recommended applied at all.

Conveniently calculated fracture energy, G_f, may successfully quantify fracture toughness for tests at sufficient low temperatures (if neglect the other energy dissipations). However, it is inappropriate to assess the toughness of asphalt mixtures at high temperatures when the material deforms in an elastic–plastic manner. The G_f values obtained at small scale yielding conditions (very low temperature testing conditions) can be utilized to estimate the dimensionless and physical property, G_{IC}. However, at relatively higher temperatures, test results tend to underestimate the fracture resistance of ductile materials dramatically, and overstate the benefits of stiffer mixtures for testing. If the SCB fracture energy test with conventional G_f method is selected to evaluate asphalt mixtures, SCB specimens prepared with a small-size notch are recommended. Once again, although conveniently estimated G_f values have considerable amount of biases at high temperature tests, but this does not mean it cannot distinguish very weak and tough asphalt mixtures.

Based upon research findings and experimental practice, a fracture energy protocol is only recommended for low temperature tests. Even then, the validation of the test assumption should be completed case-by-case, depending upon the plastic zone size of the asphalt mixture. For test temperatures above -20°C, the fracture energy test results should be verified by testing samples with different notch sizes. Diversified results indicate the small scale yielding condition is unsatisfied and the estimated G_f and K value cannot be used for toughness estimation. The SCB fracture toughness experiments should be conducted.

The J_{IC} fracture toughness test with different notch sizes, based on Begley and Landes' (1972) experiment is a promising approach for testing asphalt mixtures and needs future research.

References

Mull, M.A., Stuart, K., and Yehia, A., 2002. Fracture resistance characterization of chemically modified crumb rubber asphalt pavement. *J. Mater. Sci.*, 37(3), 557-566.

Wu, Z., Mohammad, L.N., Wang, L.B., and Mull, M.A., 2005. Fracture resistance characterization of superpave mixtures using the semi-circular bending test. *Journal of ASTM International*, 2(3), 135-149.

Shu, X., Huang, B., and Vukosavljevic, D., 2008. Laboratory evaluation of fatigue characteristics of recycled asphalt mixture. *Construction Building Materials*, 22(7), 1323-1330.

Li, X. and Marasteanu, M.O., 2010. Using semi circular bending test to evaluate low temperature fracture resistance for asphalt concrete. *Experimental Mechanics*, 50, 867-876.

Landes, J.D., and Begley, J.A., 1972. The effect of specimen geometry on J_{IC}. *ASTM STP 514, American Society for Testing and Materials*, Philadelphia, 24-29.

Begley, J.A., and Landes, J.D., 1972. The J-integral as a fracture criterion. *ASTM STP 514, American Society for Testing and Materials*, Philadelphia, 1-20.

ASTM E1820. Standard test method for measurement of fracture toughness, *American Standard of Testing Materials.*

ASTM E1823. Standard terminology relating to fatigue and fracture testing, *American Standard of Testing Materials.*

Griffith, A.A., 1920. The phenomena of rupture and flow in solids. *Philosophical Transactions*, 221, 163-198.

Irwin, G.R., 1956. Onset of fast crack propagation in high strength steel and aluminum alloys. *Sagamore Research Conference Proceedings*, 2, 289-305.

Rice, J.R., 1968. A path independent integral and the approximate analysis of strain concentration by notches and cracks. *Journal of Applied Mechanics*, 35, 379-386.

Little, D.N., Lytton, R.L., Williams, D., and Kim, Y.R., 1997. Propagation and healing of microcracks in asphalt concrete and their contributions to fatigue. *Asphalt Science and Technology*, 149-195.

Little, D.N., Lytton, R.L., Williams, D., and Kim, Y.R., 1999. An analysis of the mechanism of microdamage healing based on the application of micromechanics first principles of facture and healing. *Journal of the Association of Asphalt Paving Technologists*, 68.

Cheng, D., Little, D.N., Lytton, R.L., and Holste, J.C., 2002. Surface energy measurement of asphalt and its application to predicting fatigue and healing in asphalt mixtures. *Transportation Research Records*, 1810, 44-53.

Kim, Y., 2009. *Modeling of Asphalt Concrete*. New York, NY: McGraw Hill.

Irwin, G.R., 1948. Fracture dynamics, *Fracturing of Metals*, American Society for Metals, 147-166.

Orowan, E., 1948. Fracture and strength of solids. *Report on Progress in Physics*, XII, 185-232.

Irwin, G.R., 1957. Analysis of stress and strains near the end of a crack traversing a plate. *Journal of Applied Mechanics*, 24, 361-364.

ASTM E399. Standard test method for linear-elastic plane-strain fracture toughness K_{IC} of metallic materials, *American Standard of Testing Materials*.

ASTM E561. Standard test method for K-R curve determination, *American Standard of Testing Materials.*

ASTM E813. Standard test method for J_{IC}, a measure of fracture toughness, *American Standard of Testing Materials*.

ASTM E1152. Standard test method for J-R curves, *American Standard of Testing Materials*.

ASTM E1737. Standard test method for J-integral characterization of fracture toughness, *American Standard of Testing Materials.*

Anderson, T.Y., 1991. *Fracture mechanics.* Boca Raton, FL: CRC Press, Inc.

Wells, A.A., 1961. Unstable crack propagation in metals: cleavage and fast fracture. *Proceedings of the Crack Propagation Symposium*, 1, 84-98.

ASTM E1290. Standard test method for crack opening displacement (CTOD) fracture toughness measurement, *American Standard of Testing Materials.*

Zhu, X.K., and Joyce, J.A., 2012. Review of fracture toughness (G, K, J, CTOD, CTOA) testing and standardization. *Engineering Fracture Mechanics*, 85, 1-46.

Li, X., and Marasteanu, M.O., 2004. Evaluation of the low temperature fracture resistance of asphalt mixtures using the semi-circular bend test. *Journal of the Association of Asphalt Paving Technologists*, 73, 401-426.

Lim, I.L., Johnston, I.W., and Choi, S.K., 1993. Stress intensity factors for semi-circular specimens under three-point bending. *Engineering Fracture Mechanics*, 44(3), 363-382.

Hu, X.Z., and Wittmann, F.H., 2000. Size effect on toughness induced by crack close to free surface. *Engineering Fracture Mechanics*, 64(2), 209-221.

Hu, X.Z., 2002. An asymptotic approach to size effect on fracture toughness and fracture energy of composites. *Engineering Fracture Mechanics*, 69(5), 555-564.

Duan, K., Hu, X. Z., and Wittmann, F.H., 2003. Boundary effect on concrete fracture and non-constant fracture energy distribution. *Engineering Fracture Mechanics*, 70(16), 2257-2258.

Hu, X.Z., and Duan, K., 2010. Mechanism behind the size effect phenomenon. *Journal of Engineering Mechanics – ASCE*, 136(1), 60-68.

Yang, S.T., Hu, X.Z., and Wu, Z.M., 2011. Influence of local fracture energy distribution on maximum fracture load of three-point-bending notched concrete beams. *Engineering Fracture Mechanics*, 78(18), 3289-3299.

Li, X. and Marasteanu, M.O., 2006. Investigation of low temperature cracking in asphalt mixtures by acoustic emission. *Road Materials and Pavement Design*, 7/4, 491-512.

CHAPTER 3. THE MODIFIED SEMI-CIRCULAR BENDING (SCB) TEST AND DATA ANALYSIS BASED ON FRACTURE MECHANICS APPROACH

A paper to be submitted to International Journal of Pavement Engineering

Sheng Tang and R. Christopher Williams

Abstract

This paper first reviews several key elements of fracture mechanics and summarizes the current fracture toughness experimental methods from the American Standard of Testing Materials (ASTM). Generally, none of these standards can be directly and conventional applied to inhomogeneous asphalt mixtures by using specimens machined in a relatively small size. Inspired and guided by ASTM standards, a new semi-circular bending (SCB) toughness test suitable for asphalt mixtures was developed, based upon Begley and Landes' paper (1972). This modified SCB test is able to provide measurements to estimate toughness J_{SS}, representing fracture resistance for cracks extension at a steady state. Both the current SCB fracture energy test and the newly proposed SCB fracture toughness test were applied on asphalt mixtures with reclaimed asphalt materials to demonstrate and investigate tests' effectiveness and suitability to evaluate materials' fracture properties at three low temperatures (-10, -20, and -30°C) .

Comparison analysis of testing results obtained from both original SCB fracture energy and SCB toughness testing methods shows the peak load is inefficient for classifying asphalt mixtures because of its extensive variance of outcomes and miscorrelation with fracture toughness. Simple measurement of the fracture energy has biases and is inaccurate to classify asphalt mixtures tested at high temperatures (non-brittle) when the material deforms more in

an elastic–plastic manner. Conveniently estimated fracture energy, G_f, is a geometry-dependent value and cannot serve as a good fracture resistance estimator unless the small-scale yielding condition is met. The proposed new SCB toughness test can provide a better J_{SS} toughness parameter to evaluate asphalt mixtures subjected at brittle-ductile transition temperatures. Based on the aforementioned findings and experimental observations, this paper addresses the suitability for the semi-circular bend (SCB) test protocol to evaluate the fracture resistance of asphalt mixtures containing reclaimed asphalt materials.

Introduction

Asphalt mixtures are complex materials involving sensitive rheological properties, including the binder's viscoelastic properties and mixture's composite material property. They experience linear and nonlinear behaviors under stress, and are temperature and time dependent. The fracture resistance parameters (fracture energy, peak load, and toughness) obtained from varying SCB fracture tests must be carefully selected to correctly analyze and evaluate asphalt mixtures' fracture mechanical properties. Since SCB notch size can significantly affect fracture energy measurements as well as testing variability, when conducting the convenient fracture energy test, there are concerns regarding the effectiveness and suitability for utilizing this fracture energy test distinguished from fracture toughness in fracture mechanics. Questions have been raised for application conditions, such as test temperature ranges and SCB sample sizes for fracture energy testing. Moreover, how to properly measure fracture toughness and correctly interpret fracture toughness testing results draw researchers' attention as well. The purpose of this paper is to introduce the American Standard of Testing Materials (ASTM) fracture toughness methods and design an applicable

SCB fracture toughness test for asphalt mixtures, as well as to investigate the feasibility of using both fracture energy and toughness tests, and their resulting parameters to evaluate asphalt mixtures at low temperatures.

Fundamental Fracture Mechanics

Fracture mechanics is the field that focuses on the study of crack initiation and propagation for materials. Fracture toughness is a parameter used to quantify a material's resistance against cracking at different states. This parameter can be estimated by a series of different fracture experiments at varying defined conditions.

Generally, three critical experimental measurements—(1) stress intensity factor, K_C, (2) energy release rate, G_C, or J-integral ,J_C, and (3) Crack-Tip Opening Displacement (CTOD δ_C)—can be utilized to assess fracture toughness, based on three different perspectives (ASTM 1823). K_C is based on stress intensity, G_C and J_C are established from energy release and consumption concepts, respectively, and the CTOD (δ_C) is grounded in the correlation between fracture resistances with crack-tip geometry. Their differences and applications are described in the following sections.

Fracture Toughness Parameters in Terms of K_C, G_C, J_C, and δ_C

For materials under linear elastic and small scale yielding conditions, K_C is often selected to define the fracture toughness of brittle materials, such as glass. In linear elastic fracture mechanics (LEFM), fracture toughness parameters are all interrelated (Begley and Landes 1972). Under the plane-strain condition with the "opening" mode loading, the relationship can be shown as,

$$G_C = J_C = \frac{1-v^2}{E} K_C^2 = \delta_C \sigma_Y \,, \qquad \text{(equation 17)}$$

where v is the Poisson's ratio. The subscript "C" denotes the parameter as a critical value at the onset of fracture instability. Beyond the LEFM condition, the validation for applying fracture parameters is summarized in Table 3. Elastic-plastic fracture mechanics (EPFM) were developed to solve the problem with large scale yielding. Without estimating the plastic zone size, any conclusions or comparisons generated, based on the measurements of K or G, and are inappropriate. For low-strength and high-toughness materials able to sustain large- plastic deformations, such as rubber, toughness should be characterized by parameters in terms of J-integral or CTOD (δ) (Zhu and Joyce 2012).

Table 3. Summary of the application range for theories and fracture parameters

Theories and Measurements		Surface energy	Stress Intensity Factor	Elastice Energy Release Rate	J Integral	Open Displacement
Fracture Mechics	Deformation scale	Griffith Theory	K	G	J	CTOD
LEFM	Brittle					
	Small scale					
EPFM	Large scale					

Resistance Curve

The crack growth resistance curve (R-curve) is the plot of the fracture toughness function by using crack extension (crack advancing distance) as a variable (Anderson 1991). Functions generally can be expressed as,

$$K_R = K_R(\Delta a), J_R = J_R(\Delta a) \; or \; \delta_R = \delta_R(\Delta a) \,, \qquad \text{(equation 18)}$$

where Δa is the advancing crack distance from the preexisted crack, α_0.

The R-curve illustrates the crack growth resistance of a material, which continuously demonstrates the value of fracture toughness is dependent upon the crack extension, while controlling other variances (Figures 18 and 19). Different fracture states can be clearly observed. The R-curve of ductile materials sustaining large-plastic deformations usually utilizes J-integral (J) or CTOD (δ) to quantify fracture resistance (Figure 18). In contrast, the R-curve of brittle materials normally uses the critical value of stress intensity factor K to represent fracture toughness and appears like a step function (Figure 19).

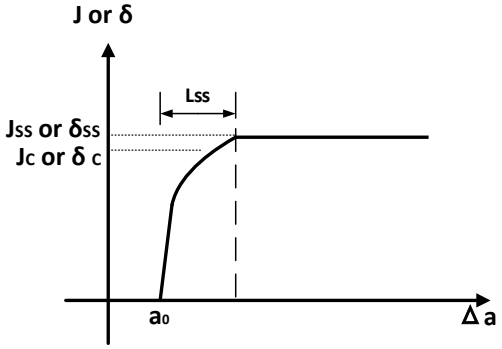

Figure 18. R-curve of material under the large scale yielding condition

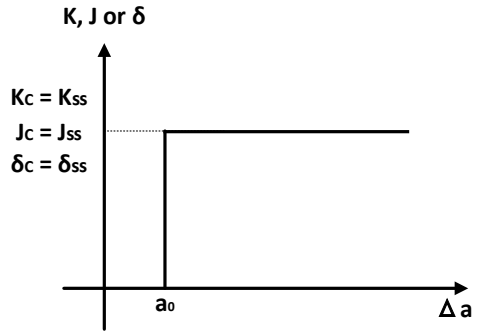

Figure 19. The idealized R-curve as a step function for brittle materials

When the stress field of the inelastic region achieves a constant value, the crack extends at a steady state. Fracture toughness ideally attains a plateau value, noted as J_{SS} or δ_{SS}, and the subscript "$_{SS}$" signifies steady state. The length of the additional crack extension needed to attain a steady state is noted as "L_{SS}" (the steady-state bridging zone size) and is comparable to the size of the plastic zone when the crack advances in the steady state. When ductile steel deforms under the elastic-plastic condition, L_{SS} is around one centimeter. Fracture resistance first increases from zero to J_C where the facture initiates, and then achieves J_{SS} after the crack slowly and stably extends L_{SS} (Figure 18). The fracture onset point toughness (J_C) is smaller

than or equal to steady-state fracture toughness, J_{SS}. The difference between them depends upon ductility of the material; in other words, the length of L_{SS} or the size of plastic processing zone. For brittle materials or ductile materials when the small scale yielding condition is fulfilled, L_{SS} is very small relatively compared to the overall size of the testing specimen, and the R-curve is more like a step function as shown in Figure 19. J_{SS} or δ_{SS} are equal to J_C or δ_C. The crack stage transition associated with the R-curve can also be well illustrated and explained graphically in Figure 20. The R-curve and its association with varying toughness values at different crack states can be used to demonstrate why there are size effects for the SCB test at relatively high temperatures when the asphalt is more ductile, but there is almost no size effect at relatively low temperatures when the asphalt mix is brittle.

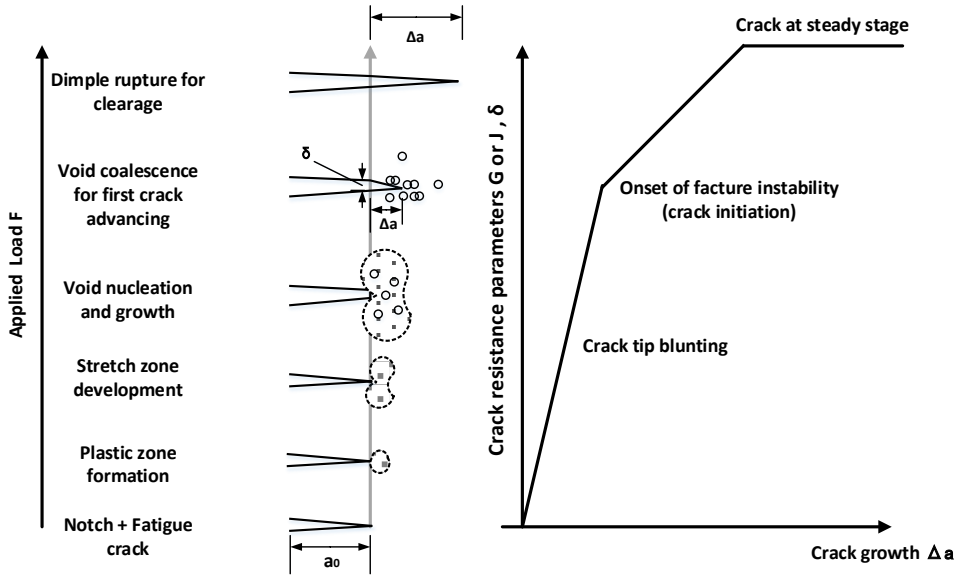

Figure 20. Cracking states transition associated with the R-curve

When a crack tip is sufficiently sharp and other geometry constraints are satisfied for plane-strain condition, the experimental measurement can be defined as plane-strain toughness, marked with the subscript "IC" for type I fracture. Plane-strain toughness (K_{IC}, G_{IC},

J_{IC}, and δ_{IC}) is considered the intrinsic physical property of materials, a geometric independent value, and represents the lower bound of all other toughness with regard to different crack states.

Current ASTM Standard Test Methods

In the asphalt research field, the semi-circular bend (SCB) test is still an evolving method used to measure fracture resistance of asphalt mixtures. No standard SCB test proposal for asphalt mixtures has been accepted by ASTM yet. Depending upon the unique properties of asphalt materials, toughness parameter, testing procedure, and even data analysis method should be appropriately selected to obtain the suitable fracture parameter. The fracture-mechanics-based approaches are necessary and should be adopted to better analyze testing data.

In this section, the review of the current ASTM toughness test protocols is introduced first. Next, the reasons for not directly applying these ASTM standards used for metallic materials to test asphalt mixtures are described.

Many ASTM methods are available for testing homogeneous metallic materials, ASTM E399, E561, E813, E1152, E1290, E1737, and E1820. ASTM E1820 is a universal standard combining all other toughness test procedures cited previously. Only ASTM E1921 is the standard designed for testing a non-homogeneous material, ferritic steel, with respect to the orientation of individual grains.

All ASTM tests mentioned above are intended to measure plane-strain fracture toughness (except E1921), since it is a geometric independent value representing the physical

property of materials. ASTM toughness testing protocols can be divided into two categories: (1) either measuring the single value of toughness at the onset point of the fracture instability (typically for brittle materials) or (2) constructing the R-curve composed by multiple fracture resistance measurements, which umbrellas all toughness from crack initiation to after the onset of significant stable tearing crack extension. For the analysis, once the R-curve is obtained, one can apply a shift line on the R-curve to estimate the plain-strain value (typically for ductile materials). Regardless which procedures are followed, the testing of notched and fatigue pre-cracked bend or compact specimens is involved.

Generally, to calculate toughness in terms of the stress intensity factor K or J-integral, the loading force versus load-line displacements plot should be generated, and include the crack initiation and extension information. T quantify toughness in terms of CTOD (δ), the crack tip opening displacement and crack advancing data are required measurements.

By applying the single point toughness experimental methods (ASTM E399, E813 and E1820) for materials with small-scale yielding, test results can be substantially effected by the peak load and initial crack length (notch size + fatigue pre-cracking distance) as well as other geometry constraints. To obtain precise and conservative peak load measurements with less variations, all ASTM standards for single point measurement first strictly define the acceptable notch envelopes. Second, a fatigue pre-cracking treatment should be implemented with the purpose of having equivalent crack tip sharpness. Even after fracture testing, ASTM single point toughness test specifications recommend a 5% secant line method and other criteria to determine qualified peak load, P_Q, utilized to determine critical K value. High precision, optical measurements are applied to obtain the initial and final physical crack sizes (locations). ASTM

standards require the cracking distance measurement have an accuracy of 0.025mm (0.001 in). Unfortunately, none of these requirements are applicable for asphalt mixture tests, due to the lack of equipment, the inhomogeneity of asphalt mixtures and relatively small-size specimen. The variance of peak load cannot be reduced, if the crack-tip front randomly locates in an aggregate or the asphalt, and specimens are machined in a relatively small size. Thus, the equivalent sharpness tip treatment is of little value as well.

If R-curve methods (ASTM E561, E1152, E1290, E1737, and E1820) are applied, the measurements of crack extensions are priorities. Based upon toughness functions ($\frac{\partial U}{B\partial a}$ or $\frac{\partial CTOD}{B\partial a}$), the deviations of energy or CTOD corresponding to crack extensions must be recorded to identify toughness. Input energy can be easily obtained from load displacement curve, and the CTOD can be calculated directly from the data collected by a crack mouth opening displacement (CMOD) device. The most difficult task for measuring fracture toughness in R-curve format tests is to precisely determine crack extension data used to answer the questions—where is the crack and how far does it extend, responding to certain amount of energy input or crack tip openings?

There are three major methods to obtain crack extension data. The first method is the basic procedure (Begley and Landes 1972) requiring multiple samples prepared with different initial crack sizes (notch size + fatigue pre-cracking distance). The difference between initial crack sizes is the crack extension distance. So, it is predetermined when test samples are prepared. The other two methods are more advanced and recommended by ASTM: (1) elastic compliance method and (2) electric potential method. Both techniques need only one specimen prepared with one notch size to obtain a toughness measurement.

The elastic compliance method utilizes crack mouth opening displacement measured by a CMOD gauge to estimate crack extension through the load and unloading processes. The application of the electric potential method estimates crack growth directly by the change of electric potential for the testing sample. However, these advanced methods are neither easy nor suitable for asphalt mixture research. The elastic compliance method increases the requirement of the load device and requires better control software. The electric potential method may only work for metallic materials.

ASTM E1921 documents the testing standard for non-homogeneous metallic materials. Among ductile-brittle transition temperatures, ferritic steels are considered non-homogeneous materials, due to the orientation of individual grains and the boundaries among themselves. Thus, the Weilbull distribution is recommended to characterize measurements of the statistical features. This statistical analysis method can be transferred to asphalt mixture testing and examined for further research. The standard is considered the most suitable testing and analysis protocol for asphalt mixtures. However, ASTM E1921 defines a toughness parameter, K_{JC}, an elastic-plastic equivalent intensity factor derived from the J-integral toughness J_C measured by applying the R-curve method mentioned previously. Some modifications must be completed to make them applicable for asphalt mixtures. This is a promising candidate test.

These existing ASTM fracture toughness tests have the need for measurements with high accuracy, and precision for crack initiation and extension, unsuitable for an engineering approximation in the asphalt industry. More importantly, difficulty to control notch sharpness and a lack in homogeneity of asphalt mixtures cause the high accuracy level to be impractical for testing the SCB sample in relatively small sizes. All unique features of asphalt mixture

materials lead to experimental variability using small specimens. Therefore, obtaining the fracture toughness of an asphalt mixture by applying a simplified method (approximation approach) is thought to appropriately provide more realistic data. The original SCB fracture energy test is practical, since it ignores the process like "fatigue pre-cracking," does not need precise controls and measurements, and uses the approximation approach to calculate the average fracture energy, but this conventional data analysis method is too lumpy. When applying the conventional "average method," fracture resistance has been underestimated for ductile materials tested at high temperatures. Therefore, two other SCB fracture toughness test protocols are introduced to assess J_{IC} and J_{SS} separately when the small-scale yielding condition cannot be satisfied.

Basic J_{IC} Fracture Toughness Test

The J_{IC} toughness test was introduced by Begley and Landes in 1972. Basically, they tested aluminum samples with different crack lengths (Begley and Landes 1972). The load displacement curves for center cracked specimens are plotted in Figure 21. Also, the crack-initiation data were recorded (the red dots). The letter "a" signifies crack length.

Based on the load displacement curves (Figure 21), work can be calculated by integrating the area under the curve from the original point to certain load-line displacement, δ (green line). Then, work vs. crack length plot (Figure 22) is generated. The height of the green dots represents the integrated work values and the black lines connect these green dots, if energy is integrated to the same load-line displacement (δ). The three yellow lines illustrate all of the green dots that belong to three samples with three different crack lengths. The slopes (green

triangle) of the black lines can be utilized to determine the values of J-integral (not the toughness), based upon equation,

$$J = -\frac{1}{B}\left(\frac{\partial U}{\partial a}\right)_{\Delta}, \qquad \text{(equation 19)}$$

where *U* is work (strain energy), *B* is the specimen thickness, and *a* is the crack length. The Δ suffix means the derivative is taken at a certain load-line displacement (δ). The J-integral vs. load-line displacement (δ) (Figure 23) can finally be created.

Based on the crack initiation record, J_{IC} toughness in the plane-strain condition can be determined by applying the same technique described above, based upon equation,

$$J_{IC} = -\frac{1}{B}\left(\frac{\partial U}{\partial a}\right)\Big|_{\Delta_{Crack\ Initiation}}, \qquad \text{(equation 20)}$$

where the Δ suffix means the derivative is taken at a critical load-line displacement ($\delta_{critical}$), where crack initiates. The J_{IC} toughness (red dots) illustrated in Figure 23 are calculated based upon the slopes from the red line in Figure 22. The average value of the critical J-integral measurements is the estimated J_{IC}.

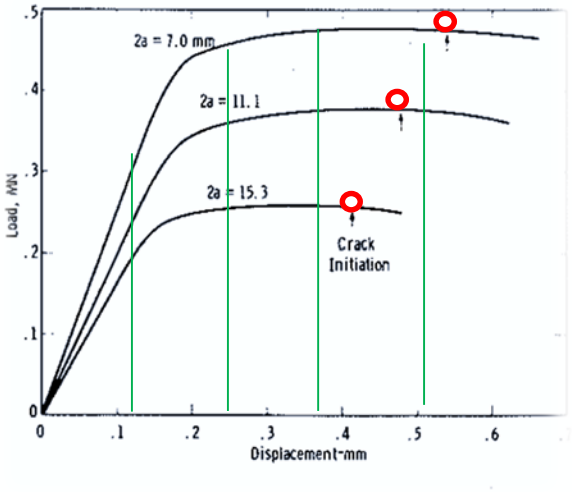

Figure 21. Load displacement curves for samples with crack length 7, 11.1 and 15.3 mm (Begley and Landes 1972)

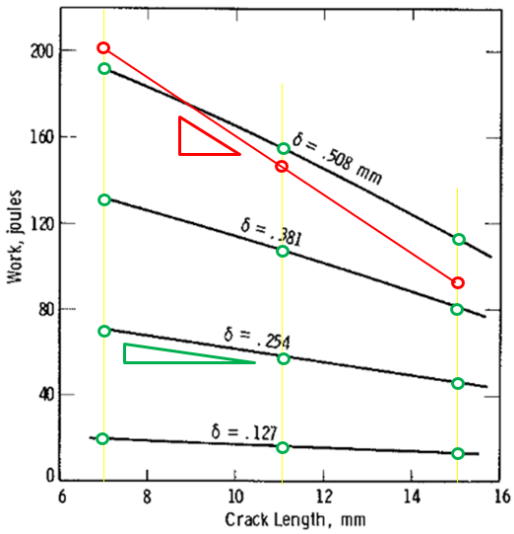

Figure 22. Work to a fixed load-line displacement vs. crack length (Begley and Landes 1972)

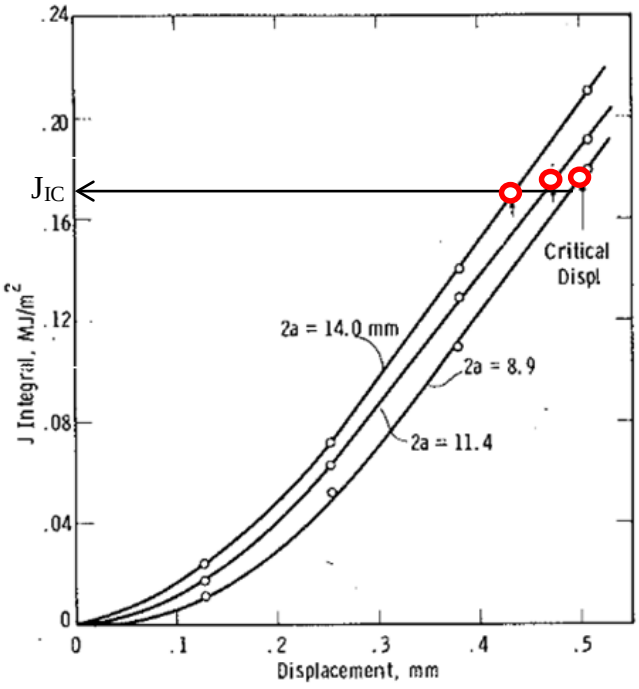

Figure 23. J-integral vs. load-line displacement under the plane-strain condition (Begley and Landes 1972)

Kim and Mohammad (2012) applied this method to test asphalt mixtures at 25ºC. Fair correlation can be found between their estimated J_{IC} toughness with pavement field cracking performance evaluations (Kim et al. 2012). The only shortcoming for conducting this basic J_{IC} fracture toughness test is the difficulty to determine crack initiation displacements, shown in Figure 21, used to integral the critical work (energy input for crack initiation). This critical work eventually affects J_{IC} toughness value. Other researchers (Kim et al. 2012) make the assumption crack initiation occurs when peak load appears. This assumption is reasonable for brittle materials, but is not always for ductile or non-homogeneous materials demonstrated by Figures 21 and 24. Figure 24 demonstrates a test of asphalt mixture at -20ºC, which provides several peak loads (red line). Thus, the challenge is to determine which one should be used to integrate the critical work.

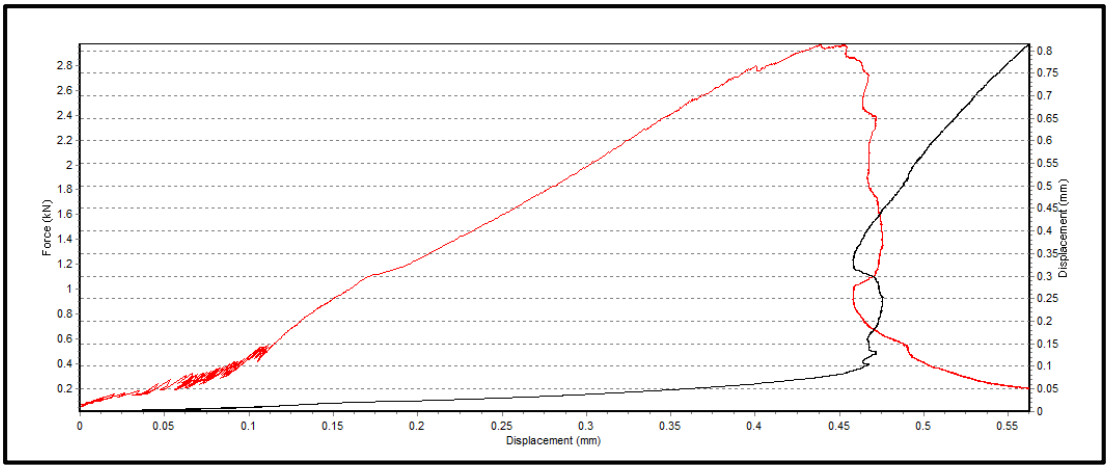

Figure 24. SCB Test Plot of force vs. displacement

Comparing with Begley and Landes' method, ASTM standard protocols do not have this problem for determining fracture initiation. The ASTM single point methods are designed for brittle materials; crack initiation can be signified when peak load appears. The ASTM R–curve

methods designed for ductile and non-homogenous materials alleviate the problem by defining fracture initiation takes place at 0.2 mm of crack extension beyond the initial tip blunting.

Since the basic J_{IC} fracture toughness has this shortcoming, a new SCB J_{SS} fracture toughness test protocol is proposed in the next section. Generally, the new J_{SS} toughness test procedure is the same as the classical J_{IC} test, but avoids the crack initiation question by integrating all work under the entire load displacement curve and results in a different toughness measurement Jss. The difference between J_{SS} and J_{IC} depends upon the material property. Very ductile materials with a long cracking bridging distance, Lss, tend to have J_{SS} larger than J_{IC}. For linear elastic brittle materials, they are almost equal.

Experimental Materials and Methods

Generally, asphalt mixtures for SCB testing were prepared with volumetric criteria including film thickness. The virgin binder utilized has a performance grade (PG) of 58-28. Reclaimed asphalt pavement (RAP) materials were added to replace 30, 40, and 50% of the optimum binder content by mass. This mixture batching method is often referred as the binder replacement method.

The RAP materials were mixed with limestone aggregate and virgin binder to prepare asphalt mixtures for SCB fracture testing. The designed and actually applied gradations of the three mixtures are summarized in Table 4. All samples were produced to include 7% ± 1% air voids at the same 5.00% optimum binder content. Since the mixtures are prepared by using the binder replacement method with the same gradation, the mixture's performance should be associated with binder's rheological behavior. Four replicate samples were prepared for each

type of mixture to evaluate via the SCB test. All SCB samples for one type of mixture were shuffled for random sampling purposes.

Table 4. Design gradation of the mixtures by adding RAP

	3/4"	1/2"	3/8"	No. 4	No. 8	No. 16	No. 30	No. 50	No. 100	No. 200
Designed 30% RAP Mixture	100	93.2	83.6	62.3	44.7	33.2	22.1	13.0	6.2	5.0
Designed 40% RAP Mixture	100	93.6	84.6	62.9	45.0	33.5	22.6	13.3	6.7	5.5
Designed 50% RAP Mixture	100	94.2	85.7	63.6	45.5	33.9	23.1	13.6	7.3	5.9
Actually Used For All % Samples	100	93.7	84.6	62.9	45.1	33.6	22.6	13.3	6.7	5.5

The SCB test setup with one asphalt specimen for both fracture energy and toughness tests is shown in Figure 25. The semi-circular asphalt specimens were tested with a UTM hydraulic testing machine. All experiments were performed in an environmental chamber, which uses liquid nitrogen to stabilize ambient temperatures at -10, -20, and -30°C.

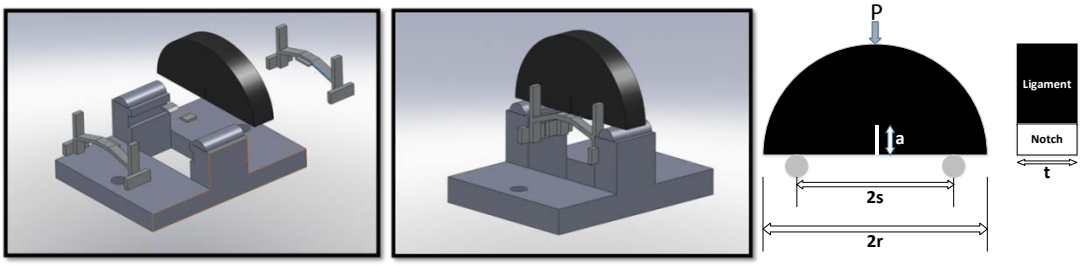

(a) **(b)** **(c)**

Figure 25. The SCB experiment setup (a) and (b) with one asphalt specimen (c)

The SCB sample shown in Figure 25 (c) was supported by two fixed rollers with a span of 120mm. The span-to-radius ratio (s/r) is confined to 0.8. Vaseline was placed on the rollers to reduce friction. Two lateral fixtures were designed and utilized to prevent sample tilts during testing. The load-line displacement in the vertical direction was record by the loading actuator. The crack-mouth opening displacement (CMOD) in the horizontal direction was measured by

an Epsilon clip gauge hung between two knife edges. These two knife edges were attached at the bottom of the specimens. The CMOD measurements controlled the loading system during the major part of loading processes. Thus, a constant crack mouth opening rate at 0.0005 mm/s was aimed and achieved. This prevents samples suddenly crashing. A slow-stable crack extension was anticipated for experiment conducted at sufficient high temperatures.

The SCB Fracture Energy Test and Its Fracture Parameters

The original SCB fracture energy protocol is found elsewhere (InTrans website under AMPP). Load displacement data is used to calculate G_f by the following equation,

$$G_f = \frac{W_f}{A_{lig}}\ , \qquad \text{(equation 21)}$$

where:

$G_f = fracture\ energy\ (J/m^2)$,

$W_f = \int Pdu$,

$P = applied\ load\ (N)$,

$u = average\ load\ line\ displacement\ (m)$,

$A_{lig} = ligament\ area\ (m^2)$,

$A_{lig} = (r - a) \times t$,

$r = specimen\ radius\ (m)$,

$a = notch\ length\ (m)$, and

$t = speciment\ thickness\ (m)$.

An assumption is presumed to apply this G_f conventional equation: the W_f is an equivalent to work of fracture and all other energy dissipations are neglected.

Additionally, in current SCB facture energy test protocol, another fracture toughness parameter, K_{IC} (maximum value of K), is estimated by a suggested equation shown below. K_{IC} defines the fracture resistance at the onset of crack extension by substituting the peak loading, P_{max}.

$$\frac{K_I}{\sigma_0\sqrt{\pi a}} = Y_{I(0.8)} \ , \qquad \text{(equation 22)}$$

where:

$\sigma_0 = \frac{P}{2rt}$,

$P = \ applied\ load\ (MN)$,

$r = specimen\ radius\ (m)$,

$t = specimen\ thickness (m)$,

$a = notch\ length\ (m)$, and

$Y_I = the\ normalized\ stress\ intensity\ factor\ (dimensionless)$.

Based upon the semi-circular geometry and dimensions of specimen used in this test method, Y_I is approximately given by (Lim et al. 1993; Li and Marasteanu. 2004),

$$Y_{I(0.8)} = 4.782 + 1.219\left(\frac{a}{r}\right) + 0.063\, exp\left[7.045\left(\frac{a}{r}\right)\right]. \qquad \text{(equation 23)}$$

The Proposed New J_{SS} SCB Testing Calculation and Procedure

There are many toughness tests providing varying toughness measurements. Plane-strain toughness is a unique one, since only the measurement under the conditions fulfilling all the strict geometric requirements and obtained at the onset of crack instability can be considered as the plane-strain toughness. Meanwhile, many other toughness parameters (J_C, J_u, J_m, and K_{JC}) are also carefully defined by ASTM standards and can be used to describe the fracture

resistance of materials at different crack states under varying conditions. The Jss SCB test method here is designed to estimate the J-integral after significant fracture when the slow-stable crack extension occurs at a *steady state*.

The proposed new SCB J_{SS} toughness test has the similar test procedure as the basic Begley and Landes' J_{IC} protocol, which tests additional samples with varying notch depths, but with a subsequent different calculation method to obtain the energy changing rate. The main difference between the proposed new SCB J_{SS} test and the SCB J_{IC} protocol is the SCB J_{SS} test integrates all energy under the entire load displacement curve.

As shown in Figure 26, there are two fracture resistance curves for testing identical SCB specimens using the same material, but with different initial notch size, a_1 and a_2, based on the concept toughness is a function describing the energy changing rate per crack length divided by sample thickness ($\frac{\partial U}{B\partial a}$). The difference between the total energy, ΔU (the shaded area in Figure 26), is used for dividing by the notch size difference ($\Delta a1$) and sample thickness. The result is used to estimate fracture toughness value, Jss, since the notch size difference , $\Delta a1$, equals crack extension distance, $\Delta a2$. Here, the consumed energy for a sample (unit thickness) per crack length is calculated after the significant fracture when the slow-stable crack extension occurs in a steady state. The J_{SS} can be expressed as,

$$J_{ss} = -\frac{1}{B}\left(\frac{\partial U}{\partial a}\right)_{\Delta \text{ Steady State}} , \qquad \text{(equation 24)}$$

where the value of ∂U is the changing area under the entire load displacement curve, when multiple samples with a notch in varying sizes are tested and ∂a is the size difference.

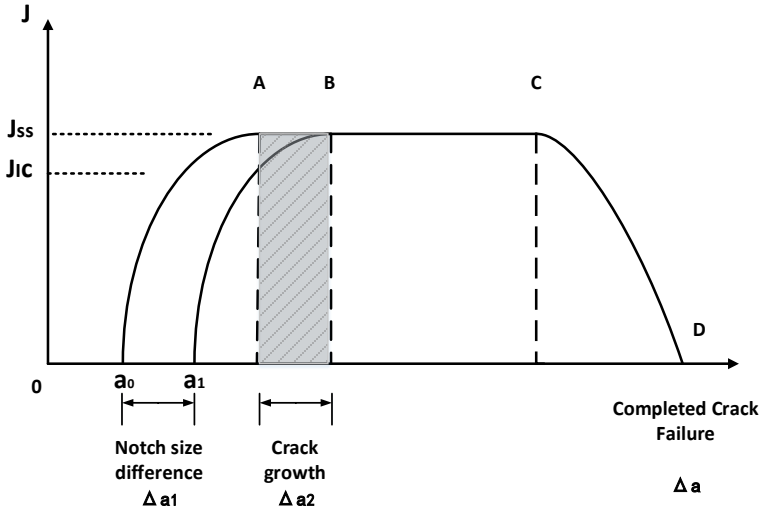

Figure 26. R-curve plot for the proposed new SCB protocol

This Jss represents the energy changing rate for a crack approaching its steady state for testing ductile materials with large scale yielding. This J_{SS} is an interesting parameter, when an elastic-plastic material needs evaluation for its full resistance of fracture extension.

Additionally, the experimentally obtained J_{SS} value can be utilized to assess $J_{IC.}$ When brittle materials are tested with small scale yielding, they are quantitatively equal.

For ductile materials with the elastic-plastic deformation, the J_{SS} value will be larger than J_{IC}. In other words, the energy to initiate cracking is less than the energy needed to maintain the slow-stable fracture continuing to extend. However, for brittle materials with small scale yielding, J_{IC} and J_{SS} are almost equal, quantitatively.

Experimental Results and Analysis

Both the current SCB fracture energy (G_f) test and the proposed Jss SCB fracture toughness test are applied on the same asphalt mixtures containing reclaimed asphalt materials to investigate their efficiencies and suitability to estimate asphalt mixture fracture resistant

properties. As previously shown, Figure 24 illustrates a typical load displacement plot for SCB experiment conducted at -20°C. The x-axis is the load-line displacement captured by the testing machine's actuator movement or LLD /LVDT devices. The y-axis on the left-hand side is the loading force, and the y-axis on the right-hand side is the crack-mouth opening displacement recorded by a CMOD gauge. The red line in Figure 24 is the load displacement curve and the area under the curve is the "work" (energy input). The black curve represents the crack-mouth opening CMOD at each load-line movement.

Table 5 summaries the SCB test results for asphalt specimens prepared with three notch sizes containing 30, 40, and 50% RAP materials. In general terms, both conveniently calculated G_f (total energy per fracture area) and total work (total energy) values decrease with a decrease in test temperature drop or with an increase in notch size, when all other factors are kept constant. Figure 27 illustrates the G_f values are sensitively notch-size dependent at -10°C, but are less geometry-dependent from -20°C to -30°C.

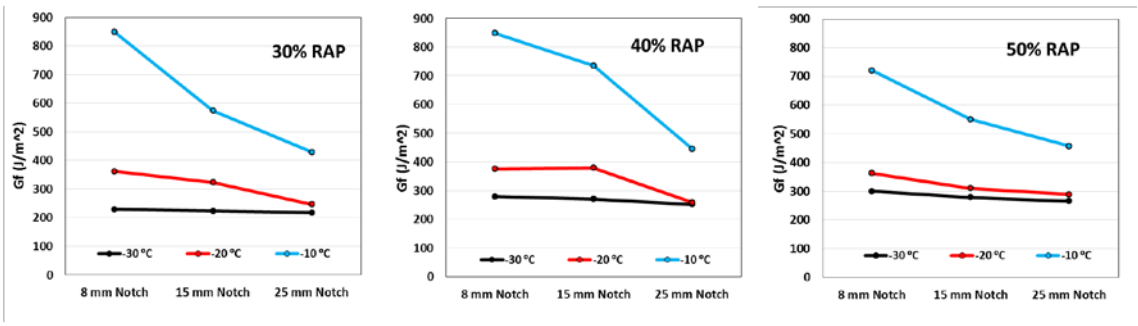

Figure 27. Geometry dependences of G_f at temperature -10, -20, and, -30°C

"Total Work vs. Crack Advancing Distance" plots are shown in Figure 28 by using the data from Table 5. Experimental results illustrate a strongly positive linear relationship between total energy and cracking extension at -30°C, and reasonably well at -20°C. A nonlinear relationship is observed for the experiments performed at -10°C.

Table 5. Fracture energy, total loading work, and crack propagation distance

8mm Notch Size Sample					15mm Notch Size Sample					25mm Notch Size Sample				
	RAP	30%	40%	50%		RAP	30%	40%	50%		RAP	30%	40%	50%
Gf (J/m^2)	-10°C	848.58	848.00	720.63	Gf (J/m^2)	-10°C	574.23	734.89	551.08	Gf (J/m^2)	-10°C	428.90	445.17	457.25
	-20°C	361.48	375.04	362.57		-20°C	323.86	378.57	310.74		-20°C	246.79	258.16	289.44
	-30°C	229.47	279.14	300.61		-30°C	223.69	270.28	278.70		-30°C	218.14	252.37	265.89
	RAP	30%	40%	50%		RAP	30%	40%	50%		RAP	30%	40%	50%
Total W (J)	-10°C	1.37	1.41	1.17	Total W (J)	-10°C	0.86	1.10	0.84	Total W (J)	-10°C	0.53	0.56	0.57
	-20°C	0.60	0.62	0.61		-20°C	0.47	0.56	0.45		-20°C	0.33	0.31	0.34
	-30°C	0.38	0.47	0.50		-30°C	0.34	0.40	0.41		-30°C	0.27	0.31	0.32
	RAP	30%	40%	50%		RAP	30%	40%	50%		RAP	30%	40%	50%
Δa (mm)	-10°C	64.22	65.85	64.25	Δa (mm)	-10°C	59.50	59.60	60.74	Δa (mm)	-10°C	49.53	50.49	50.05
	-20°C	66.55	66.11	66.86		-20°C	58.77	59.38	58.56		-20°C	50.08	48.43	46.73
	-30°C	66.40	66.75	67.08		-30°C	59.91	59.12	58.31		-30°C	49.80	49.84	47.93

The estimated K_{IC} and peak load measurements are summarized in Figures 29 and 30 with sample standard deviations, respectively. The estimated K_{IC} values are reduced extensively when the temperature is decreased from -10°C to -20°C, but there are few fluctuations when the temperature is further reduced from -20°C to -30°C. No clear trend was determined with K_{IC} value or peak load regarding the effects of the RAP content. However, the notch size shows a positive relationship with the estimated K_{IC} and the increased notch size clearly decreases the peak load. The efficiency and suitability for both parameters to evaluate asphalt mixtures will be discussed later.

The conveniently calculated fracture energy, G_f, data are summarized in Table 6 and shown in Figure 31. The results illustrate G_f decreases with a drop in temperature. The G_f values decline substantially when the temperature decreases from -10°C to -20°C, but are less temperature-dependent, similar to K_{IC} estimations and peak load measurements.

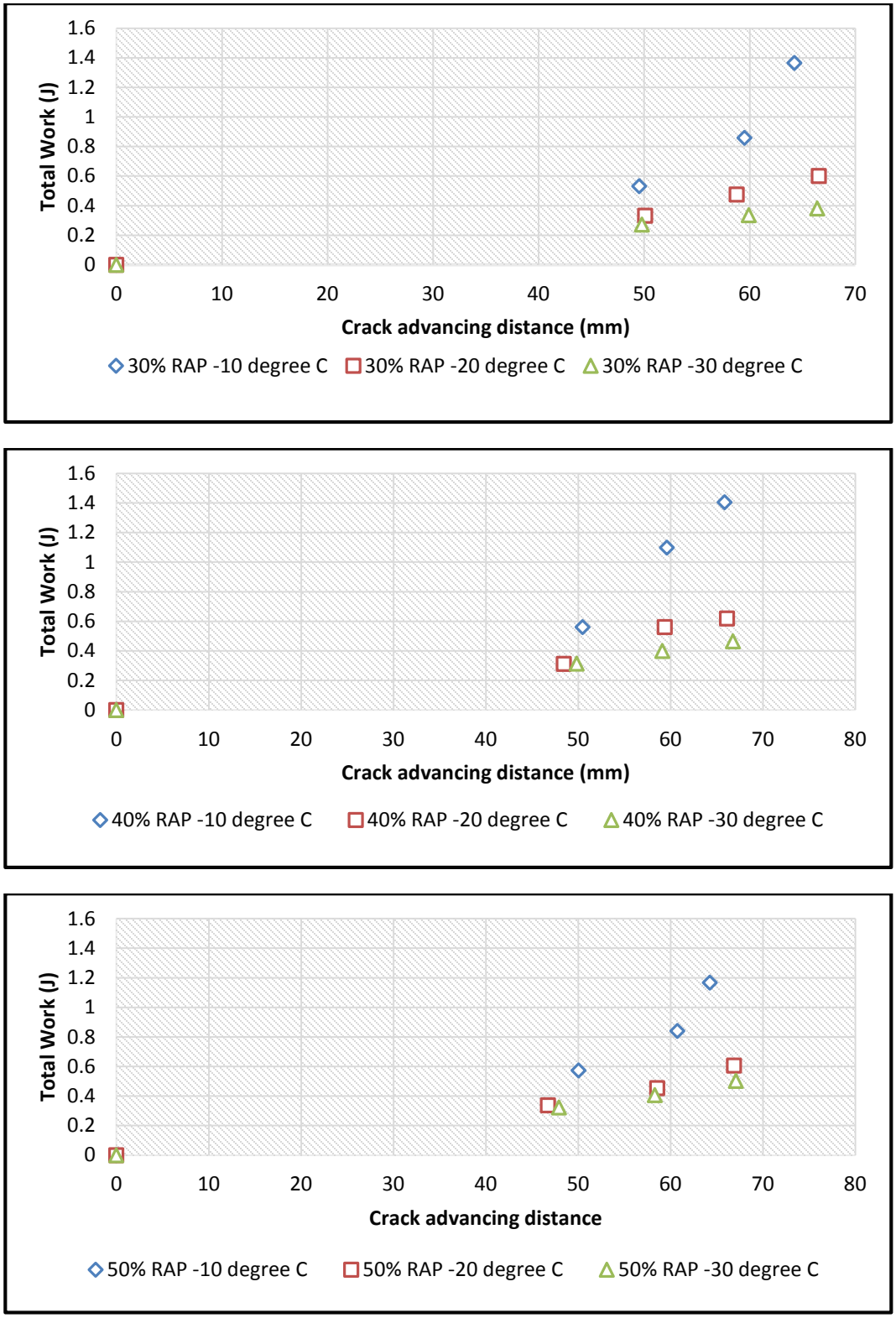

Figure 28. Total work vs. crack advancing distance plots for 25mm thickness SCB samples containing 30, 40, and 50% RAP materials

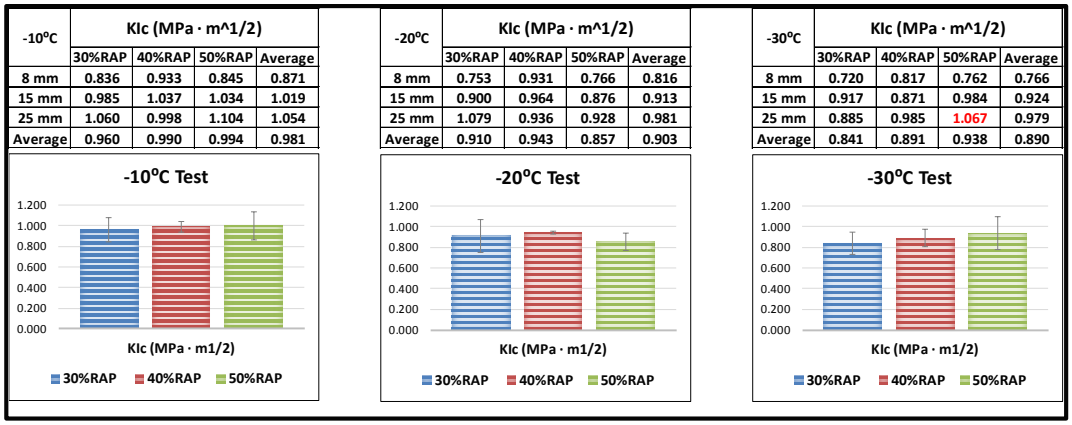

Figure 29. K_{IC} data for specimens with different notch sizes at three test temperatures

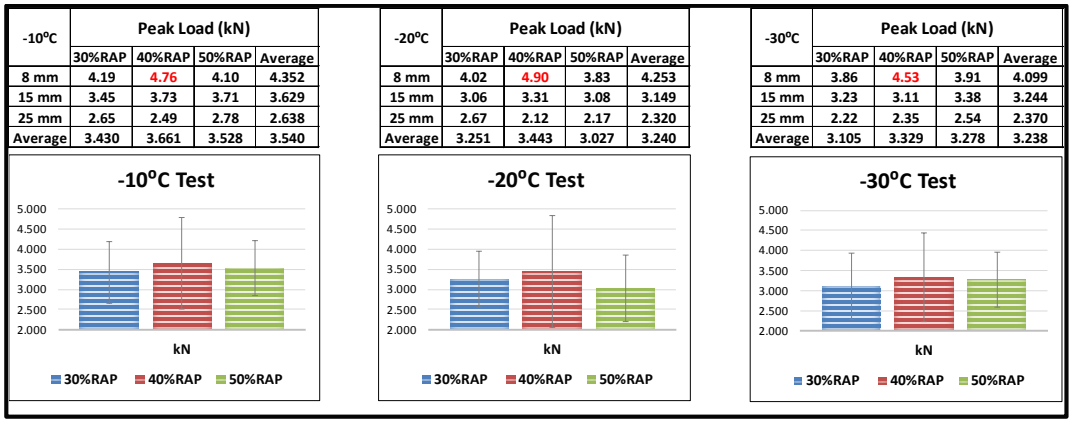

Figure 30. Peak load data for specimens with different notch sizes at three temperatures

Table 6. Fracture energy and its coefficient of variation

Test at -10°C				Test at -20°C				Test at -30°C			
Gf fracture energy (J/M^2)	30% RAP	40% RAP	50% RAP	Gf fracture energy (J/M^2)	30% RAP	40% RAP	50% RAP	Gf fracture energy (J/M^2)	30% RAP	40% RAP	50% RAP
8mm	848.58	848.00	720.63	8mm	361.48	375.04	362.57	8mm	229.47	279.14	300.61
15mm	574.23	734.89	551.08	15mm	323.86	378.57	310.74	15mm	223.69	270.28	278.70
25mm	428.90	445.17	457.25	25mm	246.79	258.16	289.44	25mm	218.14	252.37	265.89
COV	34.53%	30.73%	23.16%	COV	18.82%	20.32%	11.72%	COV	2.53%	5.10%	6.23%
Average Gf	617.24	676.02	576.32	Average Gf	310.71	337.26	320.92	Average Gf	223.76	267.27	281.73
	623.19				322.96				257.59		

Figure 32 shows the results of the estimated fracture toughness J_{SS} for different mixtures, based on the proposed SCB J_{SS} test protocol with the J-integral values summarized in Table 9. The estimated J_{SS} values were calculated from the slope of the curves/lines shown in Figure

28. These values either represent the material's ability to resist stable cracking at a steady state under elastic-plastic deformations for ductile materials, or the critical toughness at crack initiation under linear-elastic deformations for brittle materials. The J_{SS} results suggest (Figure 32) adding more RAP materials benefits asphalt mixtures to prevent cracking at -30°C to -25°C. However, this advantage diminishes with increased temperatures. The mixtures with less RAP materials demonstrate better fracture performance when increasing temperatures from -25°C to -10°C.

J_{SS} values are used as benchmarks to assess effectiveness and suitability for other fracture parameters obtained from the original SCB fracture energy test. The differences between estimated fracture energy, G_f, with estimated toughness J_{SS} are illustrated in Figure 33.

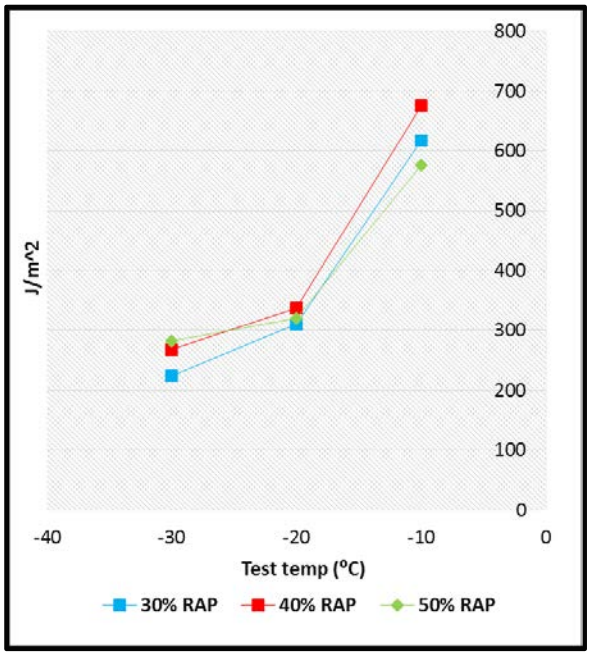

Figure 31. The fracture energy G_f (J/M^2)

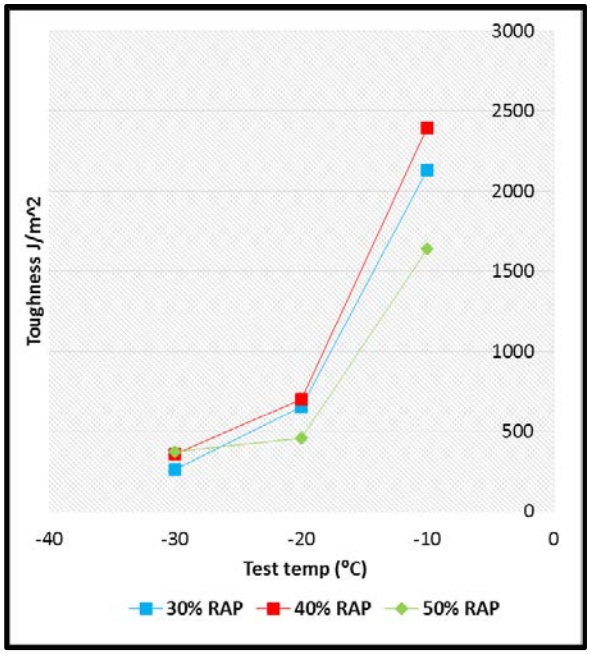

Figure 32. The estimated J_{SS} fracture toughness (J/M^2)

From Figure 33, the values of G_f (conveniently calculated fracture energy) obtained under the linear-elastic condition with small scale yielding (very low test temperatures) are close to the estimated J_{SS} toughness, but begin to diverge from J_{SS} measurements dramatically with increasing test temperatures. Generally, for testing at relatively higher temperatures, G_f results tend to underestimate the fracture resistance of ductile materials and overstate the benefits of stiffer mixtures. Table 7 lists the underestimated ratio by utilizing the differences shown in Figure 33 divided by the estimated J-integral toughness. The ranking list comparison is summarized in Table 8. If top, median and low classifications based upon fracture resistance are assigned with numbers 3, 2, and 1 correspondingly, Figure 34 demonstrates graphically the data in Table 8.

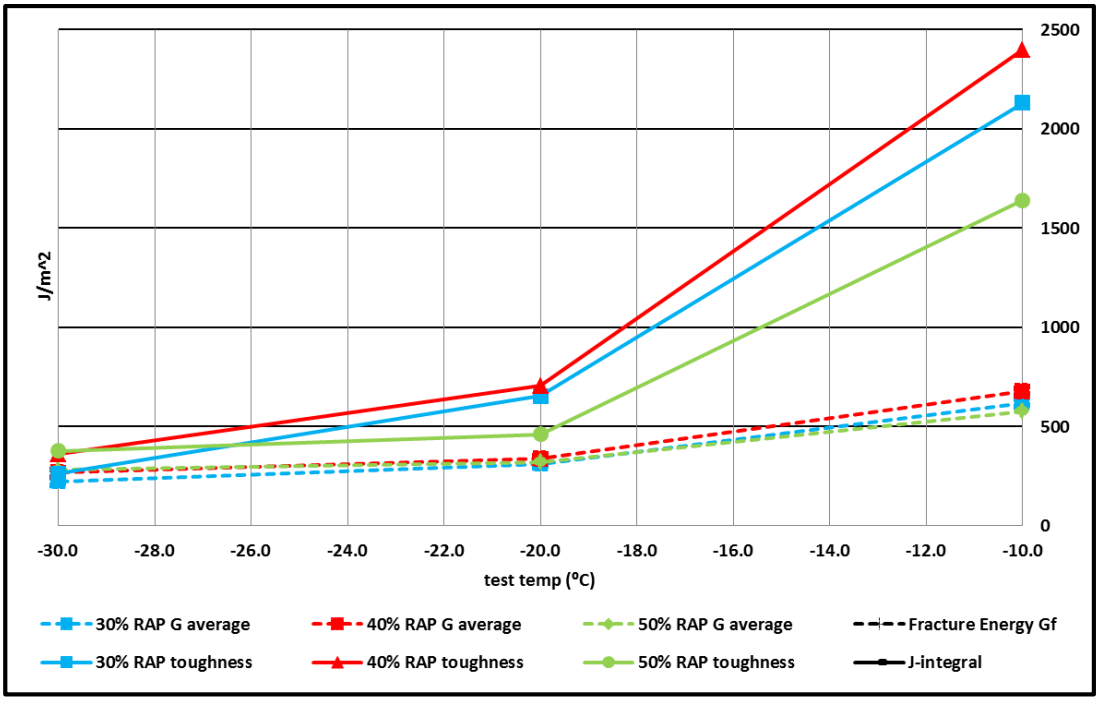

Figure 33. Fracture energy vs. Fracture toughness

Table 7. Underestimated ratio

Underestimated rate			
	30% RAP	40% RAP	50% RAP
-10°C	71.03%	71.79%	64.86%
-20°C	52.47%	52.14%	30.39%
-30°C	14.58%	25.73%	25.04%

Table 8. Ranking list for parameters

Parameters	-10°C	-20°C	-30°C
Kic	50%>40% >30%	40%>30%>50%	50%>40%>30%
PeaK Load	40%>50%>30%	40%>30%>50%	40%>50%>30%
Gf	40%>30%>50%	40%>50%>30%	50%>40%>30%
J toughness	40%>30%>50%	40%>30%>50%	50%>40%>30%

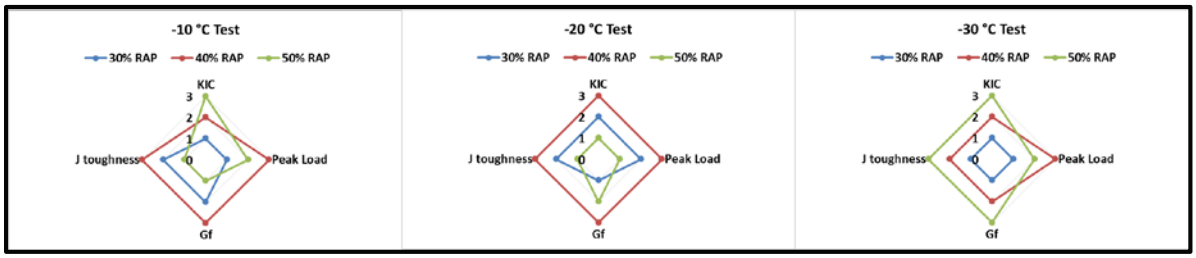

Figure 34. Ranking lists comparison analysis of introducing RAP materials

Energy is the production of force with the load-line movement distance. One brittle, but stiffer, mixture does not mean its toughness is less than a ductile, but softer mixture. At -30^{0}C, the mixture with 50% RAP materials actually has a little higher strain energy (production) per additional cracking advancing than the other mixtures (Figures 32 and 34). At

this temperature, if none of the mixtures can deform into large amounts and sustain a sufficient movement distance (the softer binder cannot help the SCB sample deform more without cracking), the mixtures containing more RAP result in higher stiffness (higher strength) and can perform better than the others against cracking. When temperatures rise higher, both 30 and 40% RAP mixtures are able to sustain more deformations (longer crack bridging distance) to reveal their advantages. The production per cracking propagation allows 40% RAP mixtures to perform outstandingly at -20°C to -10°C. Then, perhaps the 30% Rap mixture might become even better at environments above -10°C.

Analysis for Notch Size Effect

Figure 35 summaries the average values of the coefficient of variation (CV) for G_f from all mixtures at three test temperatures. The values for variations listed in Table 6 were calculated, based on sample data from the same asphalt mixtures with different notch sizes. Therefore, this plot shows the trend of the notch size effect on the experimental outcomes in varying test temperatures as the asphalt materials transition from pseudo-ductile (-10°C) to pseudo-brittle (-20°C), and then brittle (-30°C) material behaviors.

In general terms, the increase in temperature has a positive relationship with the variability of G_f. The coefficients of variance for the G_f values coming from notch size effects progressively rise with increasing test temperatures. As discussed previously, when the material mainly deforms under linear-elastic conditions, the notch size effect is very small and can be ignored, which happens for asphalt mixtures at very low temperatures. Thus, the SCB measured G_f can safely be used to estimate material toughness at the onset of fracture initiation. The conveniently calculated G_f is a good estimator for the true fracture energy of the material.

However, when the CV value increases, the elastic-plastic deformation dominates the phenomenon. Therefore, the G_f value is not a good estimator for any toughness. The "CV vs. Temp Plot" can be introduced to verify the suitability of applying the fracture energy method. CV values are highly associated with both indicators' efficiencies and stabilities to rank the asphalt materials with varying RAP contents.

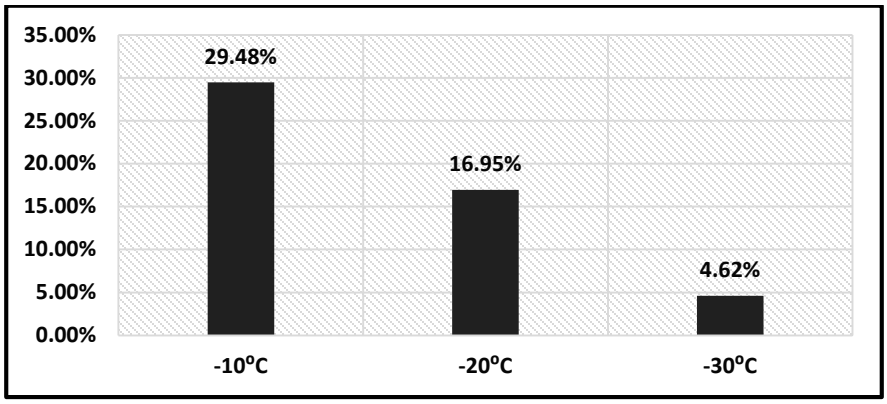

Figure 35. Coefficient of variation vs. test temperature

Correlation Coefficient Analysis for Suitability

By calculating the correlation coefficient between the estimated J_{SS} toughness with values from the other parameters, the suitability for applying other parameters to correctly classify asphalt mixtures can be assessed. The correlation coefficient value explains how strongly two variables are related to each other. One or negative one represents the strongest positive or negative linear correlation, and zero suggests two variables have no correlation. The correlation coefficients between J-integral toughness and other fracture parameters from the effect of temperatures or RAP content percentages are summarized in Tables 9 and 10, respectively.

The average correlation coefficients from Table 9 show all parameters are sound to detect temperature effects on fracture resistance, comparing with the estimated J-integral critical values. The correlation coefficient for G_f is 0.9993, estimated K_{IC} is 0.8695, and the peak load is 0.9277—strong correlations (may not be statistically significant linear correlated) with the J-integral toughness with varying temperatures for each type of asphalt mixture with varying amounts of RAP. Thus, if the relationship (only the trend) between fracture resistances with changing temperatures for only one particular material is recovered, all the aforementioned parameters can be reasonably used to provide the changing trend.

However, when it comes to ranking fracture resistance among different asphalt materials via the variation in the amount of RAP, the conclusions are different as shown in Table 10. All parameters can generally be used to rank the materials at the -30°C testing temperature. The estimated K_{IC} and peak load may even rank the asphalt materials fairly at -20°C; whereas, G_f does not. However, the G_f does provide the correct rank at the -10°C test temperature; whereas, the estimated K_{IC} and peak load do not. For temperatures above -20°C where the materials are pseudo ductile, there are no alternative parameters from the original SCB fracture energy test that can be used to appropriately evaluate the toughness of asphalt materials, except by conducting the SCB toughness test. It is interesting to note, even without correctly and quantitatively estimating the fracture resistance, as long as the materials have dramatic differences in fracture resistance, G_f can still provide a reasonable ranking list for comparing the materials. The proposed SCB toughness experiment for testing samples with varying notch sizes should be applied to assess toughness for appropriate comparisons when quantitative information are required.

Table 9. Correlation coefficient among parameters due to the effect of temperatures

	30% RAP					40% RAP					50% RAP			
Unit	K Factor MPa · m^1/2	Peak Load Kn	Gf J/m^2	J toughness J/m^2	Unit	K Factor MPa · m^1/2	Peak Load Kn	Gf J/m^2	J toughness J/m^2	Unit	K Factor MPa · m^1/2	Peak Load Kn	Gf J/m^2	J toughness J/m^2
-10°C	0.96	3.43	617.24	2130.31	-10°C	0.99	3.66	676.02	2395.98	-10°C	0.99	3.53	576.32	1640.00
-20°C	0.91	3.25	310.71	653.66	-20°C	0.94	3.44	337.26	704.69	-20°C	0.86	3.03	320.92	461.04
-30°C	0.84	3.11	223.76	261.96	-30°C	0.89	3.33	267.27	359.88	-30°C	0.94	3.28	281.73	375.85

	K Factor	*Peak Load*	*Gf*	*J toughness*
K Factor	1			
Peak Load	0.9886548	1		
Gf	0.9190016	0.96779452	1	
J toughness	0.9142851	0.96475635	0.9999	1

	K Factor	*Peak Load*	*Gf*	*J toughness*
K Factor	1			
Peak Load	0.9743485	1		
Gf	0.9211939	0.98512952	1	
J toughness	0.9204523	0.98480101	1	1

	K Factor	*Peak Load*	*Gf*	*J toughness*
K Factor	1			
Peak Load	0.9948916	1		
Gf	0.7327403	0.79769398	1	
J toughness	0.7737846	0.83377794	0.9981	1

	K Factor	0.8695073
AVERAGE	Peak Load	0.92777844
Value	Gf	0.99932631
	J toughness	1

Table 10. Correlation coefficient among parameters due to RAP content percentages

	-10°C					-20°C					-30°C			
Unit	K Factor MPa · m^1/2	Peak Load Kn	Gf J/m^2	J toughness J/m^2	Unit	K Factor MPa · m^1/2	Peak Load Kn	Gf J/m^2	J toughness J/m^2	Unit	K Factor MPa · m^1/2	Peak Load Kn	Gf J/m^2	J toughness J/m^2
30% RAP	0.96	3.43	617.24	2130.31	30% RAP	0.91	3.25	310.71	653.66	30% RAP	0.84	3.11	223.76	261.96
40% RAP	0.99	3.66	676.02	2395.98	40% RAP	0.94	3.44	337.26	704.69	40% RAP	0.89	3.33	267.27	359.88
50% RAP	0.99	3.53	576.32	1640.00	50% RAP	0.86	3.03	320.92	461.04	50% RAP	0.94	3.28	281.73	375.85

	K Factor	*Peak Load*	*Gf*	*J toughness*
K Factor	1			
Peak Load	0.7377348	1		
Gf	-0.028677	0.65365663	1	
J toughness	-0.297134	0.42539431	0.963	1

	K Factor	*Peak Load*	*Gf*	*J toughness*
K Factor	1			
Peak Load	0.9964261	1		
Gf	0.4978547	0.5693316	1	
J toughness	0.9822802	0.96293874	0.3265	1

	K Factor	*Peak Load*	*Gf*	*J toughness*
K Factor	1			
Peak Load	0.7485671	1		
Gf	0.966133	0.89431426	1	
J toughness	0.9311479	0.93880574	0.9937	1

Conclusions and Recommendations

Fracture Toughness Evaluation for Asphalt Mixtures Containing RAP Materials

Fracture toughness tests performed on asphalt mixtures containing 30, 40, and 50% RAP reveal the ranking list changes with varying temperatures (Figure 32). None of asphalt mixtures evaluated in this research preserves its own advantage for the entire temperature range from -30 to -10°C.

Fracture Parameter Evaluations

At -30°C, all parameters from the original SCB fracture energy test can fairly analyze the testing results. The variations accounted from the specimen geometry and notch tip sharpness eliminate application to finely ranked material at relatively higher temperatures by utilizing relatively small size specimens. Once again, peak load, estimated K_{IC}, and G_f data have substantial variance, which limit application, but does not mean it cannot rank the fracture property between very weak and strong mixtures. Because the fatigue precracking treatment is skipped, the preexisting crack tip sharpness, the tip location (stone or sand or binder), and relatively small specimens result in certain variations of the fracture toughness K_{IC}, when relatively small specimens are utilized.

Fracture energy, G_f, successfully quantifies fracture toughness at -30°C. However, test results tend to underestimate the ductile material dramatically and overstate the stiffer material with increasing test temperatures. In other words, as the temperature rises above the glass transition value of the asphalt binder, the fracture energy estimator, G_f, tends to underestimate the ability of the more ductile asphalt mixture against cracking. The higher the testing

temperature, the more underestimation in the results. If the original SCB test protocol is selected for study, the sample with a small size notch is recommended.

Based on research findings and experimental practice, the original fracture energy protocol is only recommended for low temperatures. Even then, validation varies case-by-case, depending upon the plastic zone size of the asphalt mixture when it deforms. For tests above -20°C, the application of the old protocol should be suspected.

The proposed new procedures provide much better toughness parameters. However, they still have limitations. The J_{IC} fracture toughness test, based on Begley and Landes' experiment, has the shortcoming of requiring more extensive work. The SCB J_{SS} experiment provides experimental values for J_{SS}, which could be a number between the actual J_{IC} and J_{SS}. Whether the experimentally estimated J_{SS} is closed to the actual J_{IC} or J_{SS} depends upon the material's deformation yielding scale and the distance for approaching a steady-state cracking. Therefore, in the future, the elastic compliance should be introduced into the asphalt SCB test and follow the ASTM standard to measure the J R-curve. At this point, the old SCB test will completely change. The CMOD will not be used for loading rate control, but for estimating crack extension. Data from only one sample can produce a J R-curve and test data from multiple samples can be utilized to obtain an average J R-curve with a higher confidence level. Table 11 summarizes the efficiencies and suitability for all parameters from SCB tests.

Table 11. Summary of efficiencies and suitability for all parameters

Experiment	Notch Size for one mixture (mm)	Efficent Experimental Parametor	Feasibility Application Condition	Practicability Temp Range (°C)	Note
Original Current SCB	15	Gf (J/M^2)	LEFM	≤-20°C (For ordinary binder)	only applied to very low temp when mixture is brittle
		KIc (MPa · m^0.5)			
		Stiffness (S)			
The new *J* ss SCB	8, 15, 25	Gf (J/M^2)	LEFM	≤-20°C (For ordinary binder)	only applied to very low temp when mixture is brittle
		KIc (MPa · m^0.5)			
		Stiffness (S)			
		Experimental estimated *J* ss (J/M^2)	LEFM & EPFM	No Limits (but for very ductile and fine mixture used for inter layer applications, the SCB speciment size need be increased)	at LEFM condition, experimental esimated Jss = JIC = Gf, at EPFM condition experimental estimated Jss ≈ Jss.
The new J_{IC} SCB	8, 15, 25	Gf (J/M^2)	LEFM	≤-20°C (For ordinary binder)	only applied to very low temp when mixture is brittle
		KIc (MPa · m^0.5)			
		Stiffness (S)			
		Experimental estimated Jss (J/M^2)	LEFM & EPFM	No Limits (but for very ductile and fine mixture used for inter layer applications, the SCB speciment size need be increased)	at LEFM condition, experimental estimated Jss = J_{IC} = Gf, at EPFM condition experimental estimated Jss ≈ Jss and experimental J_{IC} ≈ J_{IC}
		Experimental estimated J_{IC} (J/M^2)	LEFM & EPFM	No Limits	

References

Landes, J.D. and Begley, J.A., 1972. The effect of specimen geometry on J_{IC}. *ASTM STP 514, American Society for Testing and Materials*, Philadelphia, 24-29.

Begley, J.A. and Landes, J.D., 1972. The J-integral as a fracture criterion. *ASTM STP 514, American Society for Testing and Materials*, Philadelphia, 1-20.

ASTM E1823. Standard terminology relating to fatigue and fracture testing, *American Standard of Testing Materials.*

Zhu, X.K. and Joyce, J.A., 2012. Review of fracture toughness (G, K, J, CTOD, CTOA) testing and standardization. *Engineering Fracture Mechanics*, 85, 1-46.

Anderson, T.Y., 1991. *Fracture mechanics.* Boca Raton, FL: CRC Press, Inc.

ASTM E399. Standard test method for linear-elastic plane-strain fracture toughness K_{IC} of metallic materials, *American Standard of Testing Materials*.

ASTM E561. Standard test method for K-R curve determination, *American Standard of Testing Materials.*

ASTM E813. Standard test method for J_{IC}, a measure of fracture toughness, *American Standard of Testing Materials*.

ASTM E1152. Standard test method for J-R curves, *American Standard of Testing Materials*.

ASTM E1290. Standard test method for crack opening displacement (CTOD) fracture toughness measurement, *American Standard of Testing Materials.*

ASTM E1737. Standard test method for J-integral characterization of fracture toughness, *American Standard of Testing Materials.*

ASTM E1820. Standard test method for measurement of fracture toughness, *American Standard of Testing Materials.*

ASTM E1921. Standard test method for determining od reference temperature T_0 for ferritic steels in the transition range, *American Standard of Testing Materials.*

Kim, M., Mohammad, L.N., and Elseifi, M., 2012. Characterization of fracture properties of asphalt mixtures as measured by semicircular bend test and indirect tension test. *Journal of the Transportation Research Board*, 2296, 115-124.

Lim, I.L., Johnston, I.W., and Choi, S.K., 1993. Stress intensity factors for semi-circular specimens under three-point bending. *Engineering Fracture Mechanics*, 44(3), 363-382.

Li, X. and Marasteanu, M.O., 2004. Evaluation of the low temperature fracture resistance of asphalt mixtures using the semicircular bend test. *Journal of the Association of Asphalt Paving Technologists*, 73, 401-426.

CHAPTER 4. FRACTURE TOUGHNESS DETERMINATION OF ASPHALT MIXTURES CONTAINING RECLAIMED ASPHALT PAVEMENT (RAP) MATERIALS

A paper to be submitted to Construction and Building Materials

Sheng Tang and R. Christopher Williams

Abstract

The semi-circular bending (SCB) fracture energy method has been selected to evaluate the low-temperature fracture resistance for asphalt pavement materials due to its convenience. However, under certain temperature conditions, these parameters can be inappropriately employed, leading to incorrect conclusions. The proper application of the current fracture energy test is limited by SCB specimen geometry size and sample testing temperature. A new fracture mechanics-based SCB toughness J_{SS} test, suitable for asphalt mixtures, is applied in this research. The modified SCB toughness test can provide better measurements by estimating J_{SS}, representing the fracture resistance for cracks extended at a steady state. Both the current SCB fracture energy test and the SCB fracture toughness test are applied on asphalt mixtures to investigate their fracture resistance in relationship to various proportions of reclaimed asphalt pavement materials' contents (30, 40, and 50%) and batching methods (Traditional and Fractionated Methods) at different low temperatures (-10, -20, and -30°C).

Generally, fracture energy and experimental estimated toughness rise with increasing test temperatures. The experimental outputs of both traditional and fractionated batched mixtures suggest adding more reclaimed asphalt materials benefits asphalt mixtures to prevent cracking at -30°C. However, this advantage, by introducing reclaimed asphalt materials,

diminishes with increased temperatures. When temperatures rise above -30°C, mixtures with less reclaimed asphalt materials start to demonstrate better fracture performance. When evaluating and comparing all six asphalt mixtures studied in this research, none preserves its own advantage for the entire temperature range from -30 to -10^{0}C.The estimated toughness of traditional batched mixtures is generally slightly higher than the fractionated prepared mixtures between the tested temperature range (-30 to -10^{0}C). This may be due to additional asphalt binder content and more fine aggregate materials.

Introduction

Reclaimed asphalt pavement technology has been applied in the United States for more than 30 years. There is a tendency for many owner agencies to utilize more reclaimed asphalt material due to environmental and economic benefits. Florida Department of Transportation shows, by utilizing reclaimed asphalt pavement materials (RAP), 15 to 30% construction costs can be saved (Page and Murphy 1987, Page 1988). This increasing RAP utilization is and will continue to be driven by historically high asphalt binder prices, high quality aggregates existing in pavement rehabilitation projects, and increasing awareness of environmental stewardship and sustainability issues.

However, increasing RAP utilization may adversely lead to pavement deterioration from distress, including thermal cracking, raveling, and weathering (Solaimanian and Kennedy 1995). Most of the concerns for applying RAP are related to low temperature cracking, considering the stiffness of the asphalt mixture can dramatically increase through introducing RAP (Sargious and Mushule 1991, McDaniel et al. 2000). Correctly and conveniently evaluating fracture resistances for asphalt mixtures is critically important for pavement mixture

design, material selection, and in-situ service performance modeling. A fair correlation between measured toughness of asphalt mixtures at 25°C with in-situ pavement performance index has been established (Kim et al. 2012). Fracture toughness in terms of the J-integral has been determined a useful parameter for evaluating fracture resistance of asphalt mixtures subjected to moderate temperature environments (25°C). However, fracture resistance at low temperature for asphalt mixtures containing high percentages RAP has not been correctly estimated by utilizing toughness parameters, yet. More research to correctly assess fracture toughness of asphalt mixtures at low temperatures and its correlation with low temperature cracking is required.

The purpose of this paper is to apply the adopted SCB fracture toughness J_{SS} test to estimate asphalt mixtures toughness in relationship to various proportions of RAP contents and batching methods at different low temperatures.

Experimental Materials and Methods

Generally, asphalt mixtures for SCB testing were prepared, based upon volumetric criteria. The utilized virgin binder has a performance grade (PG) 58-28. Reclaimed asphalt pavement materials were added to replace 30, 40, and 50% of the optimum binder content by mass. This mixture design method is often referred as the binder replacement method. All samples were designed to include 7% ± 1% air voids at the optimum binder content, using aggregates with the design gradation.

Three RAP percentages with two different RAP addition method (Traditional and Fractionated Methods) combinations developed six different asphalt mix designs. RAP

materials were mixed with virgin limestone aggregate and binder to prepare asphalt mixtures for SCB fracture tests. The mixed asphalt mixture materials are compacted into 170mm (high) x 150mm (diameter) cylinders by a gyratory compactor. Those asphalt-mixture cylinders with different RAP contents were machined into semi-circular shape specimens with 25mm in thickness. Thirty-six SCB specimens with three notch sizes (8, 15, and 25mm), respectively, were fabricated from cylinders for each mix design. This results in a total of 216 specimens tested at three different low temperatures (-10, -20, and -30°C). SCB samples for each type of mixtures were shuffled before notch cutting for random sampling purposes. Additionally, all the values of radius, thickness, and notch size for each SCB specimen were determined as an average of two measurements. This is critically important for sequential calculations and analysis. The plan for the experimental design is illustrated in Table 12.

Table 12. Experimental design for the SCB fracture tests

Batch Method	Test Temp	Mixture with 30% RAP			Mixture with 40% RAP			Mixture with 50% RAP		
Traditional Method	-10(°C) -20(°C) -30(°C)	SCB Samples with 8mm Notch	SCB Samples with 15mm Notch	SCB Samples with 25mm Notch	SCB Samples with 8mm Notch	SCB Samples with 15mm Notch	SCB Samples with 25mm Notch	SCB Samples with 8mm Notch	SCB Samples with 15mm Notch	SCB Samples with 25mm Notch
Fractionated Method	-10(°C) -20(°C) -30(°C)	SCB Samples with 8mm Notch	SCB Samples with 15mm Notch	SCB Samples with 25mm Notch	SCB Samples with 8mm Notch	SCB Samples with 15mm Notch	SCB Samples with 25mm Notch	SCB Samples with 8mm Notch	SCB Samples with 15mm Notch	SCB Samples with 25mm Notch

Reducing the number of experimental variables is the key to focus on evaluating the performance of the RAP binder and its influence on fracture performance. Thus, aggregate gradation must be controlled to isolate the binder effect when one RAP adding method is applied. Therefore, only two gradations for the six different mixtures were developed with the primary difference being the higher percentage of material passing the #30 sieve for the traditional RAP based mixes. The differences between the mixes prepared by two RAP

addition methods were still preserved, while the gradation variations among the mixes applying the same RAP adding method were minimized. This similarity of gradation can be achieved by adding varying amounts of virgin aggregate with different aggregate sizes regarding the RAP contents and gradations. The final gradations of the six mixtures containing RAP materials are shown in Table 13. The optimal binder contents are 5.34 and 5.0% for traditional and fractionated batch samples, respectively.

Table 13. Design gradations of the mixtures by adding RAP

	3/4"	1/2"	3/8"	No. 4	No. 8	No. 16	No. 30	No. 50	No. 100	No. 200
All % RAP Samples applying traditional batch method	100	90.0	80.0	60.4	44.5	33.8	23.3	14.1	7.6	6.3
All % RAP Samples applying fractionated batch method	100	93.7	84.6	62.9	45.1	33.6	22.6	13.3	6.7	5.5

Asphalt Binder Test

RAP binder extraction and recovery tests, and performance grading tests were performed to evaluate binders' rheological properties. The aged binder from RAP materials first was dissolved in toluene. Then, two centrifuges with low and high operational speeds were applied to separate the solvent, containing binder, from the aggregate (Figure 36).

Since toluene has a lower boiling temperature than the asphalt binder, a rotary evaporator system (Figure 37) can be utilized to distill toluene and retain the RAP binder in the container. The asphalt binder extraction and recovery tests were implemented in accordance with AASHTO T164 and AASHTO T319 standards, utilizing the centrifuge and rotary evaporator system (ASASHTO T164, T319). Minimizing additional aging of the binder during the recovering process can be achieved by introducing nitrogen. Next, the extracted binder was blended with virgin binder in 30, 40, and 50% for the sequential binder testing on a mass basis.

The aged binder replacement percentage is consistent with the RAP percentages for the mix testing.

(a) **(b)**

Figure 36. Low-Speed (a) and High-Speed (b) centrifuges

Figure 37. A rotary evaporator system

A dynamic shear rheometer (DSR) was used to test two replicate samples for each RAP and virgin binder combination, according to ASTM D 7175 (2005), to characterize the

rheological properties of the binders at high and intermediate temperatures. The complex modulus (G*) and phase angle (δ) were determined with a DSR for the initial binder and residual binder after every asphalt aging treatment (RTFO, PAV). The complex modulus (G*) and phase angle (δ) were used later to determine the high and intermediate critical temperatures, and the binder grade ranges.

A bending beam rheometer (BBR) was applied to evaluate the treatment group's susceptibility to thermal cracking at low service temperatures (The Asphalt Institute 2003). Two key properties, stiffness (S) and change in stiffness (m-value) were recorded according to ASTM 6648 (2001). The BBR test was utilized to determine the low critical temperatures.

The SCB Fracture Testing

The SCB test setup for fracture toughness tests is shown in Figure 38(a) and (b). Semi-circular asphalt specimens with a notch in varying sizes (8, 15, and 25mm) were tested with a UTM hydraulic testing machine. All experiments were performed in an environmental chamber, using liquid nitrogen to stabilize the ambient temperatures at -10, -20, and -30°C.

The SCB sample in Figure 38(c) is supported by two fixed rollers with a span of 120mm. The span-to-radius ratio (s/r) is confined to 0.8. Vaseline was placed on the rollers to reduce friction. Two lateral fixtures were designed and utilized to prevent sample tilts during testing. The load-line displacement in the vertical direction was recorded with a loading actuator. The crack-mouth opening displacement (CMOD) in the horizontal direction was measured by an Epsilon clip gauge hung between two knife edges. These two knife edges were attached at the bottom of the specimens. Both loading actuator and CMOD measurements were utilized to control the loading system. In other words, the loading system applies the load such that

constant deformation speed is obtained. A loading procedure with slow constant deformation speeds intends to stabilize fracture extension.

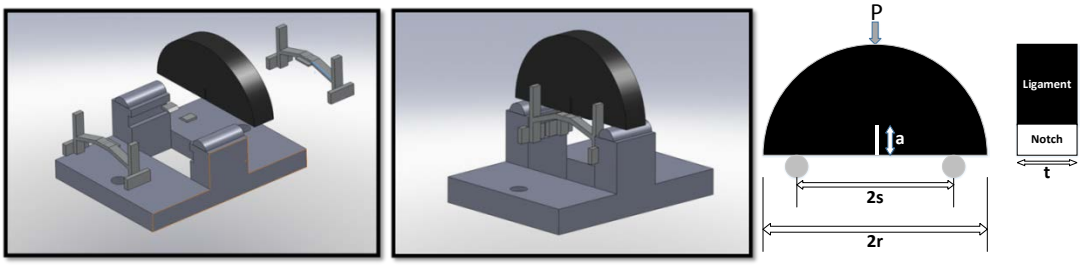

(b) **(b)** **(c)**

Figure 38. The SCB experiment setup (a) and (b) with one asphalt specimen (c)

The entire loading procedure was separated into four loading blocks, and was controlled to achieve four displacement speeds (0.05, 0.005, 0.001, and 0.0005mm/s). These speeds are sequentially and progressively dropped to prevent samples suddenly crashing. Figure 39 illustrates the loading actuator and CMOD displacements data recorded during a typical loading process. Constant slopes of lines in Figure 39 represent constant deformations speed. Red lines (1, 2, and 3) illustrate the loading actuator displacements at rates (1) 0.05, (2) 0.005, and (3) 0.001mm/s, respectively. These loading actuator displacement speeds govern three loading blocks. The CMOD displacements are shown as black line 4. Once the loading force (1kN) was reached, the loading system triggered was governed by the CMOD starting from the arrow point with a displacement rate 0.0005mm/s. Tests were terminated, when the vertical loading was smaller than 0.5kN.

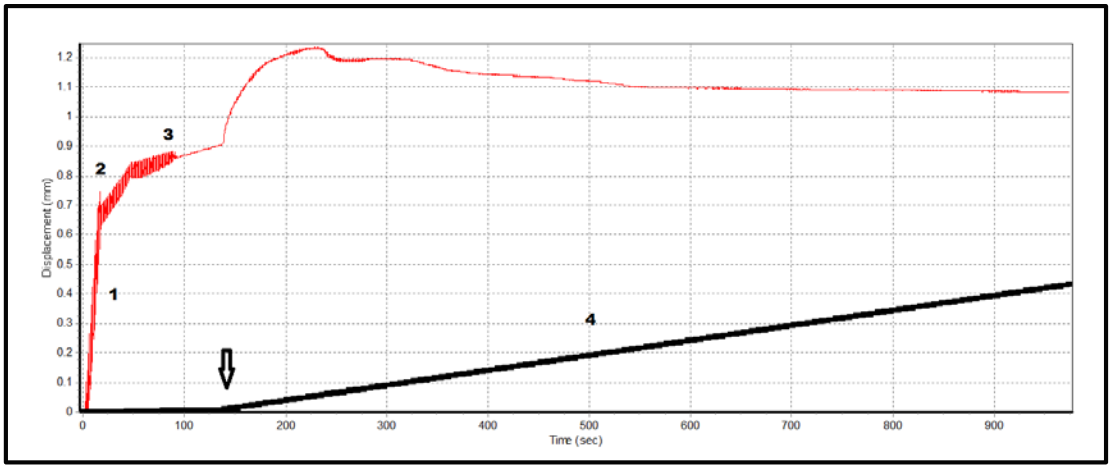

Figure 39. Loading rates (mm/s) at (1) 0.05, (2) 0.005, (3) 0.001, and (4) 0.0005

The SCB Fracture Energy Method

The original SCB fracture energy protocol is found elsewhere (InTrans website under AMPP). Load displacement curve (Figure 40) can be used to obtain G_f by the following,

$$G_f = \frac{W_f}{A_{lig}}, \qquad \text{(equation 25)}$$

where:

$G_f = fracture\ energy\ (J/m^2)$,

$W_f = \int Pdu$,

$P = applied\ load\ (N)$,

$u = average\ load\ line\ displacement\ (m)$,

$A_{lig} = ligament\ area\ (m^2)$,

$A_{lig} = (r - a) \times t$,

$r = specimen\ radius\ (m)$,

$a = notch\ length\ (m)$, and

$t = speciment\ thickness\ (m)$.

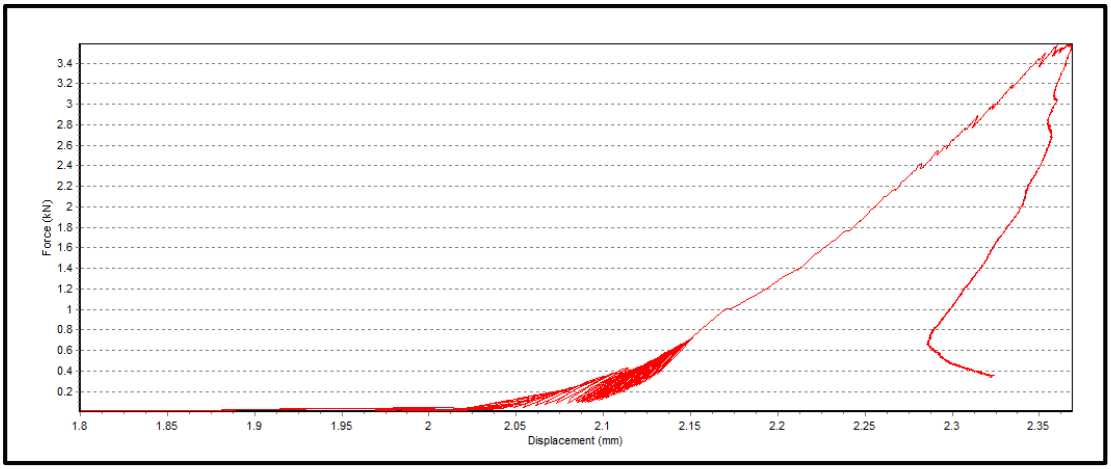

Figure 40. The SCB test plot with load displacement curve

Figure 40 illustrates a typical load displacement plot for a SCB fracture experiment with a single notch conducted at -30°C. The x-axis is the load-line displacement captured by the machine's loading actuator. The y-axis is the loading force.

Total work is the area under the entire load-line displacement curve, a red curve in Figure 40, for a particular SCB sample in certain geometries (radius, thickness, and notch size). The conveniently-calculated G_f (if neglecting the viscous dissipation of the material and kinetic energy transfer) is utilized to assess fracture resistances when the small-scale yielding condition is satisfied. However, when the small scale yielding condition is not satisfied, the measured value of G_f will be extremely geometry-dependent, and diverse from its true fracture toughness.

The SCB J-integral Method

The SCB J_{SS} experiment has the same test procedure as the SCB fracture energy G_f test, except testing additional SCB samples with varying notch depths and applying subsequent different calculations, based upon Begley and Landes' method (Begley and Landes 1972). This

SCB J-integral method provides a critical energy changing rate J_{SS} rather than applying the conventional average method to obtain G_f.

The Jss integral represents the critical energy-changing rate for cracks approaching a steady state. This is an interesting parameter when an elastic-plastic material needs evaluation for its full resistance of fracture extension. This J_{SS} can be expressed as,

$$J_{ss} = -\frac{1}{B}\left(\frac{\partial U}{\partial a}\right)_{\Delta \text{ Steady State}}, \qquad \text{(equation 26)}$$

where the value of ∂U is the changing area under the entire load-line curve, when multiple samples with a notch in varying sizes are tested and ∂a is the size difference. Since ∂U is the changing area under the entire load displacement curve, the steady-state fracture is presumed. The SCB J-integral method can be used, even if the small-scale yielding condition is not satisfied, which provides a broader application. The Jss toughness in this research is determined, based upon the slope of the total work versus crack propagation distance as shown in Figure 41.

Experimental Results and Analysis

PG grading test results for asphalt binders containing RAP binder in varying percentages are summarized in Table 14. Little difference was observed between the control group (no recovering treatments) with the recovering treated group. This indicates an additional aging of the binder was minimized by introducing nitrogen during the recovering process. PG grading test results of recovered asphalt binder can represent binder's rheological properties. Both the BBR and DSR testing results indicate the binder becomes stiffer with an increasing amount of

aged binder. However, the changes are insignificant between specimens with 30 and 40% RAP binder, until the 50% RAP binder was introduced.

Table 14. Binder performance grading data

Sample		Critical High Original (^{O}C)	Critical High RTFO(^{O}C)	Test at -18 ^{O}C		Test at -12 ^{O}C		Low Critical Temp(^{O}C)	PG Grade
				M-Value	Stiffness	M-Value	Stiffness		
50%RAP	1	72.35	71.11	0.261	329	0.324	164	-22	PG 70-22
	2	71.70	71.58	0.26	335	0.331	160		
40%RAP	1	70.51	69.03	0.277	272	0.345	116	-22	PG 64-22
	2	69.20	69.26	0.274	306	0.347	130		
30%RAP	1	67.42	68.12	0.289	283	0.356	125	-22	PG 64-22
	2	67.22	68.19	0.281	301	0.35	132		
0% RAP	Control Group	61.46	60.50	0.299	269	0.355	122	-28	PG 58-28
		61.76	60.63	0.299	256	0.369	112		
	Recovered Group	60.95	62.05	0.299	269	0.356	123	-28	
		61.02	63.30	0.304	276	0.361	119		

Table 15 summarizes the average SCB test results for asphalt specimens prepared with three notch sizes (8, 15, and 25mm), containing 30, 40, and 50% RAP materials, tested at three low temperatures (-10, -20, and -30°C), and prepared by applying the traditional and fractionated addition methods. Each number is the average value of test results from four experimental replicates. In general terms, both G_f (energy per fracture area) and total work (total energy) values decrease with a drop in test temperature or with an increase in the notch size and all other factors constant. The crack propagation distance (crack advancing distance), Δa, equals the radius of the SCB sample subtracted by the notch size. The total work is the energy integrated for the 25mm thickness SCB sample from the beginning of the loading to the test's termination.

Table 15. Average fracture energy, total work, and crack propagation distance

8mm Notch Size Trad Sample					15mm Notch Size Trad Sample					25mm Notch Size Trad Sample				
	RAP	30%	40%	50%		RAP	30%	40%	50%		RAP	30%	40%	50%
Gf (J/m^2)	-10°C	1026.70	841.30	895.54	Gf (J/m^2)	-10°C	680.96	741.48	596.82	Gf (J/m^2)	-10°C	460.58	431.55	409.73
	-20°C	331.40	364.38	413.15		-20°C	323.79	344.28	344.44		-20°C	274.13	288.06	323.37
	-30°C	299.34	318.45	317.21		-30°C	253.29	264.56	278.30		-30°C	274.41	276.76	283.66
	RAP	30%	40%	50%		RAP	30%	40%	50%		RAP	30%	40%	50%
Total W (J)	-10°C	1.704	1.377	1.449	Total W (J)	-10°C	0.992	1.117	0.886	Total W (J)	-10°C	0.571	0.549	0.525
	-20°C	0.563	0.586	0.666		-20°C	0.470	0.510	0.516		-20°C	0.343	0.348	0.410
	-30°C	0.493	0.504	0.515		-30°C	0.368	0.386	0.415		-30°C	0.342	0.355	0.364
	RAP	30%	40%	50%		RAP	30%	40%	50%		RAP	30%	40%	50%
Δa (mm)	-10°C	66.42	65.43	64.72	Δa (mm)	-10°C	58.19	61.78	59.36	Δa (mm)	-10°C	49.51	50.83	51.32
	-20°C	65.88	64.37	64.56		-20°C	58.53	59.32	59.85		-20°C	50.13	48.58	50.69
	-30°C	65.88	63.37	64.91		-30°C	58.10	58.40	59.73		-30°C	49.82	51.25	51.34

8mm Notch Size Frac Sample					15mm Notch Size Frac Sample					25mm Notch Size Frac Sample				
	RAP	30%	40%	50%		RAP	30%	40%	50%		RAP	30%	40%	50%
Gf (J/m^2)	-10°C	848.58	848.00	720.63	Gf (J/m^2)	-10°C	574.23	734.89	551.08	Gf (J/m^2)	-10°C	428.90	445.17	457.25
	-20°C	361.48	375.04	362.57		-20°C	323.86	378.57	310.74		-20°C	246.79	258.16	289.44
	-30°C	229.47	279.14	300.61		-30°C	223.69	270.28	278.70		-30°C	218.14	252.37	265.89
	RAP	30%	40%	50%		RAP	30%	40%	50%		RAP	30%	40%	50%
Total W (J)	-10°C	1.366	1.405	1.167	Total W (J)	-10°C	0.858	1.099	0.839	Total W (J)	-10°C	0.531	0.562	0.574
	-20°C	0.601	0.619	0.605		-20°C	0.475	0.562	0.453		-20°C	0.332	0.313	0.337
	-30°C	0.380	0.466	0.501		-30°C	0.335	0.400	0.407		-30°C	0.272	0.314	0.322
	RAP	30%	40%	50%		RAP	30%	40%	50%		RAP	30%	40%	50%
Δa (mm)	-10°C	64.22	65.85	64.25	Δa (mm)	-10°C	59.50	59.60	60.74	Δa (mm)	-10°C	49.53	50.49	50.05
	-20°C	66.55	66.11	66.86		-20°C	58.77	59.38	58.56		-20°C	50.08	48.43	46.73
	-30°C	66.40	66.75	67.08		-30°C	59.91	59.12	58.31		-30°C	49.80	49.84	47.93

The "Total work vs. Crack propagation distance" plots are shown in Figure 41 by using data from Table 15. Mainly, the experimental results illustrate a strong, positive linear relationship between total energy and cracking propagation at -30^{0}C, and reasonably well at -20^{0}C. A nonlinear relationship is observed for the experiments performed at -10^{0}C, regarding the starting point of cracking propagation. The results show the values of total work drop substantially when the temperature decreases from -10 to -20^{0}C, but then change less from -20 to -30^{0}C. When the testing temperate approaches the glass transition ranges of asphalt binders, the fracture resistances are much less temperature dependent. From Figure 41, the values of total work are very close for tests conducted at -20 and -30^{0}C, and relatively far from the experiment results at -10^{0}C.

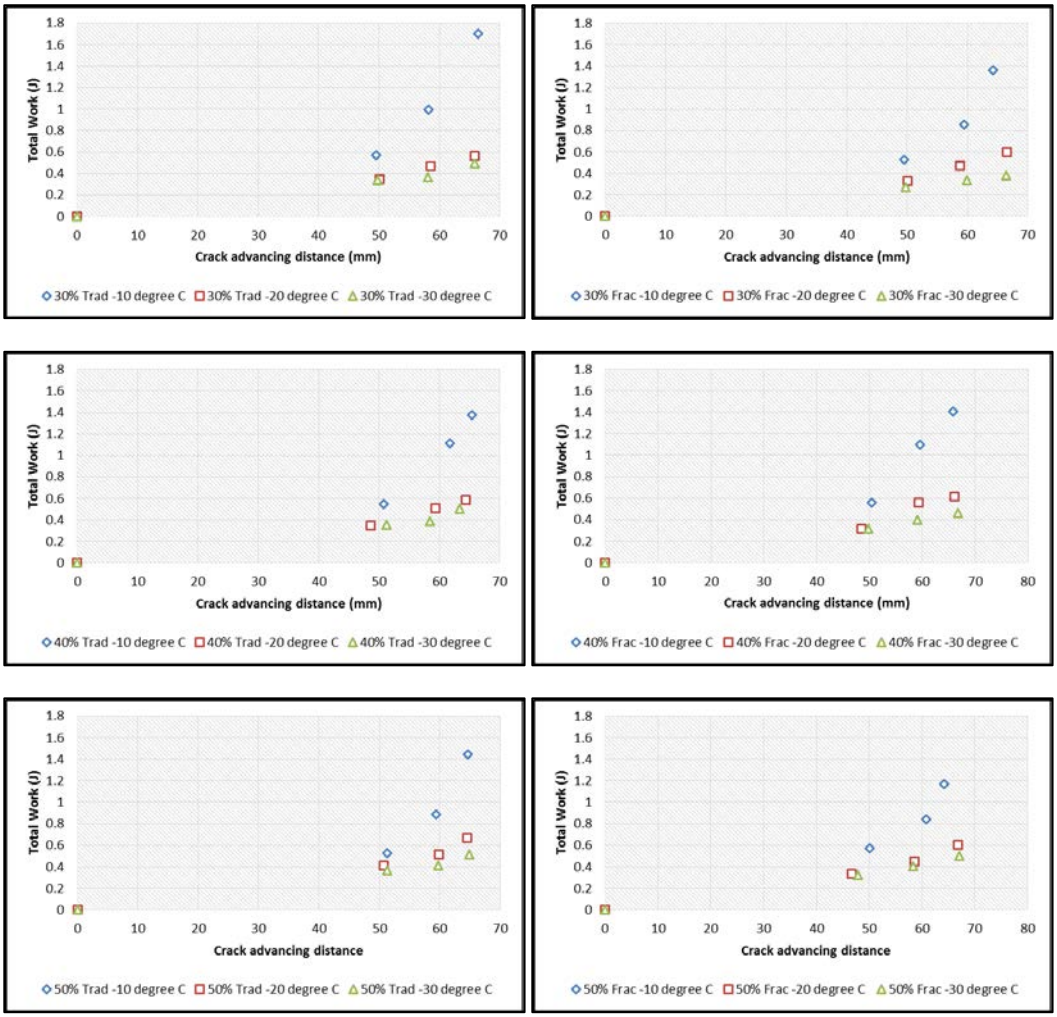

(a) **(b)**

Figure 41. Total work vs. Propagation distance for (a) Trad and (b) Frac samples

The calculated J-integral is the consumed energy per notch depth in unit thickness at a particular loading condition. From the perspective of graphic interpretation, the value of J-integral is equal to the slope for the fitting curve or line at particular locations in Figure 41 divided by sample thickness. The value of J_{SS} is obtained by taking the slope at the end of the right tail of the curves divided by sample thickness. Thus, J_{SS} represents the critical values of the J-integral for fracture at a steady state. The conventional G_f calculation simply uses the entire area under the load-line curve divided by the total ligament area. The ligament area is

the product of the crack advancing distance with sample thickness. Graphically shown on the total work vs. propagation distance plot (Figure 41), the estimated fracture energy G_f is the slope of any straight line connected between the points on the fitting curve with the original zero point and then divided by the sample thickness.

The estimated fracture energy G_f data and their coefficients of variations (CV) are summarized in Table 16 and 17—traditional and fractionated batching methods separately. These variations were calculated, based on data of the samples from the same asphalt mixtures, but with different notch sizes. Therefore, the CV values are the normalized measurements of the dispersion, due to the notch size effect at a certain temperature for a particular asphalt mixture.

Generally, CV values rise with increasing test temperatures progressively from below 10% to more than 30%. When the material mainly deforms linearly and elastically, the notch size effect is very small and can be ignored. This occurs for asphalt mixtures tested at very low temperatures and the values of CV for all experimental mixtures are not greater than 10%. When the CV value increases to 30%, due to increased test temperature, the elastic-plastic deformation dominates the phenomenon. Hence, the size effect is remarkable. In this situation, the estimated fracture energy with huge bias is a poor estimator for fracture resistance. CV values can be applied to evaluate the efficiencies and stabilities to utilize estimated fracture energy to rank different asphalt materials.

Table 16. Fracture energy G_f and coefficient of variation for Trad samples

Test at -10°C				Test at -20°C				Test at -30°C			
Gf fracture energy (J/M^2)	30% RAP Trad	40% RAP Trad	50% RAP Trad	Gf fracture energy (J/M^2)	30% RAP Trad	40% RAP Trad	50% RAP Trad	Gf fracture energy (J/M^2)	30% RAP Trad	40% RAP Trad	50% RAP Trad
8mm	1026.70	841.30	895.54	8mm	331.40	323.79	274.13	8mm	299.34	318.45	317.21
15mm	680.96	741.48	596.82	15mm	364.38	344.28	288.06	15mm	253.29	264.56	278.30
25mm	460.58	431.55	409.73	25mm	413.15	344.44	323.37	25mm	274.41	276.76	283.66
COV	39.48%	31.82%	38.65%	COV	11.13%	3.52%	8.60%	COV	8.36%	9.86%	7.20%
Average Gf	722.75	671.44	634.03	Average Gf	369.64	337.50	295.18	Average Gf	275.68	286.59	293.06
	676.07				334.11				285.11		

Table 17. Fracture energy G_f and coefficient of variation for Frac samples

Test at -10°C				Test at -20°C				Test at -30°C			
Gf fracture energy (J/M^2)	30% RAP Frac	40% RAP Frac	50% RAP Frac	Gf fracture energy (J/M^2)	30% RAP Frac	40% RAP Frac	50% RAP Frac	Gf fracture energy (J/M^2)	30% RAP Frac	40% RAP Frac	50% RAP Frac
8mm	848.58	848.00	720.63	8mm	361.48	375.04	362.57	8mm	229.47	279.14	300.61
15mm	574.23	734.89	551.08	15mm	323.86	378.57	310.74	15mm	223.69	270.28	278.70
25mm	428.90	445.17	457.25	25mm	246.79	258.16	289.44	25mm	218.14	252.37	265.89
COV	34.53%	30.73%	23.16%	COV	18.82%	20.32%	11.72%	COV	2.53%	5.10%	6.23%
Average Gf	617.24	676.02	576.32	Average Gf	310.71	337.26	320.92	Average Gf	223.76	267.27	281.73
	623.19				322.96				257.59		

The averaged fracture energy results from all 8, 15, and 25mm samples are illustrated in Figure 42 (a) for Trad mixture and (b) for Frac mixture. Generally, the averaged fracture energy values increase with increasing temperatures. Both plots suggest adding more RAP materials benefits the asphalt mixture to prevent cracking at -30^{0}C, but this advantage diminishes with increased temperatures for both traditional and fractionated prepared samples. The mixtures with less RAP materials demonstrate better fracture performance when changing from -20 to -10^{0}C generally, and the ranks between traditional and fractionated prepared samples are slightly different.

Figure 43 shows the results of fracture toughness for different mixtures, based upon the SCB JSS method. The estimated toughness J values are calculated from the slope of the curves/lines shown in Figure 41. These values represent the material's ability to resist cracking

at steady state. With increasing temperature, the toughness for both traditional and fractionated prepared samples increases. This general trend agrees with the conclusion generated from fracture energy G_f results. However, fracture resistance values for evaluating each mixture are different compared with the G_f method, which ranks these RAP-added mixtures in a different sequence.

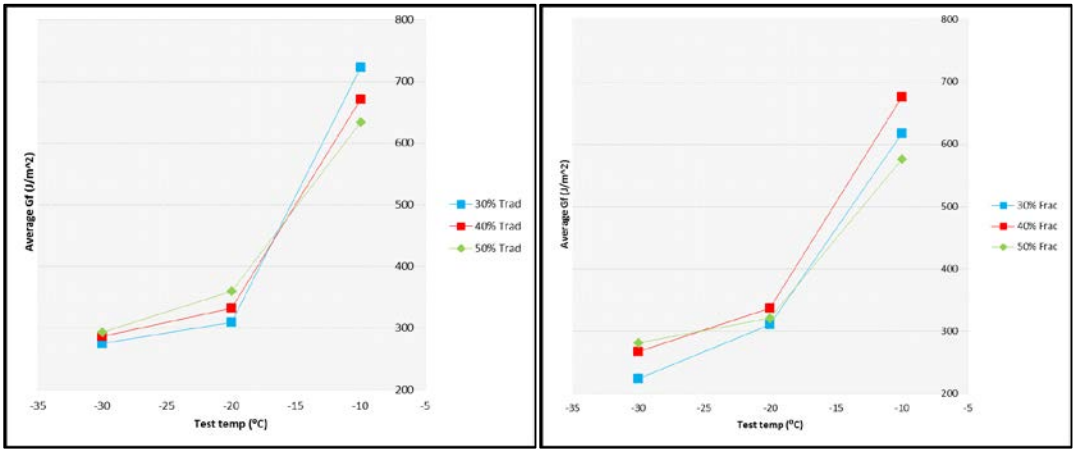

(a) **(b)**

Figure 42. The average fracture energy G_f (J/M^2) of 8, 15, and 25mm samples for (a) Trad and (b) Frac mixtures

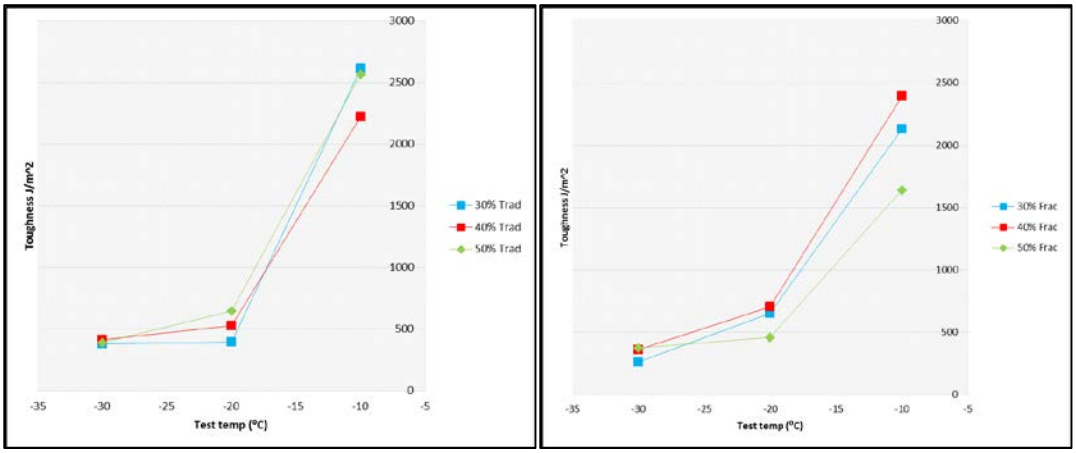

(a) **(b)**

Figure 43. The estimated J_{SS} fracture toughness (J/M^2) for (a) Trad and (b) Frac mixtures containing 30, 40, 50% RAP

Energy is the production of force with changed distance in force direction. One stiffer mixture does not mean its toughness is less than a softer one. Toughness also depends on how much deformation the materials can sustain. At -30^{0}C, the mixture with 50% RAP materials actually has a little higher strain energy (production) per additional crack advancing than the other mixtures. At this temperature, if none of the mixtures deform too much and are subject to a large movement distance (the softer binder cannot help the SCB sample deform more without cracking at the binder glass transition temperature), the mixtures containing more RAP with higher stiffness (higher strength) can even perform better than others to resist cracking extension. When temperatures rise to a higher value, both 30 and 40% RAP mixtures are able to sustain larger deformation (longer crack bridging distance) and reveal their advantages by absorbing more input energy.

Based on observations in Figure 43, this phenomenon is dependent upon the batching method and RAP binder content. For samples batched by applying the traditional method, which have a higher binder content and also may contain more RAP (aged) binder due to additional fine RAP materials, the 30% RAP samples will not show their benefits in toughness until the temperature rises to -15^{0}C. For fractionated prepared samples, immediately after -30^{0}C, 40 and 30% RAP samples start to perform better than the sample with 50% RAP. Continuously, the 40% RAP mixture is distinctive at -20 to -10^{0}C. Hence, RAP percentages and batching methods affect the toughness of asphalt mixtures.

By using the J integral toughness value as the benchmark to assist suitability for applying the SCB fracture energy test, the differences between the G_f fracture energy with toughness are illustrated in Figure 44.

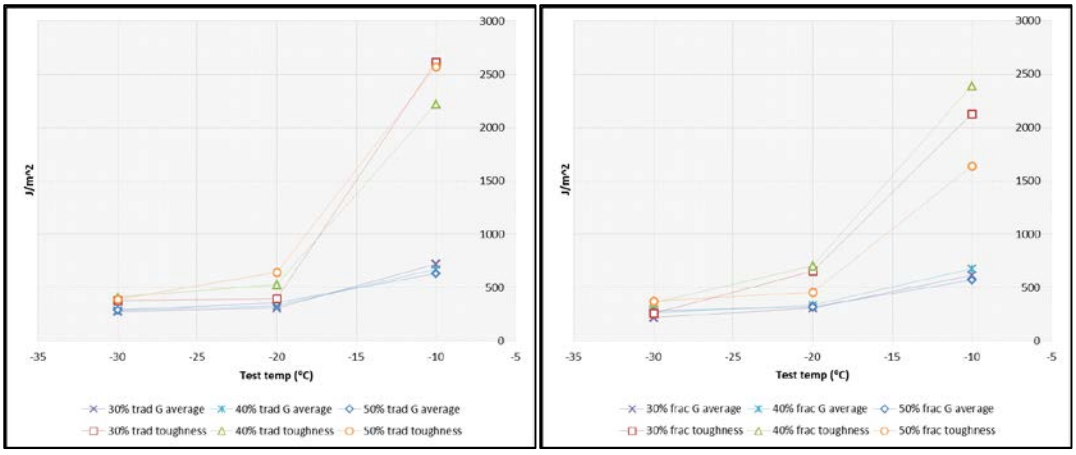

(a) **(b)**

Figure 44. Average fracture energy vs. Fracture toughness for (a) Trad and (b) Frac mixtures

The G_f fracture energies obtained at the elastic test condition (very low test temperature) are very close to J integral toughness, but begin to diverge dramatically with an increasing test temperature. Generally, the G_f test method tends to underestimate the ductile material dramatically and provides too much credit to the stiffer one at high testing temperatures. Table 18 lists the underestimated ratio by utilizing the differences shown in Figure 44 divided by the J toughness. Table 19 summarizes the ranking list comparison. No statistically significant difference is detected between the traditional and fractionated mixtures, even though the toughness of traditional batched mixtures is generally larger than the fractionated prepared mixtures.

Table 18. Underestimated ratio for (a) Trad and (b) Frac mixtures

(a)

Underestimate rate			
	30% Trad	40% Trad	50% Trad
-10°C	72.34%	69.80%	75.30%
-20°C	21.90%	36.98%	44.22%
-30°C	28.04%	31.15%	25.33%

(b)

Underestimate rate			
	30% Frac	40% Frac	50% Frac
-10°C	71.03%	71.79%	64.86%
-20°C	52.47%	52.14%	30.39%
-30°C	14.58%	25.73%	25.04%

Table 19. Ranking lists

Parameters	-10°C Test						-20°C Test						-30°C Test					
Gf (J/M^2)	30%Trad>	40%Frac>	40%Trad>	50%Trad>	30%Frac>	50%Frac	50%Trad>	40%Frac>	40%Trad>	50%Frac>	30%Frac>	30%Trad	50%Trad>	40%Trad>	50%Frac>	30%Trad>	40%Frac>	30%Frac
	722	676	664	634	616	576	360	337	332	320	310	309	293	287	282	275	267	223
J toughness (J/M^2)	30%Trad>	50%Trad>	40%Frac>	40%Trad>	30%Frac>	50%Frac	40%Frac>	30%Frac>	50%Trad>	40%Trad>	50%Frac>	30%Trad	40%Trad>	50%Trad>	30%Trad>	50%Frac>	40%Frac>	30%Frac
	2613	2566	2396	2223	2130	1640	705	654	646	527	461	397	416	392	383	375	359	262

Parameters	-10°C Test	-20°C Test	-30°C Test
Gf (J/M^2)	30%Trad>40%Trad>50%Trad	50%Trad>40%Trad>30%Trad	50%Trad>40%Trad>30%Trad
J toughness (J/M^2)	30%Trad>50%Trad>40%Trad	50%Trad>40%Trad>30%Trad	40%Trad>50%Trad>30%Trad

Parameters	-10°C Test	-20°C Test	-30°C Test
Gf (J/M^2)	40%Frac>30%Frac>50%Frac	40%Frac>50%Frac>30%Frac	50%Frac>40%Frac>30%Frac
J toughness (J/M^2)	40%Frac>30%Frac>50%Frac	40%Frac>30%Frac>50%Frac	50%Frac>40%Frac>30%Frac

Conclusions and Recommendations

The fracture toughness tests performed on 30, 40, and 50% RAP-contained asphalt mixtures reveal ranking changes with varying temperatures (Figure 43). None preserves its own advantage for the entire temperature range. One mixture presenting a better fracture performance between certain temperature ranges does not mean it will always be better than others at other temperatures. It is possible, but there is no guarantee. It is inappropriate to infer the conclusion only relies on one temperature testing. Consequently, the decision about which asphalt mixture should be selected for a project should be based on the major application temperature range.

Generally, the experimental estimated toughness increases with increasing temperature for mixtures. Both traditional and fractionated RAP samples suggest adding more RAP materials benefits the asphalt mixture to prevent cracking at -30^0C, but this advantage diminishes with increased temperatures for both traditional and fractionated prepared samples. The mixtures with less RAP materials demonstrate better fracture performance when changing from -20 to -10^0C.

The toughness of traditional batched mixtures is generally larger than the fractionated prepared mixtures. However, a statistically significant difference is undetected.

Fracture energy G_f results agree with fracture toughness measurements at -30^{0}C. However, it is insufficiently accurate to rank the asphalt mixture in high temperatures when the material deforms more in an elastic-plastic manner. The G_f values obtained at elastic condition (very low temperature testing condition) can be utilized only to estimate the dimensionless, physical property—G_{IC}. However, test results tend to underestimate the ductile material dramatically and provide too many credits to the stiffer material with increasing test temperature. In other words, as the temperature rises above the glass transition value of the asphalt binder, the fracture energy parameter tends to underestimate the ability of the more ductile asphalt mixture against cracking—the higher the testing temperature, the greater the underestimation. If the SCB G_f test protocol is selected for utilization, the sample with the smallest notch size is recommended. The CV values can be applied to evaluate the efficiencies and stabilities for utilizing fracture energy to rank different asphalt materials.

In the future, elastic compliance should be introduced into the asphalt SCB test and follow the ASTM standard to measure the J-R curve. The CMOD will not be used only for load rate control, but for estimating crack extension. Data from only one sample can produce a J R-curve and test data from multiple samples can be used to obtain an average J R-curve with a higher confidence level.

References

Page, G.C., and Murphy, K.H., 1987. Hot-mix recycling saves Florida DOT $38 million. *Asphalt*, 1.

Page, G.C., 1988. Florida's experience in hot-mix asphalt recycling. *Hot-mix asphalt technology*, Spring.

Solaimanian, M., and Kennedy, T. W., 1995. Production variability analysis of hot-mix asphalt concrete containing reclaimed asphalt pavement. Center for Transportation Research, Bureau of Engineering Research, The Univ. of Texas, Austin, Tex.

Sargious, M., and Mushule, N., 1991. Behavior of recycled asphalt pavements at low temperatures. *Can. J. Civ. Eng*, 18, 428–435.

McDaniel, S.R., Soleymani, H., Anderson, R.Mj., Turner, P., and Peterson, R., Oct. 2000. Recommended use of reclaimed asphalt pavement in the superpave mix design method. *National Cooperative Highway Research Program*, Washington, D.C.

Kim, M., Mohammad, L.N., and Elseifi, M., 2012. Characterization of fracture properties of asphalt mixtures as measured by semicircular bend test and indirect tension test. *Journal of the Transportation Research Board*, 2296, 115-124.

AASHTO T164. Standard method of test for quantitative extraction of asphalt binder from hot mix asphalt (HMA), *American Association of State Highway and Transportation Officials*.

AASHTO T319. Standard method of test for quantitative extraction and recovery of asphalt binder from asphalt mixtures, *American Association of State Highway and Transportation Officials*.

ASTM D7175. Standard test method for determining the rheological properties of asphalt binder using a dynamic shear rheometer, *American Standard of Testing Materials*.

Asphalt Institute, 2003. *The superpave performance graded asphalt binder specifications and testing superpave (SP-1)*. Third Edition, Lexington, Kentucky.

ASTM D6648. Standard test method for determining the flexural creep stiffness of asphalt binder using the bending beam rheometer, *American Standard of Testing Materials*.

CHAPTER 5. THE EVALUATION OF ASPHALT MIXTURES CONTAINING RECLAIMED ASPHALT PAVEMENT THROUGH DISSIPATED ENERGY

A paper to be submitted to International Journal of Pavement Engineering

Sheng Tang, R. Christopher Williams, and Andrew A. Cascionec

Abstract

When applying reclaimed asphalt technology in a flexible pavement project, most performance concerns are related to low temperature and fatigue cracking, since the stiffness of the HMA mixture could dramatically increase through adding a high percentage of reclaimed asphalt pavement (RAP) material. The purpose of this study is to evaluate asphalt mixtures with high RAP contents, prepared using two RAP addition methods, for their performance based on fatigue cracking resistance rather than relying on volumetric properties. Asphalt mixture samples were prepared with three RAP binder content replacement percentages (30, 40, and 50%) using two preparation methods: the as-is RAP gradation (Traditional method) and the splitting of the RAP gradation into coarse and fine fractions (Fractionated method). Asphalt mixture beam fatigue and binder fatigue time-sweep tests were performed at 20°C. Beam fatigue samples also underwent freeze-thaw cycling for freeze-thaw damage evaluation. Rather than based solely on S-Nf curves to illustrate the fatigue performance, the beam fatigue test data was analyzed through a dissipated energy approach. Faster fatigue degradation was observed for the 40% RAP binder and beam mixture when subjected to repeated loading. From a morphology aspect, the binder's phase separation and physical hardening effects can explain this.

Introduction

Reclaimed asphalt material technology has been applied in the United States for more than 30 years, and there is a tendency for many owner agencies to utilize more reclaimed asphalt material (RAP) by increasing the RAP percentage. This increasing RAP utilization is and will continue be to be driven by historically high asphalt binder prices, high quality aggregates existing in pavement rehabilitation projects, and increasing awareness of environmental stewardship and sustainability issues.

From the application perspective, one of the challenges of the mix design process for using high percentage RAP in the United States is to meet the volumetric mix design criteria. Often a large amount of fine materials introduced into the asphalt mix via RAP often makes volumetric criteria including film thickness requirements difficult to achieve. Two RAP addition methods (Traditional and fractional methods) were examined to demonstrate the relationship between the mix methods and film thickness in order to fulfil the film thickness design criteria. The only difference between the two mix procedures is the Fractionated method removes a portion of fine RAP material passing the No.30 sieve (0.6mm), so the RAP material remaining on and above the No. 30 sieve could be used to add into mixtures. This sieve size could be changed depending on the design purpose and the RAP gradation. Most of the concerns for applying RAP are related to low temperature and fatigue cracking performance, considering the stiffness of the asphalt mixture can dramatically increase through introducing RAP (McDaniel et al. 2000). This paper focuses on the two RAP methods and the effects on fatigue cracking performance rather than only on volumetric parameters. The asphalt mixture beam fatigue and binder fatigue tests (binder fatigue test) were performed at 20°C . Normally

examining the traditional S-Nf fatigue curve (strain level vs. cycles to failure) is used to illustrate mix fatigue testing results. In this paper, the beam fatigue test data is also analyzed through a dissipated energy approach.

Materials and Methods

The asphalt mixtures for beam fatigue testing were prepared based upon volumetric criteria including film thickness. The virgin binder utilized has a performance grade (PG) 58-28. RAP materials were added to replace 30, 40 and 50% of the 5.4% optimum binder content by mass. This method is often referred to as the binder replacement method. This means that the mixture is prepared by adding RAP until 30, 40 and 50% of the total binder is replaced by the RAP binder, and it is assumed that all of the RAP binder is being used to displace virgin binder. Since the mixtures were prepared by using the binder replacement method, the binders' rheological behavior should be associated with the mixtures' performance.

Three different RAP percentages and two different RAP addition methods combinations were used to develop six different asphalt mix designs. Six beams were procured for each mix design resulting in 36 beams being fatigue tested at 20°C. Similar gradations for the six different mixtures were developed with the primary difference being the higher percentage of material passing the #30 sieve for the Traditional RAP based mixes. Thus the differences between the mixes prepared by two RAP addition methods were still preserved while the gradation variations among the mixes applying the same RAP adding method were minimized. Limiting the number of experimental variables was one of the primary goals of this study in order to focus the assessment on the performance of the RAP binder and its influence on performance. The gradations of the six mixtures are shown in Table 20 below.

Table 20. Gradations of the six mixtures

	3/4"	1/2"	3/8"	No. 4	No. 8	No. 16	No. 30	No. 50	No. 100	No. 200
Traditional RAP mixes prepared with 30%, 40%, and 50% RAP	100.0	93.4	84.6	67.3	49.6	67.7	26.2	17.0	10.8	9.2
Fractionated RAP mixes prepared with 30%, 40%, and 50% RAP	100.0	93.6	85.2	66.6	48.9	36.2	24.1	15.3	9.0	7.4

The fine virgin aggregate was adjusted to achieve comparable gradations as reasonably possible between the mixes with the varying RAP percentages. For example, 2.1% of the virgin fine aggregate passing No. 30 sieve was removed from the mix design when using the Fractionated RAP preparation method so the combined aggregate gradation matched the mix design of the Traditional RAP preparation method.

For the beam fatigue testing at 20°C, the strain amplitude was kept constant and the stress on the samples was varied to achieve the target strain. According to AASHTO T321-03 testing standard, the test termination point was defined as when 50% of initial stiffness was achieved. The initial stiffness was recorded at the 50th load cycle allowing for some “seating” of the samples. Six beams were prepared for each mix method with 7% ±1% air voids and tested at six different strain levels ranging from 1000 to 375 micro-strain.

Twelve additional beams using a mix design with 15% RAP were also prepared using the Traditional RAP preparation method to demonstrate the weakness of evaluating asphalt mixtures based on the AASHTO T321 criteria. Six of the twelve beams were unconditioned and tested in the beam fatigue apparatus. The other six beams were conditioned according to ASTM C666 by being subjected to 120 freeze-thaw cycles. Those six beams were saved after the beam fatigue test and subjected to an additional 120 freeze-thaw cycles, then retested in

the beam fatigue apparatus. This was again followed by a third round of freeze-thaw conditioning and beam fatigue testing.

The asphalt binder extraction and recovery tests were done in accordance with AASHTO 164 and AASHTO T319 standards utilizing a centrifuge and rotary evaporator, minimizing additional aging of the binder during the process. The extracted binder could then be blended with virgin binder in varying percentages on a mass basis consistent with the RAP percentages for the mix testing. This allows for subsequent binder test results to be compared with the mix performance test results.

Binder performance grading tests including Rolling Thin Film Oven (RTFO), Pressure Aging Vessel (PAV), Dynamic Shear Rheometer (DSR) and Bending Beam Rheometer (BBR) were performed to evaluate the binders containing the extracted RAP at replacement rates of 30, 40 and 50 percent.

The time-sweep test (Bahia et al. 1999) utilizing a dynamic shear rheometer (DSR) was also carried out at 20°C to assess the fatigue behavior of the RTFO aged binder. Three samples for each blend containing 30, 40, and 50% RAP binder were tested. The time-sweep testing was conducted at 10Hz and 20°C consistent with the mixture beam fatigue testing parameters. The strain level for the binder test was set to 0.04 mm/mm in order to accelerate the fatigue progress, so the test could be completed in 10 to 15 hours. Previous research (Kim 2009) has shown that G* or G*sin (δ) of the binder does not correlate well with mix beam fatigue performance. However the time-dependent rheological behavior of the binder involving the shear-induced breakdown of the internal structure is associated with the mixture's fatigue behavior.

Results and Discussion

Performance Grading of Binders at 30, 40, and 50% Replacement Rates

Table 21 shows that all the three blended binders containing the virgin binder and corresponding RAP binder percentage have a 64-22 performance grade. Both the BBR and DSR testing results indicate that the binder is increasing in stiffness with an increasing amount of RAP binder. Generally, all the binders' rheological properties are in the linear viscoelastic region and are relatively similar. Based on the critical high temperatures for those binders, the blend with the 50% RAP binder should have the highest initial stiffness for the fatigue tests at 20° and the 30% RAP blend should be the softest one.

Table 21. Binder performance grading data

Sample		Test at -18 °C		Test at -12 °C		Low Critical Temp	Critical High Original (°C)	Critical High RTFO(°C)	PG Grade
		M-Value	Stiffness	M-Value	Stiffness				
50%RAP	1	0.261	329	0.324	164	-22	67.96	67.82	PG 64-22
	2	0.26	335	0.331	160		68.01	68.43	
40%RAP	1	0.277	272	0.345	116	-22	65.88	65.81	PG 64-22
	2	0.274	306	0.347	130		65.29	65.28	
30%RAP	1	0.289	283	0.356	125	-22	64.88	64.1	PG 64-22
	2	0.281	301	0.35	132		64.69	64.85	
0% RAP	PG 58-28								

Traditional Fatigue Analysis for HMA Mixture

The beam fatigue test protocol with a test termination at 50% of initial stiffness tends to rank softer materials as better performing than stiffer materials if the conclusion is based on the traditional S-Nf plots of the mix beam fatigue testing. To demonstrate this phenomenon, an additional aspect to the experiment was performed which evaluated the effect of material compliance (softness) from freeze-thaw cycling as shown in Figure 45. Twelve samples for beam fatigue test were prepared with same conditions by using the same HMA material, an

asphalt mixture with 15% RAP. Half of the samples were tested in the beam fatigue apparatus before any freeze-thaw cycling as shown by the solid line in Figure 45. This line represents the benchmark S-Nf curve for the mixtures. The dashed lines in Figure 45 represent the other six beams after freeze-thaw conditioning. After the first 120 freeze-thaw cycles and beam fatigue testing, the same beams were reconditioned and retested for another 120 freeze-thaw cycles. The beams were then subjected to the same process for a third time for a total of 360 freeze-thaw cycles. Each conditioning cycle and fatigue test enhanced the damage of the beams physically. Figure 45 summarizes the test data and illustrates that the sample set before undergoing freeze-thaw testing exhibited poorer performance than the samples that have undergone the 120 freeze-thaw cycles. Figure 46 illustrates the visual condition of a beam after successive freeze-thaw cycling and clearly demonstrates the deterioration of the beam after freeze-thaw cycling.

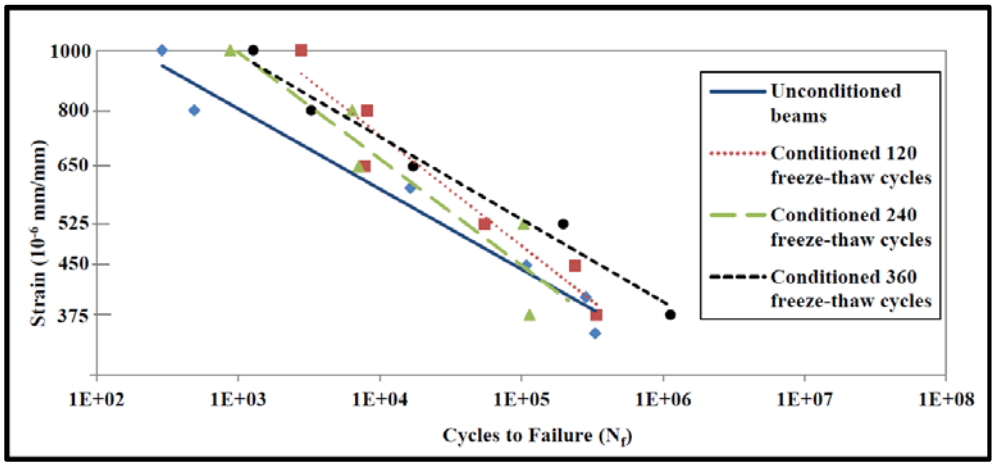

Figure 45. Number of cycles vs. testing strain levels

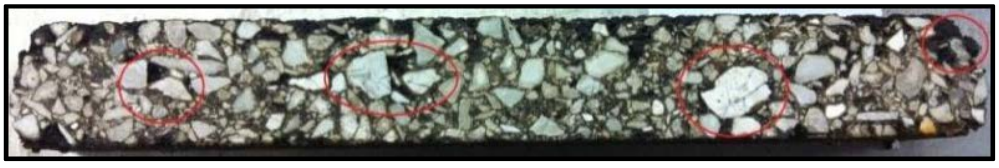

Figure 46. Cracking for the beams after 120 freeze-thaw cycles

The problem may arise from the 50% stiffness reduction “failure” test protocol. Figure 47 illustrates the typical beam fatigue test results of stiffness vs. cycle curve when testing the same beam twice. The Nf cycle (cycles to “failure”) is obtained when 50% of the stiffness is reduced. Since the curve is usually represented by an exponential distribution, and when the tail portion of the distribution part gets flatter, a change in one unit of stiffness will result in an increasing number of cycles to failure. Clearly, Cycle A is shorter than Cycle B with same reduction in stiffness in Figure 47. The “softer” beam material represented by Cycle B has a higher number of cycles to failure than Cycle A for the constant strain test.

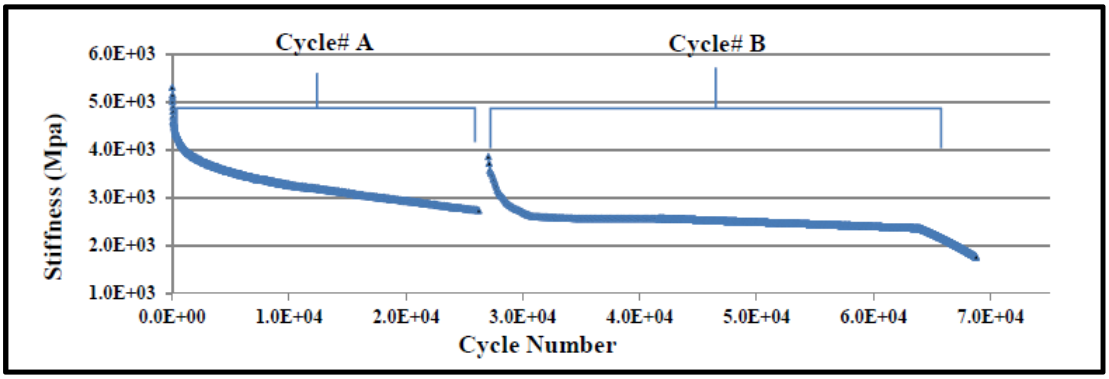

Figure 47. Stiffness vs. number of cycles

Figure 48 shows the traditional S-Nf curve summarized for all of the Traditional and Fractionated mixes with the varying levels of RAP. It could be misleading as previously described to rely on the reduced stiffness of materials with varying levels of stiffness. It is also hard to rank mixtures that have intersecting lines of “performance”, even when using best fit equations including the use of statistical methods. Thus, only using cycles to “failure” criteria is not sufficient to define the fatigue resistance ability, and other test data collected could be utilized. One such example is the calculation of dissipated energy.

A dissipated energy plot illustrates the transferred energies that are consumed by the material during testing, and it may be a reasonable alternative approach to demonstrate the fatigue resistance features of mixes. A stiffer mix has a higher dissipated energy than a softer mix in the initial loading cycles for achieving the same deformation at a constant strain level, and the total cumulative energy integrated with cycle counts can be used to represent the performance of a mix maintaining structural adequacy.

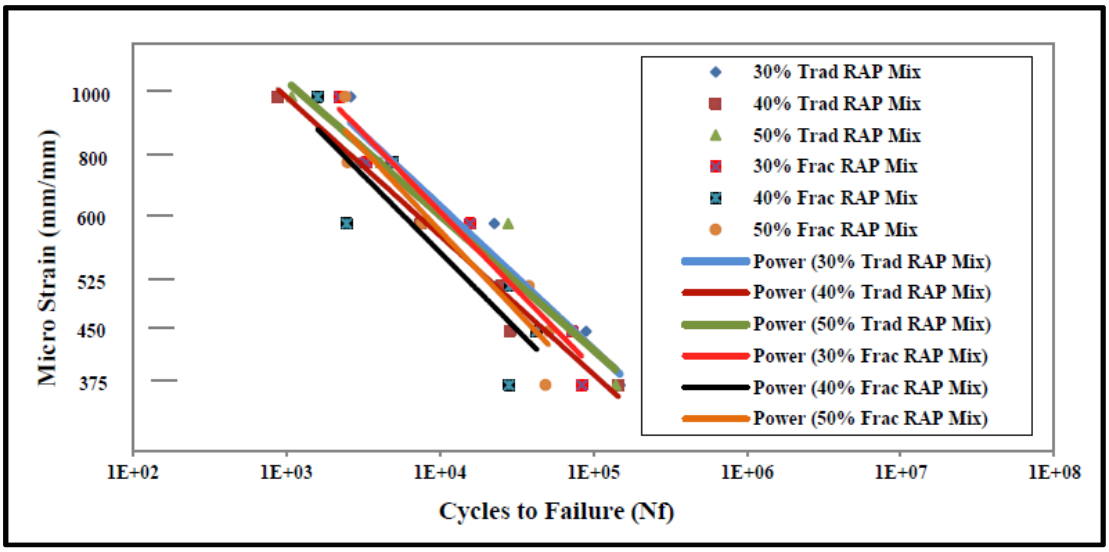

Figure 48. Testing strain level vs. Number of cycles

Figures 49 and 50 illustrate the dissipated energy curves for 375 and 1000 micro strain tests at 20°C , respectively. Increasing RAP usage in the mixture has been shown to improve the stiffness modulus, and more energy is needed to generate deformation. However, it is noteworthy that some stability problems with these RAP mixtures have also been observed. The dissipated energy for 40% RAP mixture drops faster than the 30% and 50% amounts of RAP for both the Traditional and Fractionated methods. A decreasing amount of energy was consumed or needed to achieve the constant strain deformation as the number of load cycles

increases. This indicates that the beams are becoming weaker and the stiffness is decreasing resulting in the strain energy density of the specimen being reduced (Lagoda et al. 2009).

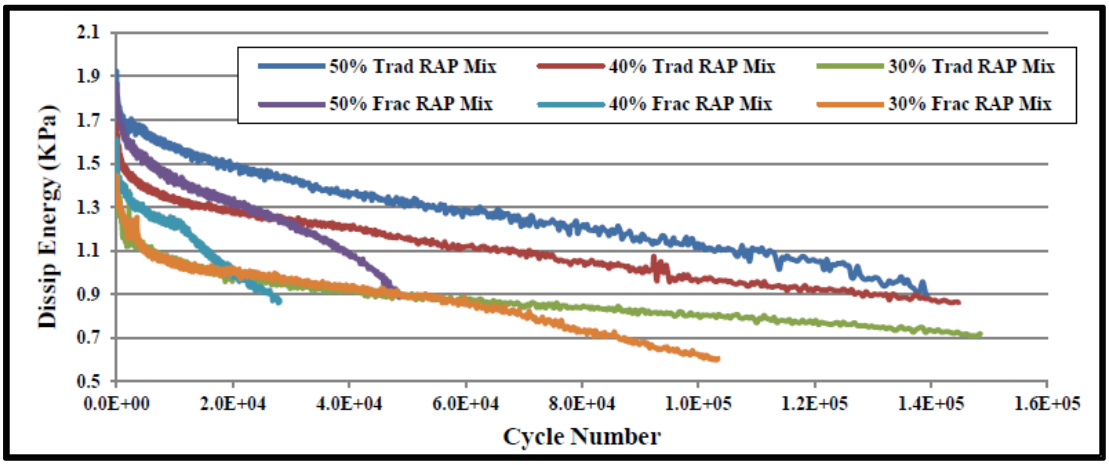

Figure 49. Number of cycles vs. dissipated energy at 375 micro-strain

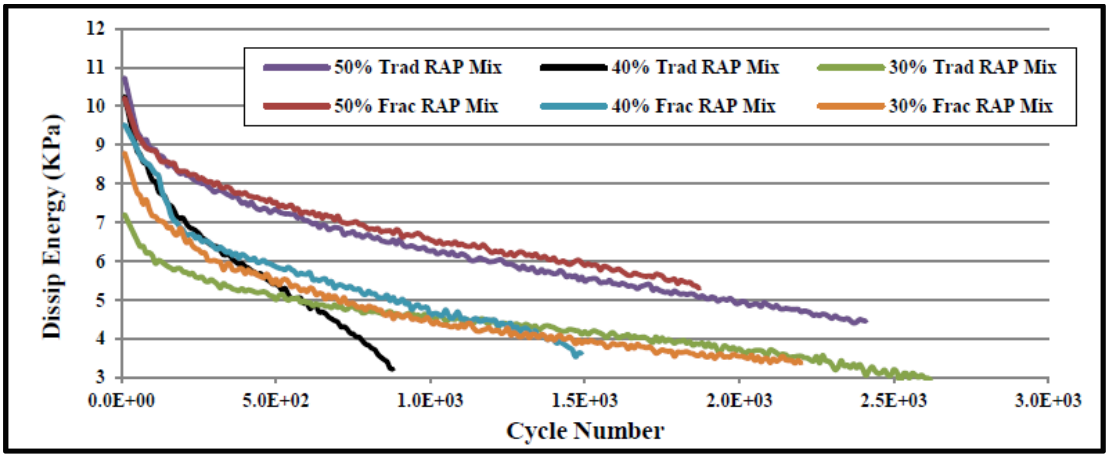

Figure 50. Number of cycles vs. dissipated energy at 1000 micro-strain

Table 22 summarizes the cumulative dissipated energy, which is the integration of the dissipated energy over the number of cycles. This cumulative energy quantifies the toughness or tenacity of the different mixtures. Mainly the 40% RAP materials are weaker than the ones with 30% and 50% RAP. Further, the traditional RAP mixes exhibit better performance than the fractionated ones.

Table 22. Cumulative dissipated energy

Cummulative Engergy (Mpa)								
Testing Strain Level (mm/mm)	375	450	525	650	800	1000	Average for each mix at different strain levels	Average for each RAP preparation method
30% Trad Sample	120.721	115.227	42.746	53.705	10.767	11.459	59.104	59.433
40% Trad Sample	146.374	42.931	53.080	26.585	18.698	5.128	48.799	
50% Trad Sample	163.010	55.620	86.815	84.113	19.990	12.820	70.395	
30% Frac Sample	86.451	86.752	12.853	41.918	12.220	10.230	41.737	38.386
40% Frac Sample	31.600	59.821	5.917	25.570	19.832	8.234	25.162	
50% Frac Sample	60.815	73.912	47.680	73.762	15.800	17.583	48.259	

Matched paired mean t-tests were performed to assess the difference of the cumulative dissipated energy between the mixtures. The data were paired by the same strain level of the fatigue test. The level of significance, σ level, was set to be 0.05 and one-side tail tests were done as understanding if there is a higher or smaller amount of cumulated energy for the various factors is of interest. The statistical test results are shown in Figures 51 and 52 for the Traditional and Fractionated RAP mixes, respectively.

The Y (vertical) axis is the difference of each pair of cumulative dissipated energy between the mixtures at same strain level in Figures 51 and 51. The horizontal (X) axis represents the mean of each pair of cumulative energy results. The red horizontal solid line is the average mean difference between two mixes and the two red dash lines are the 95% confidence bands.

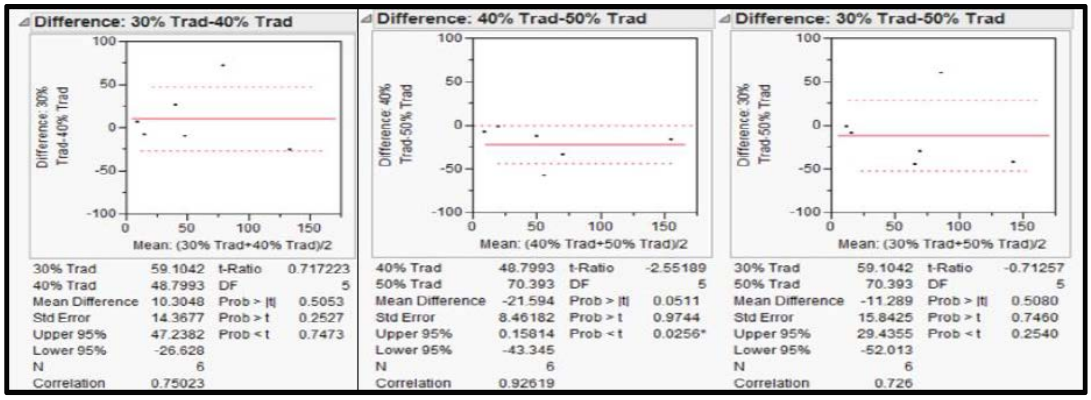

Figure 51. Matched Pairs t-Test for mixtures applying traditional method

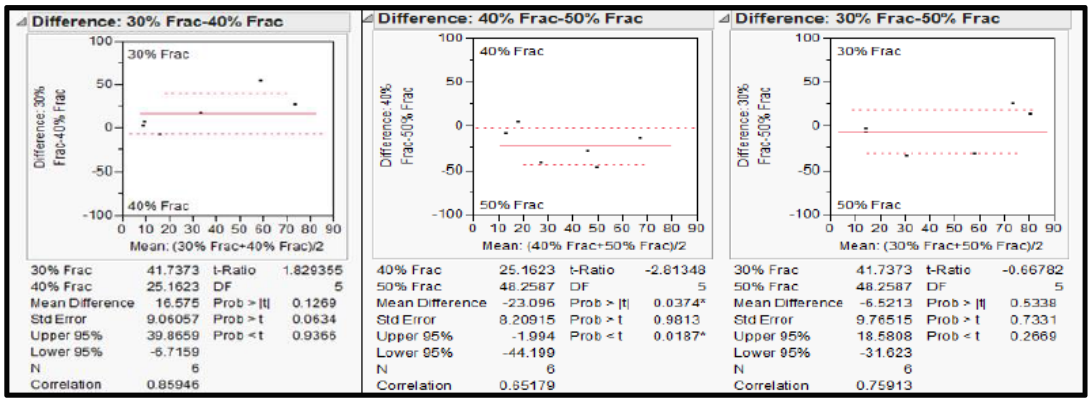

Figure 52. Matched Pairs t-Test for mixtures applying fractionated method

The t-test results (Figures 51 and 52) suggest that the cumulated dissipated energy of 40% RAP mix is statistically significantly smaller than the 50% RAP mixture for both the Traditional and Fractionated methods.

However, the statistical differences when comparing 30% RAP mixes with the other two are not as clear. Only the energy of 30% RAP fractionated prepared mixes are close to being significantly higher than the 40% RAP with a p-value of 0.0634 testing if 30% mixtures have a larger value. The 30 and 50% RAP mixtures do not provide any statistical difference between each other.

The reason that the 30% RAP mixes do not stand out from 40% RAP mixes is because the beam fatigue test was terminated relatively early at the various levels of strain due to the relative fast test duration to achieve the 50% reduction in stiffness.

Another t-test with a 2.421 as t-ratio and p-value (>t) at 0.011 also suggests that the mixes prepared using the Fractionated method have statistically significant lower cumulative dissipated energy than the Traditional ones.

Binder Fatigue Analysis

The original time-sweep data for the binder testing at 20°C is illustrated in Figure 53. The shear modulus (G_0*) at time zero in the linear viscoelastic region shows that as the percentage of RAP binder increases, there will also be an increase in the G* value. The 50% replacement binder is the stiffest one and the 100% virgin binder is the softest one, but the fatigue behaviour for those binders is significantly different. The binder fatigue speed could not simply be correlated to the RAP binder replacement percentage.

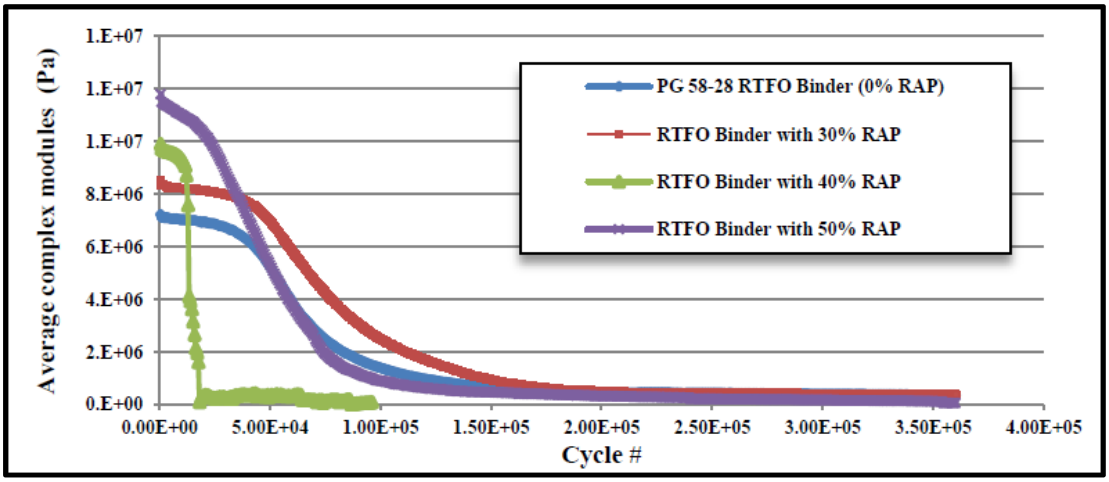

Figure 53. Number of cycles vs. Shear modulus (G*)

In order to better demonstrate the rate of fatigue and the G* dissipating process, a dimensionless structural parameter was introduced based on thixotropic theory. The fatigue failure could be described as when the material transitions from a structured state to a non-structured state. The initial G_0* at cycle N = 0 and G_∞*when cycle number N approaches to ∞ are used to define the structural parameter ψ, where ψ (N) = (G_N*-G_∞*) / (G_0*-G_∞*). When ψ = 1 would represent an initial structured state, while a ψ = 0 represents a non-structured state. By applying this method, the G* value is normalized and transferred to the ψ value. Figure 54 summarizes the number of cycle verses the structural parameter.

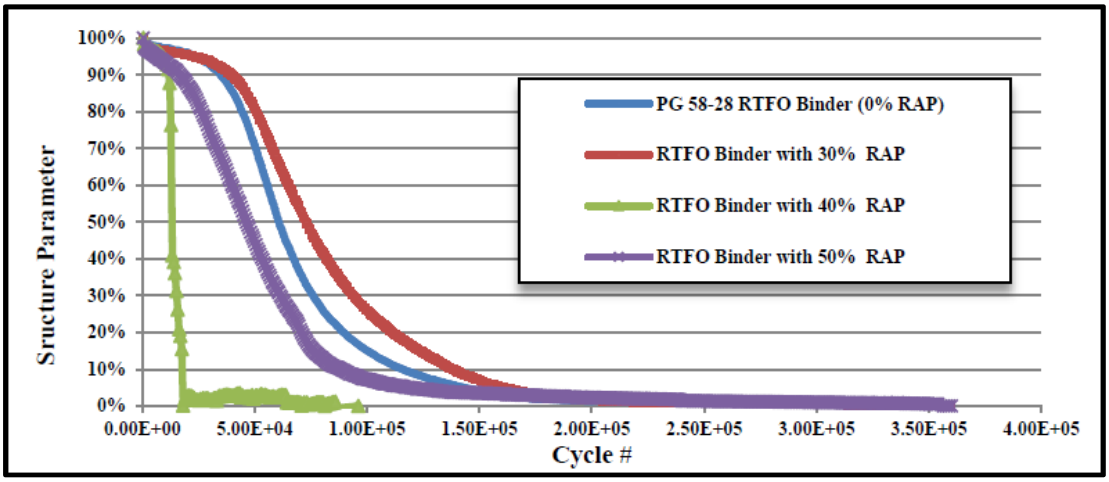

Figure 54. Number of cycles vs. Structure parameter

As shown in Figure 54, the structure breakdown rates for the different binders are illustrated. It suggests that the binder with 30% RAP binder degrades slower than the 50% and 40% binder replacement ones. And the interesting results show that the 50% ones have longer fatigue life than 40% replacement blends. Those breakdown processes appear to agree with the mixtures' fatigue test results and there is no difference when applying either the Traditional or Fractionated methods. Additionally, it indicates that the 30% RAP binder replacement mixes may be even better than the virgin mix when comparing the fatigue performance under the

condition of similar aggregate gradation when performing the binder fatigue test at the same strain level. Figures 53 and 54 illustrate that the shear modulus and the structural parameter decrease with an increase in load cycles. These binder observations agree with the outcome of the mixture beam fatigue test results using the dissipated energy approach.

Conclusions

The freeze-thaw cycle treatment did breakdown the asphalt beams, but those structure damage did not reflect on the beam fatigue test results through the traditional S-Nf curve plot. The cumulative dissipated energy may be a better method to rank the fatigue durability of materials.

The overall evaluation based on the result from both mixture and binder fatigue tests at 20°C indicate that asphalt mixes with 30% and 50% RAP could perform better than mixes with 40% RAP, when the aggregate structures are similar. It illustrates that simply limiting RAP content and performing the traditional beam tests and examining S-N_f curves for evaluating fatigue performance may not explain the actual performance.

The mixture containing a high percentage of reclaimed asphalt pavement that introduces a substantial amount of fine material could have longer fatigue life, and those fine materials may contribute to improved fatigue cracking performance as active fillers. Removing 2.1% fine aggregate (passing the #30 sieve) the from RAP may not improve the film thickness, since the thickness is a calculated value based on the volumetric data and does not account for whether the fine materials are being a void filler or acting as a surface area.

Comparing the pavement with similar aggregate structures under same service conditions, the binder fatigue behaviour dominates the overall performance related to fatigue cracking. The binder time sweep test could give a better indicator of expected fatigue performance of mixes rather than the loss modulus G".

The overall fatigue performances generally vary depending on the combinational effects from the mix volumetric properties as well as the binder's ability to resist fatigue.

From the morphology aspects, the faster fatigue degradation of the 40% RAP binder and the corresponding mix being subjected to the repeated beam fatigue loading could be explained by the phase separation of the blended binder, and physical hardening effect (crystallization) as well. In general, the phase separation makes the blended binder behave as a composite material considered being a "weaker" constituent (Keller 1992), which could be the major reason that impacts on the mechanical properties of the 40% RAP mixtures and binder. The phase separation for the asphalt binder has been observed and studied by other researchers (Masson et al. 2003, 2005, Kriz et al. 2008, Lesueur 2009). Secondly, the higher the degree of crystalline structuring possessed by crystallizable fractions (CF), such as wax, the higher the resulting tensile strength, the lower the elastic response, the lower the toughness and the more potential for fatigue cracking. Even for materials having the same CF content, the degree of crystallinity could be significantly different depending upon the thermal history of the material (Saeed et al. 1996). This thermal history can have the same effect in fatigue as the glass transition temperature has on the low temperature behaviour of binders and mixes (Kriz et al. 2008).

Future research work will use a differential scanning calorimetry (DSC) to measure the phase stability and the degree of crystalline of the blended binder with different RAP contents. This will capture the morphological features of the binders and allow for examination of any potential phase differences among the materials.

References

Iowa DOT Standard Specifications, 2012. Section 2303. *Hot Mix Asphalt Mixtures*.

McDaniel, S.R., Soleymani, H., Anderson, R.Mj., Turner, P., and Peterson, R., Oct. 2000. Recommended use of reclaimed asphalt pavement in the superpave mix design method. *National Cooperative Highway Research Program*, Washington, D.C.

Bahia., H.U., Zhai, H., Kose, S., and Bonnetti, K, 1998. Non-Linear viscoelastic and fatigue properties of asphalt binder. *Journal of the Association of Asphalt Paving Technologists*, 67, 1-41.

Kim, Y., 2009. *Modeling of Asphalt Concrete*. New York, NY: McGraw Hill.

Łagoda, T., and Sonsino, C., 2009. Application of the strain energy density parameter for estimation of multiaxial fatigue life of sintered steels with stress concentrators. *Journal of Theoretical Applied Mechanics*, 47 (1), 161-175.

Keller, A., 1992. Morphology of polymer. *Pure & Applied Chemistry*, 64 (2), 193-204.

Masson, J.F., Polomark, G., and Collins P., 2005. Glass transitions and amorphous phases in SBS-bitumen blends. *Thermochimica Acta*, 436, 96-100.

Masson, J.F., Collins, P., Robertson, G., Woods, J.R., and Margeson, J., 2003. Thermodynamics, phase diagrams, and stability of bitumen-polymer blends. *Energy and Fuels*, 17, 714-724.

Kriz, P., Stastna, J., and Zanzotto, L., 2008. Glass transition and phase stability in asphalt binders. *Road and Material and Pavement Design*, 9, 37-65.

Lesueur, D., 2009. The colloidal structure of bitumen: consequences on the rheology and on the mechanisms of bitumen modification. *Advances in Colloid and Interface Science*, 145, 42-82.

Doroudiani, S., Park, C.B., and Kotschot, M.T., 1996. Effect of the crystallinity and morphology on the microcellular foam structure of semi-crystalline polymers. *Journal of Polymer Engineering and Science*, 36 (21), 2645-2662.

Kriz, P., Stastna, L., and Zanzoto, L., 2008. Temperature dependence and thermo-reversibility of physical hardening of asphalt binders. *Proceedings of the 4th Eurasphalt and Eurobitume Congress*, 21-23 May 2008 Copenhagen, Denmark. European Asphalt Pavement Association

CHAPTER 6. SUMMARY, CONCLUSIONS, RECOMMENDATIONS, AND FUTURE RESEARCH

Summary

When applying recycled asphalt technology in a flexible pavement project, most of the concerns are related to low-temperature fracture and fatigue cracking, since the stiffness of hot mix asphalt (HMA) mixtures could dramatically increase through adding a high percentage of reclaimed asphalt pavement (RAP) materials. This study investigated fracture and fatigue resistance of asphalt mixtures in relationship to various proportions of reclaimed asphalt pavement materials' contents (30, 40, and 50%) and batching methods (Traditional and Fractionated Methods) at different temperatures (-10, -20, and -30°C for fracture tests, and 20°C for fatigue tests). Additionally, the performance grade and fatigue behavior of the asphalt binder containing RAP binder were evaluated as well.

A proposed new SCB toughness test providing a better J_{SS} toughness parameter to evaluate fracture resistance of asphalt mixtures subjected at brittle-ductile transition temperatures was implemented in this research. Rather than based solely on S-Nf curves to illustrate the fatigue performance, the beam fatigue test data were analyzed through a dissipated energy approach. Compared with normal performance grading evaluations for asphalt binder, a time-sweep test was utilized to assess the binder's fatigue behavior.

Conclusions

Fracture Parameter Evaluations

The peak load for SCB testing is not recommended as an indicator to rank asphalt mixtures' cracking resistance performance at all temperatures. The variations accounted from the specimen geometry, notch tip sharpness, and miscorrelations with fracture toughness eliminated its application to evaluate fracture resistance of asphalt materials.

When the asphalt materials could be modeled as linear elastic objects, the experimentally measured K value should be appropriate to estimate toughness, K_{IC}, theoretically. However, because fatigue pre-cracking treatment is skipped in SCB testing of asphalt mixtures, the preexisting crack tip sharpness and tip location (stone or binder) result in certain variations to K measurements. The estimated K_{IC} toughness may not be efficiently used to rank asphalt mixtures, when the experiment plan consists of a small number of replicate samples and the differences for the compared mixtures are insignificant. Test results tend to underestimate the ductile material dramatically with huge biases, when small-scale yielding is unmet.

Fracture energy, G_f, successfully quantifies fracture toughness at -30°C. However, test results tend to underestimate the ductile material and overstate the stiffer material with increasing test temperatures. In other words, as the temperature rises above the glass transition value of the asphalt binder, the fracture energy parameter, G_f, tends to underestimate the ability of the more ductile asphalt mixture against cracking. The higher the testing temperature, the greater the underestimation.

Fracture Toughness Evaluation for Asphalt Mixtures Containing RAP Materials

Fracture toughness tests performed on asphalt mixtures containing 30, 40, and 50% RAP reveal the ranking list changes with varying temperatures. None of the asphalt mixtures evaluated in this research preserves its own advantage for the entire temperature range from -30 to -10°C.

The estimated toughness J_{SS} of traditional batched mixtures is generally slightly higher than the fractionated prepared mixtures between the tested temperature range (-30 to -10^{0}C). This may be due to additional asphalt binder content and more fine aggregate materials.

Asphalt Mixtures and Binder Fatigue Analysis When Introducing RAP Materials

Faster fatigue degradation was observed for the 40% RAP binder and beam mixture when subjected to the repeated loading at 20°C. From a morphology aspect, this can be explained by the binder's phase separation and physical hardening effects. Comparing the pavement with similar aggregate structures under the same service conditions, binder fatigue behavior dominates the overall performance related to fatigue cracking. The binder time sweep test could provide a better indicator of expected fatigue performance of mixes rather than the loss modulus G".

The mixture containing a high percentage of reclaimed asphalt pavement, that introduces a substantial amount of fine material, could have a longer fatigue life. These fine materials may contribute to improved fatigue cracking performance as active fillers. Removing additional fine aggregates (passing the #30 sieve) from RAP may not improve the film thickness, since the thickness is a calculated value, based on the volumetric data and does not account for whether the fine materials are being a void filler or acting as a surface area.

Traditional vs. Fractionated RAP Addition Methods

Both fracture and fatigue experimental results suggest the traditional RAP addition method may be a better choice than the fractionated method. Although, the RAP materials for fracture and fatigue experiments were different and came from two sources, evaluating additional asphalt mixtures containing RAP from more different sources may provide firmer evidence.

Recommendations and Future Research

Based upon research findings and experimental practice, fracture energy protocols are only recommended for low temperature tests. Even then, the validation of the test assumption should be completed case-by-case, depending upon the plastic zone size of the asphalt mixture. For test temperatures above -20°C, the application of the old fracture energy protocol should be suspect and questioned. G_f test results should be verified by testing samples with different notch sizes. Diversified results indicate the small-scale yielding condition is unsatisfied and the estimated G_f and K value cannot be utilized for toughness estimation. If the original SCB test protocol is still selected for study, the sample with a small size notch is recommended. However, the SCB fracture toughness experiments are recommended for study.

The proposed new procedures provide much better toughness parameters. However, they still have limitations. The J_{IC} fracture toughness test, based on Begley and Landes' experiment, has the shortcoming of requiring more extensive work. The SCB J_{SS} experiment provides experimental values or J_{SS}, which could be a number between the actual J_{IC} and $J_{SS.}$ Whether the experimentally-estimated J_{SS} is close to the actual J_{IC} or J_{SS} depends upon the material's deformation yielding scale and the distance for facture approaching a steady state. Therefore,

in the future, elastic compliance should be introduced into the asphalt SCB test and follow the ASTM standard to measure the J R-curve. At this point, the old SCB test will completely change. The CMOD will not be used for loading rate control, but for estimating crack extension. Data from only one sample can produce a J R-curve and test data from multiple samples can be utilized to obtain an average J R-curve with a higher confidence level. From an application perspective, a transitional RAP addition method may be recommended, compared with the fractionated RAP addition methods utilizing No. 30 sieve.